# Exploring RIG-I like receptor signaling: Regulation by DHX15 and RIGing the pathway for broad-spectrum antiviral immunity

Sowmya Pattabhi

A dissertation

submitted in partial fulfillment of the

requirements for the degree of

Doctor of Philosophy

University of Washington

2014

Reading Committee:

Michael Gale Jr., Chair

Stephen J. Polyak

Christoph Grundner

Program Authorized to Offer Degree:

Pathobiology

University of Washington

## Abstract

Exploring RIG-I like receptor signaling: Regulation by DHX15 and RIGing the pathway for broad-spectrum antiviral immunity

Sowmya Pattabhi

Chair of the Supervisory Committee:
Professor Michael Gale Jr., Ph.D.
Department of Immunology

Retinoic acid inducible gene-I (RIG-I) is a cytoplasmic pathogen recognition receptor essential for recognition of RNA viruses. RIG-I engagement of viral RNA activates downstream signaling through the mitochondrial antiviral-signaling adaptor (MAVS) and results in the production of type I interferons, pro-inflammatory cytokines, and the expression of innate immune genes that suppress virus infection. My work has been focused on understanding the regulation of RIG-I signaling and developing small molecule agonists that target the RIG-I-like receptors as a strategy to develop host-targeted, broad-spectrum antivirals that work to inhibit emerging and re-emerging RNA virus infections.

This thesis focuses on the regulation of RIG-I signaling in the first part. To identify cofactors of RIG-I signaling, a proteomic approach coupled with assessment of innate immune signaling function was used to identify the DEAH-box RNA helicase,

DHX15 as a RIG-I signaling partner. My work identifies DHX15, as a positive regulator that is essential for innate immune response to control viruses of the family-*Paramyxoviridae* (Sendai virus), *Picornaviridae* (Encephalomyocarditis virus) and *Rhabdoviridae* (Vesicular stomatitis virus) and characterizes DHX15 as a RNA helicase that binds RIG-I and melanoma differentiation associated factor 5 (MDA5) basally through interactions mediated by the DHX15 N-terminus and the RLR CARDs. RNA binding studies identify DHX15 as a pathogen recognition receptor that binds non-self single-stranded RNA (ssRNA) and double-stranded RNA (dsRNA). DHX15 and RIG-I bind dsRNA more efficiently than either protein alone, indicating that DHX15 serves as a PAMP co-receptor to enhance RLR signaling.

In the second part, I hypothesize that small molecule agonists that target the RLR pathway and induce cell and tissue-wide innate antiviral immunity can be effectively used in therapeutic approaches to control RNA virus infections. A small molecule diversity library designed based on the ligand binding pocket within RIG-I, was used in a cell-based screening approach to identify compounds that drive IRF3 activation. Hit compounds identified in the screen differentially induce a discrete subset of proinflammatory cytokines, chemokines and antiviral genes. Correspondingly, compound administration before or after infection significantly decreased the viral RNA load in cultured cells that were infected with the family *Flaviviridae* West Nile virus (WNV), dengue virus (DV) and hepatitis C virus (HCV), the *Filoviridae* Ebola virus (EBOV, Zaire), Orthomyxoviridae Influenza A virus (IAV, H3N2, Udorn strain) and Paramyxoviridae respiratory syncytial virus (RSV) and concomitantly suppressed infectious virus production. This study thus identifies a novel class of immune-

modulatory molecules that activate RLR signaling to promote host antiviral responses to broadly suppress infection by RNA viruses of distinct genera. These compounds target the host and therefore could be broad-spectrum and effectively developed as a first line of defense in controlling RNA viruses.

**Acknowledgements**

I would like to express my deepest gratitude to my graduate thesis advisor, Dr. Michael Gale Jr., for his guidance through my graduate research work. He has been a tremendous source of inspiration, support and has been instrumental in my success. Dr. Yueh-Ming Loo has offered her guidance, scientific support and helped me move my projects forward. I am extremely grateful for her friendship and support.

I would like to thank my graduate thesis committee; Dr. Stephen J. Polyak, Dr. Christoph Grundner, Dr. Steven G. Reed, Dr. Deborah Fuller and Dr. Lalitha Ramakrishnan for encouraging me, meeting with me and taking the time to give me insightful and constructive feedback on my projects. I am extremely grateful to Dr. Steven G. Reed for believing in me and supporting me financially through the first year of graduate school. I am thankful to Kineta Inc. for the opportunity to work on a translational antiviral drug discovery project, which was made possible through an active collaboration with scientists and chemists at Kineta. I would like to acknowledge the financial support by the viral pathogenesis pre-doctoral training grant (T32AI083203) that provided for my tuition-related expenses for the last two years. A special thanks to the Pathobiology program, especially Dr. Lee Ann Campbell and Rachel A. Reichert for helping me at every stage of the graduate program. I would like to acknowledge Melissa Petersen and her help over the last 4 years with scheduling, ordering, travel, planning and making all the time consuming tasks quick and trouble-free.

My husband, Subramanian Sundaresan (Mani) and my kids, Sneha and Shreyas Subramanian, add meaning to my life and have been very patient. They have stayed

positive, made many sacrifices and have always believed in me. My dad, Pattabhi Ramaiyer and my mom, Dr. Vasantha Pattabhi are a source of inspiration and have taken time to help me and offered their support and guidance to see me succeed both at work and in my family life. I am extremely grateful to them and all of my family including my brother Ravi Pattabhi for cheering me on and always being there for me. I am thankful to my past mentors; Dr. Victor Tsang, Dr. Kathy Hancock, Dr. Ajay Bhatia who shaped my ideas on science and taught me that science can be fun and exciting. Last but not the least, I am extremely thankful to my wonderful friends; Hong Liang, Vanitha Raman, Raodoh Mohamath, Amina Negash, Tien-Ying Hsiang and Alison Kell, who have kept me in good cheer and supported me through ups and downs.

*“I am richer by this life experience. I have learnt from everyone that has crossed paths with me!”*

*Sowmya Pattabhi*

## Table of Contents

## List of Tables

## List of Figures

## List of Abbreviations

| | |
|---|---|
| 5’-ppp | 5’ tri-phosphate |
| a.a | Amino acid |
| ADAR1 | adenosine deaminase RNA-specific 1 |
| AP1 | Activator protein-1 |
| APOBEC3 | apolipoprotein B mRNA editing enzyme, catalytic polypeptide-like 3 |
| ATF2 | activation transcription factor 2 |
| ATP | Adenosine tri-phosphate |
| CARD | Caspase activation and recruitment domains |
| CTD | C-terminal domain |
| CYLD | tumor suppressor protein cylindromatosis |
| DExD/H | DEAD-Box |
| DUB | Deubiquitinating enzymes |
| DV | Dengue virus |
| EBOV | Ebola virus |
| eIF | Eukaryotic initiation factor |
| EMCV | Encephalomyocarditis virus |
| FADD | Fas-associated protein with death domain |
| HCV | Hepatitis C virus |
| HIV | Human immunodeficiency virus |
| IAV | Influenza A virus |
| IFIT | IFN-induced protein with tetratricopeptide repeats |

| | |
|---|---|
| IFITM | Interferon-inducible transmembrane protein |
| IFN | Type-I interferon |
| IFNAR | IFN-$\alpha/\beta$ receptors |
| IKK | I-Kappa-B Kinase |
| IL | Interleukin |
| IRF | Interferon regulatory factor |
| ISG | Interferon stimulated gene |
| ISGF3 | Interferon-stimulated gene factor 3 |
| ISRE | Interferon stimulated response element |
| JAK | Janus kinase |
| JEV | Japanese encephalitis virus |
| LGP2 | Laboratory of genetics and physiology 2 |
| Lys | Lysine |
| MAM | Mitochondrial-associated membrane |
| MDA5 | Melanoma differentiation associated gene 5 |
| MFN | Mitofusin |
| MX | Myxoma resistance |
| MyD88 | Myeloid differentiation primary response gene (88) |
| NEMO | NF-kappa-B essential modulator |
| NF-$\kappa$B | nuclear factor kappa-light-chain-enhancer of activated B cells |
| NLR | NOD-like receptor |
| N-RIG | N-terminus of RIG-I |

| | |
|---|---|
| OAS | Oligo-adenylate synthase |
| PAMP | Pathogen-associated molecular patterns |
| PKR | RNA-activated protein kinase. |
| Poly-U/UC | HCV PAMP |
| Pro | Proline |
| PRR | Pathogen recognition receptors |
| PTM | Post translational modifications |
| RD | Repressor domain |
| RIG-I | Retinoic acid inducible gene |
| RIP | Receptor-interacting protein kinases |
| RLR | RIG-I like receptors |
| RNF | Ring finger protein |
| SAMHD1 | Sam-domain-and HD-domain containing protein 1 |
| SenV | Sendai virus |
| STAT | Signal transducer and activation of transcription |
| STING | Stimulator of interferon genes |
| TAK | Transforming growth factor-β-activated kinase |
| TBE | Tick-borne encephalitis |
| TBK | Tank binding kinase |
| TIM | TRAF-interacting motif |
| TLR | Toll-like receptor |
| TNF | Tumor necrosis factor |
| TOM | Translocase of outer membrane |

| | |
|---|---|
| TRADD | Tumor necrosis factor receptor type 1-associated DEATH domain |
| TRAF | TNF receptor-associated factor |
| TRIF | TIR-domain containing adapter-inducing interferon-β |
| TRIM | Tri-partite motif containing |
| USP | Ubiquitin specific peptidase |
| VSV | Vesicular stomatitis virus |
| WDR | WD repeat proteins |
| WNV | West Nile virus |
| YF | Yellow fever virus |

# Chapter 1. Introduction

Self versus non-self discrimination is a crucial step in the induction of innate immune responses that clear infections. These innate immune responses are an organism's first-line of defense against microbial infections. These responses when dysregulated, can result in auto-immunity [1-5]. RIG-I is a pathogen recognition receptor (PRR) that can sense the presence of non-self viral RNA in an infected cell and can establish innate immune programs that limit and restrict RNA virus infections. My work has been focused on understanding the regulation of RIG-I signaling, identifying novel co-factors that regulate the pathway and targeting host innate immunity as a strategy to control RNA virus infections.

## RIG-I like receptors and their role in innate immunity

RIG-I like receptors (RLR) are cytoplasmic pathogen recognition receptors that detect pathogen-associated molecular patterns (PAMP) within viral RNA. There are three main members of the RLR family, RIG-I (retinoic acid inducible gene-I), MDA5 (melanoma differentiation associated gene 5) and LGP2 (Laboratory of genetics and physiology 2). The RLRs are widely expressed in multiple cell types and in many tissues to assist with pathogen recognition [6]. The expression of the RLRs remains at low levels in the steady-state and is greatly increased upon IFN exposure or in response to virus infection [7-10]. RIG-I is the prototypical RLR that is essential for recognition of many RNA viruses through the binding of viral RNA which initiates innate immune responses and antiviral programs that control RNA virus infections [8-9, 11-12]. RIG-I signaling results in the activation of transcription factors; IRF3/7, AP1 and NF-κB,

production of type I interferons (type-I IFN), secretion of proinflammatory cytokines and drives the expression of innate immune genes [13-14]. Immune responses induced by type-I IFNs are crucial in triggering innate antiviral responses through Janus kinases and signal transducer and activator of transcription protein (JAK-STAT) signaling pathway. Type-I IFNs, when secreted from the virus-infected cell, bind to IFN-$\alpha/\beta$ receptors (IFNAR) to induce the expression of hundreds of interferon-stimulated genes (ISG) in autocrine and paracrine fashion to establish an antiviral state that limits infection (Figure 1-1) [15-19].

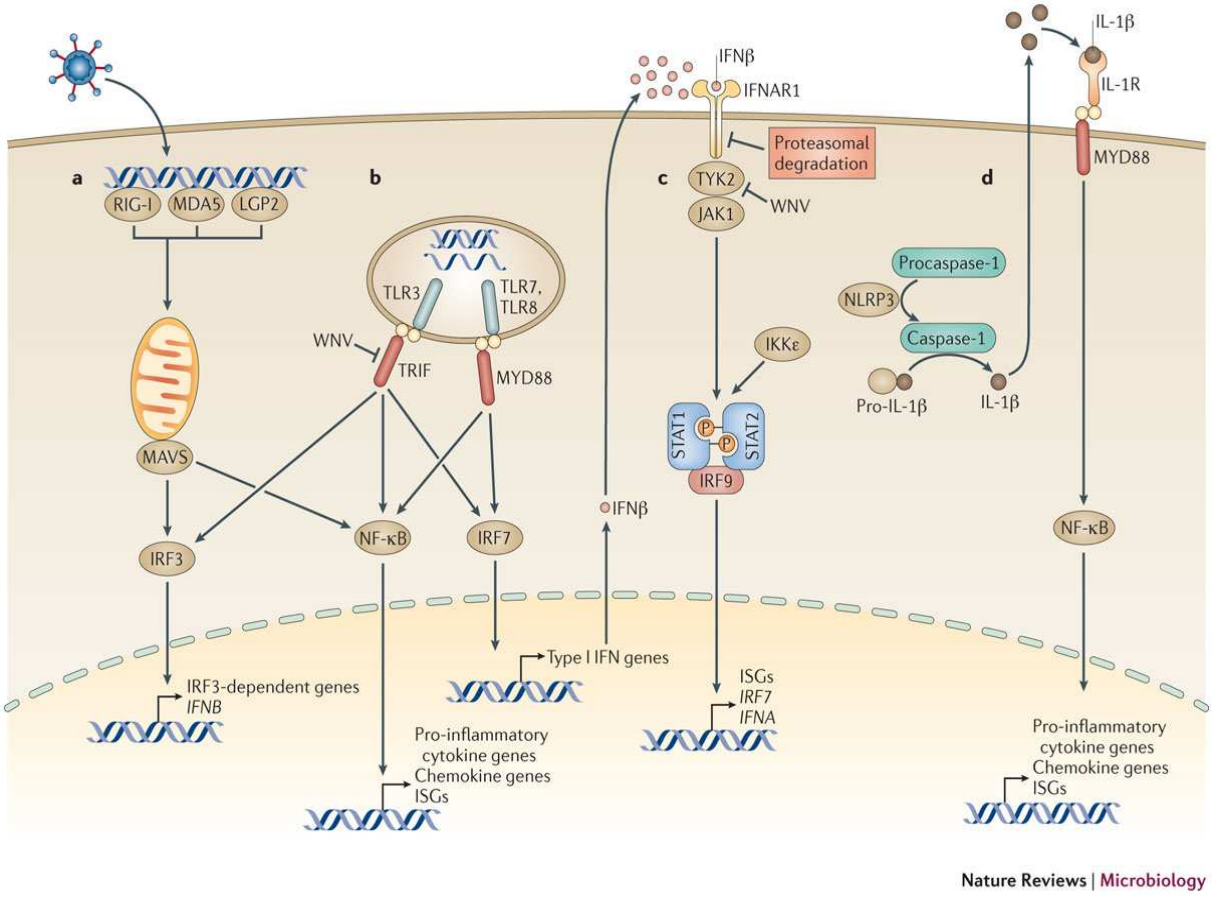


***Figure 1-1. RIG-I like receptor signaling and the interferon signaling cascade.*** (a) RIG-I like receptors are cytoplasmic pathogen recognition receptors that sense the presence of viral RNA in an infected cell and signal through a central adapter, MAVS which is

present on mitochondrial-associated membranes. Viral RNA sensing drives the activation of transcription factors IRF3/7 and NF-κB and results in the production of type I IFNs and pro-inflammatory cytokines. (b) TLR3, TLR7 and TLR8 can sense the presence of RNA in endosomal compartments and signal through the adapter TRIF to drive the activation of the transcription factors; IRF3/7 and NF-κB that can trigger ISG induction and pro-inflammatory cytokine production. (c) Type-I IFN secreted from the infected cell binds cell surface IFNAR receptors to activate JAK-STAT signaling to establish an antiviral state through the induction of hundreds of interferon-stimulated genes that control RNA virus infection. (d) RIG-I can trigger NF-κB-dependent production of pro-IL-1β and inflammasome activation in response to sensing some RNA viruses. Reproduced from Suthar M. S., 115-128, 2013 [20].

## Structure of the RLRs

Rig-I mediated antiviral immunity starts with the sensing of non-self RNA by the RLRs. The RLRs RIG-I, MDA5 and LGP2 share a DExD/H box helicase domain that constitutes the proteins' central core, a C-terminal domain (CTD) that is essential for PAMP recognition and in the case of RIG-I, for autoregulation [8-9, 21-22] and two tandem amino-terminal caspase activation and recruitment domains (CARDs) that are essential for signaling in the case of RIG-I and MDA5. The RLRs work through a central adapter mitochondrial antiviral signaling protein (MAVS) [23-27] which is present on the mitochondrial-associated membranes (MAM). The MAM has emerged as a critical platform that facilitates innate immune signaling functions [28]. The CARD's of RIG-I and MDA5 are involved in interaction with the single CARD domain on MAVS adapter molecule to trigger signaling (Figure 1-2).

In an uninfected cell, the repressor domain (RD) on RIG-I, that is part of the CTD, binds the N-terminal CARDs and represses signaling [15]. Upon sensing of non-self viral RNA by the RD followed by the helicase domain, ATP is hydrolyzed and RIG-I undergoes a conformational change and occupies an active conformation that releases

the CARD domains for signaling to MAVS [29-30]. Unlike RIG-I, MDA5 is less stringently regulated as ectopic over expression of MDA5 is sufficient to drive signaling even when the RNA ligand is absent [21]. LGP2 lacks the N terminal CARD domains and is thought to have a role in regulating RIG-I and MDA5 signaling [15, 31-34]. The RLR activation, translocation and homotypic interactions between the RLRs CARDs and MAVS involve the dynamic recruitment of several co-factors that regulate the formation of a large signaling complex also called the “signalosome” [28, 35-38].

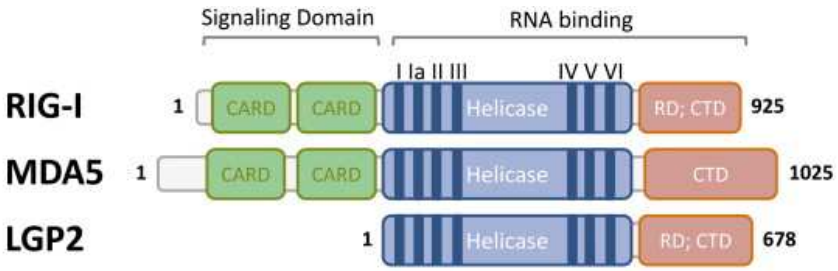


***Figure 1-2. Schematic representation of the RIG-I like receptor family.*** The RIG-I like receptor family has three main members; RIG-I (1-925 a.a), MDA5 (1-1025 a.a) and LGP2 (1-678 a.a). RIG-I and MDA5 have the N-terminus tandem caspase activation and recruitment domains (CARD) that are essential for signaling. The RLRs have a central DExD/H-box domain that can hydrolyze ATP, a helicase domain that can unwind RNA and a C-terminal domain (CTD) that is essential for making contact with the viral PAMP RNA. Image reproduced from Shih J-W, Lee Y-HW, 2013 [39].

## Pathogen sensing by RLR

RIG-I is involved in pathogen sensing of a wide range of viruses belonging to multiple families. RIG-I can sense hepaciviruses which belong to the family *Flaviviridae* and many other viruses from the families *Orthomyxoviridae, Rhabdoviridae, Paramyxoviridae, Filoviridae, Bunyaviridae, Coronaviridae, Arenaviridae,* and

*Calciviridae* [6, 8, 11-12, 40-45]. MDA5 can sense pathogens from the family *Picornaviridae* [46-47]. Some of the viruses that belong to *Flaviviridae* like West Nile virus, dengue virus, Japanese encephalitis virus (JEV) and reoviruses can signal through both RIG-I and MDA5 [11, 46, 48].

Extensive work from our lab and other labs has established that RIG-I recognizes viral RNA with 5’ ppp and stretches of poly-U/UC [40, 49-51]. Viral replication intermediates produced as a part of the viral life cycle, both positive and negative sense RNA as well as RNA polymerase III transcripts generated from DNA viruses can be sensed by RIG-I efficiently [49, 52-53]. RIG-I also has a preference for blunt ended viral RNA ligands over those with 3’ or 5’ overhangs [54]. Recently, sensing of 5’pp RNA from the reovirus genome was reported. In this recent paper, both RIG-I and MDA5 were shown to bind reoviral genomes irrespective of length, but RIG-I sensing required the presence of 5’pp on the viral genome [55]. This body of work now diversifies the PAMP recognition by RIG-I to base-paired RNA with either 5’ppp or 5’pp moiety and widens the viral PAMP features that can be recognized by RIG-I.

In comparison to RIG-I, the viral PAMP recognition by MDA5 is less well understood. MDA5 is known to recognize longer dsRNA and branched RNA structures and does not require the presence of a 5’ ppp moiety on its RNA ligand [56-58]. MDA5 has been suggested to multimerize on viral RNA and utilize energy from the hydrolysis of ATP to form higher order structures and large filaments that in turn interact with MAVS to trigger downstream signaling [59-61]. MDA5 has also been shown to

differentiate between host and viral RNA based on the 2'-O-methylation status of their 5' cap structures [62].

Recently, RIG-I and MDA5 has been shown to have a temporal response in recognizing viral PAMP RNA in the context of West Nile virus infection. RIG-I plays a role early in the infection by recognizing viral replication intermediates in a 5' ppp-dependent manner, while in RIG-I knockout cells, MDA5 has a role in recognizing viral PAMP RNA that accumulates as infection progressed resulting in type-I IFN production with delayed kinetics [48, 63]. In contrast to RNA ligands recognized by RIG-I and MDA5, the ligand specificity of LGP2 remains unclear. LGP2 is predicted to bind a variety of RNA species and has been suggested to modulate both RIG-I and MDA5-mediated signaling [15, 21, 31-34, 64].

## Regulation of the RLR signaling pathway

Self versus non-self RNA recognition is a tightly regulated process that determines the establishment of innate immunity against virus infection. RIG-I is regulated by its expression level and its conformational state in uninfected cells. In the basal state, RIG-I is autorepressed through the C-terminal repressor domain (RD), which binds and conceals the CARD domains. RIG-I is signaling "inactive" in the steady-state and requires the binding of non-self viral RNA to be activated. Viral RNA/PAMP binding to the RD and helicase domains triggers ATP hydrolysis followed by conformational change that releases the CARDs for signaling [22, 29-30, 49-50].

The RLR components are post-translationally modified and these modifications are dynamically controlled and altered based on the infection status. RIG-I transition from the “inactive” to “active” state requires recruitment of several co-factors as well as dynamic changes to the post-translational modifications (PTM) present on RIG-I. In the basal state, RIG-I is constitutively phosphorylated in its CARDs and C-terminal domain (CTD) and is rapidly dephosphorylated upon virus infection. The phosphorylation of Thr 770 and Ser 854/855 in the RIG-I CTD by casein kinase II [65] and phosphorylation of Ser 8/Thr 170 in the CARD domains of RIG-I by protein kinase C-$\alpha/\beta$ maintains RIG-I in an autorepressed basal state [66-68]. Dephosphorylation of the Ser 8/Thr 170 of RIG-I and Ser 88 of MDA5 by protein phosphatase 1 $\alpha/\gamma$ is essential for RLR activation [69].

RIG-I activation occurs in multiple steps and starts with viral PAMP binding, followed by dephosphorylation of RIG-I, which promotes binding of E3 ubiquitin ligase tripartite motif-containing protein 25 (TRIM25) to CARD1 of RIG-I, followed by K63-linked ubiquitination of Lys 172 of CARD 2 as well as riplet (a ring finger protein) dependent K63-linked ubiquitination of Lys 788 of CTD of RIG-I [15, 70-73]. The K63 polyubiquitination of RIG-I allows for its multimerization and activation. Activated RIG-I in combination with TRIM25 associates with 14-3-3ε, a mitochondrial targeting chaperone translocates from the cytoplasm and redistributes to the mitochondria-associated membranes (MAM) to interact with MAVS [36, 74]. This interaction acts as a platform for recruitment of several signaling molecules and cofactors and forms the signalosome complex that leads to amplification of signal as well as transcription factor activation (IRF3/7 and NFκB) [28, 35-38].

The ubiquitination and deubiquitination status of RIG-I and the other signaling molecules downstream of RIG-I further regulates the pathway. RIG-I is regulated by the deubiquitinating (DUB) enzymes; tumor suppressor protein cylindromatosis (CYLD), USP3 and USP2. These DUBs negatively regulate RIG-I by removing K63-linked ubiquitin chains, thus dampening RIG-I activity [75-77]. RIG-I is also regulated by K48-linked ubiquitination through the action of Ring-finger protein125 (RNF125). RNF125 induces K48-linked ubiquitination of RIG-I, MDA5 and MAVS to promote proteasomal degradation triggering a negative feedback loop that prevents excessive cytokine production [78]. The ubiquitin-editing protein A20 and linear ubiquitin assembly complex (LUBAC) composed of two E3 ligases, HOIL-1L and HOIP, negatively regulate RIG-I signaling whereas USP4 and USP15 positively regulate the pathway by removing Lys48-linked ubiquitin chains [77, 79-82].

The extensive post-translational modifications that control and regulate the activation of the RLR serve as a check point to prevent aberrant signaling and allow for rapid modulation of the steady-state in case of infection.

## MAVS as a central adapter that controls innate immune signaling

Mitochondrial antiviral signaling protein (MAVS) is a central adapter that controls innate immune signaling that is triggered by RIG-I and MDA5 in response to sensing viral PAMP RNA in the cytoplasm [83]. MAVS is constitutively expressed and localizes to the outer membrane of the mitochondria, peroxisomal membranes as well as mitochondrial-associated membranes (MAM) [28, 84-85]. MAM is an essential structure

that connects the endoplasmic reticulum to the mitochondria and has emerged as an essential platform regulating innate immune signaling. Structurally, MAVS has an N-terminal CARD domain that is essential for signaling and for making homotypic interactions with CARD domains on RIG-I and MDA5. It has a central proline-rich domain involved in protein-protein interactions and a C-terminal transmembrane domain that anchors MAVS to the intracellular membranes (Figure 1-3). Membrane localization is important for MAVS to signal. For example, the HCV NS3/4A protease targets MAVS close to the transmembrane domain to cleave MAVS from the intracellular membranes to abrogate innate immune signaling and promote HCV replication [15, 24, 28, 86-87].


***Figure 1-3. Structure of MAVS.*** Schematic shows structure of mitochondrial antiviral signaling protein (MAVS, 1-540 a.a). MAVS is a central adapter that signals through its N-terminus CARD domains. It has a central proline (Pro) rich domain involved in protein-protein interactions and a C-terminal transmembrane domain that anchors MAVS to the intracellular membranes.

The activation of signaling that occurs through the interaction of CARD domains of RLR and MAVS results in the assembly of the signalosome complex [28, 35-38]. MAVS has three TRAF-interacting motifs (TIMS) that bind TNF receptor-associated factors (TRAF3, 2 and 6). Several signaling cofactors and adapters are recruited and assembled in the intracellular membranes leading to the amplification of signaling. The cofactors that get recruited and interact with MAVS can be divided based on the functions they regulate (Table 1-1).

| Function | MAVS Interactors | Reference |
|---|---|---|
| Antiviral signaling | TRAF3, TRAF5, IKKε, WDR5,NEMO, DDX3, IRF3, IRF7 | [88-94] |
| Inflammatory response | NLRC5, NLRX1, TRAF 2, 5, 6, TAK1, IKK α/β | [93, 95-100] |
| Apoptosis | FADD, TRADD and RIP1 | [101-103] |
| Mitochondrial membrane potential | Mfn1 and Mfn2 | [104-105] |
| Mitochondrial import | Tom70 | [106] |
| Phosphorylation | IKKε, PLK1, c-Src, c-Abl | [90, 107-110] |
| Ubiquitination | RNF125, RNF5, PCBP2 | [78, 111-112] |

**Table 1-1. MAVS interactome.** Table lists proteins that interact with MAVS and regulate RLR signaling pathway. The classification is based on the functions that are regulated by the signaling cofactors or adapter molecules.

MAVS like RIG-I is regulated dynamically by post-translational modifications. MAVS is altered by both K63-linked and K48-linked polyubiquitination that modulates its activity [90, 113]. Activation of MAVS results in its multimerization to form a prion-like aggregate that acts as the active form [114-115]. The signal amplification and activation of MAVS results in the recruitment of IκB kinase-ε (IKKε), TANK-binding kinase 1 (TBK1) as well as the IKK α/β/γ complex and drives the activation of transcription factors; IRF3/7 and NF-κB. These transcription factors along with activation transcription factor 2 (ATF-2) and c-Jun induce the secretion of type-I IFNs (IFN α/β), proinflammatory cytokines, and induce antiviral gene expression (Figure 1-4). The

antiviral genes induced include the primary PRRs, RIG-I, MDA5 and LGP2 and their induction results in a positive feedback loop that amplifies the RLR response.

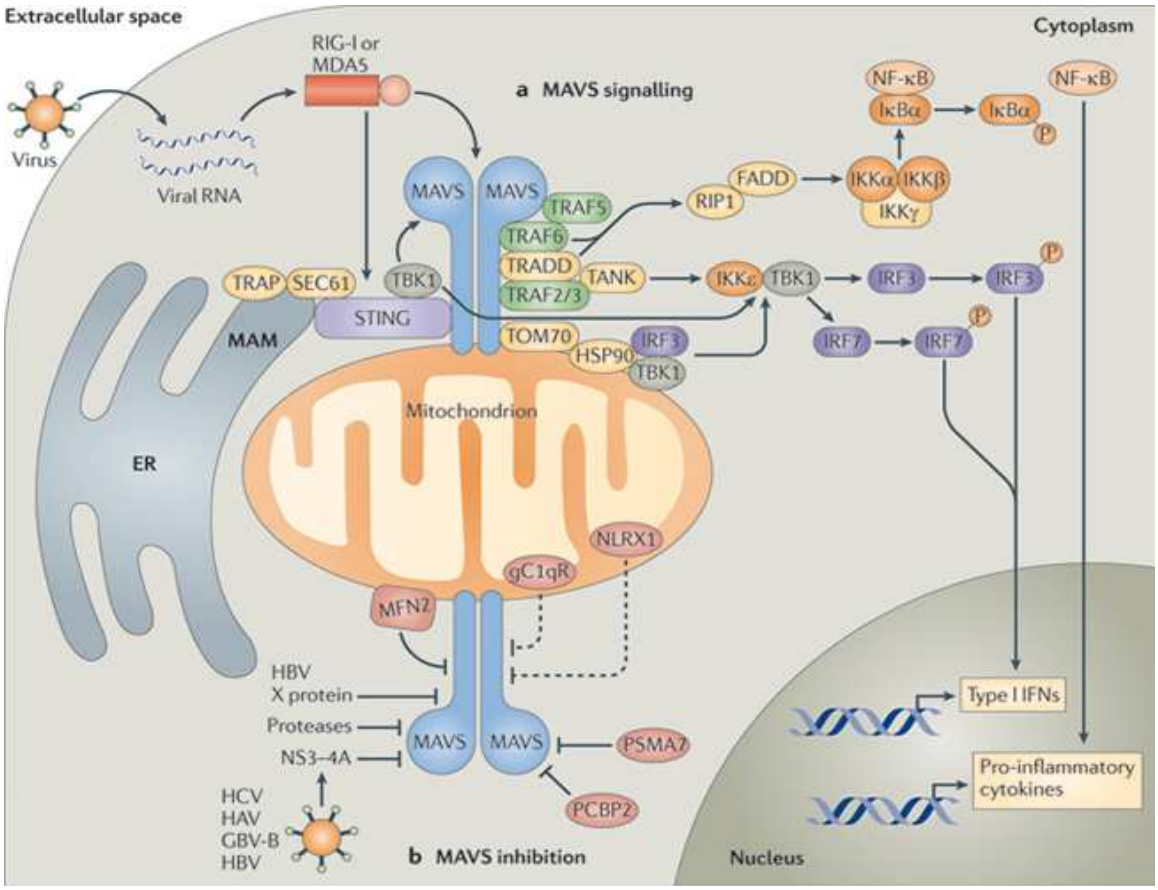


***Figure 1-4. Mitochondrial antiviral signaling pathways.*** MAVS is a central adapter that regulates signaling cascades at the intracellular membranes. Schematic shows (a) positive and (b) negative regulators that control the innate immune signaling pathway. The signaling molecules that get recruited to the activated RLR/MAVS complex lead to the activation of transcription factors IRF3/7, AP1, and NF-κB, and production of type I interferons, proinflammatory cytokines, and the expression of innate immune genes. Reproduced from West A. P., Shadel G. S., Ghosh S., 2011 [16].

## Role of DEXD/H box helicases in innate immunity to RNA viruses

In recent years, several DExD/H helicases have been characterized and shown to have a role in antiviral immunity against RNA and DNA viruses. They either help with innate immune sensing of PAMPs or have a role in mediating signaling events that are necessary to establish antiviral immunity. These helicases also have a role in triggering programmed cell death of infected cells, which acts as yet another antiviral mechanism to defend against pathogens.

DExD/H helicases are highly conserved molecular motors that hydrolyze ATP to remodel RNA or ribonucleoprotein complexes. These RNA helicases have essential roles in RNA metabolism, pre-mRNA splicing, ribosome biogenesis, transcription, translation, RNA storage and decay. RNA helicases can be broadly classified as monomeric helicases such as; SF1 and SF2 or ring-forming oligomeric/hexameric helicases such as; SF3-SF6. These helicases have a conserved helicase core that consists of two tandem Rec A-like domains with a flexible linker that connects the two domains. Within the helicase core, 12 highly conserved motifs, Q, I, Ia, Ib, Ic, II, III, IV, V, Va, Vb, VI are located sequentially in defined positions. These motifs have roles in ATP hydrolysis, RNA binding, RNA unwinding, and translocation [36, 116-118].

The majority of the eukaryotic RNA helicases belong to the SF2 family. Within this, they can be further classified as DEAD, DEAH, DExH, or DExD helicases [36, 116-118]. RLR helicases; RIG-I (DDX58), MDA5 (IFIH1) and LGP2 (DHX58) belong to the class of SF2 helicases. Several other non-RLR, DExD/H box helicases that have a role

in pathogen sensing of viruses or regulate antiviral immunity against both RNA or DNA viruses have been identified and characterized (Figure 1-5).

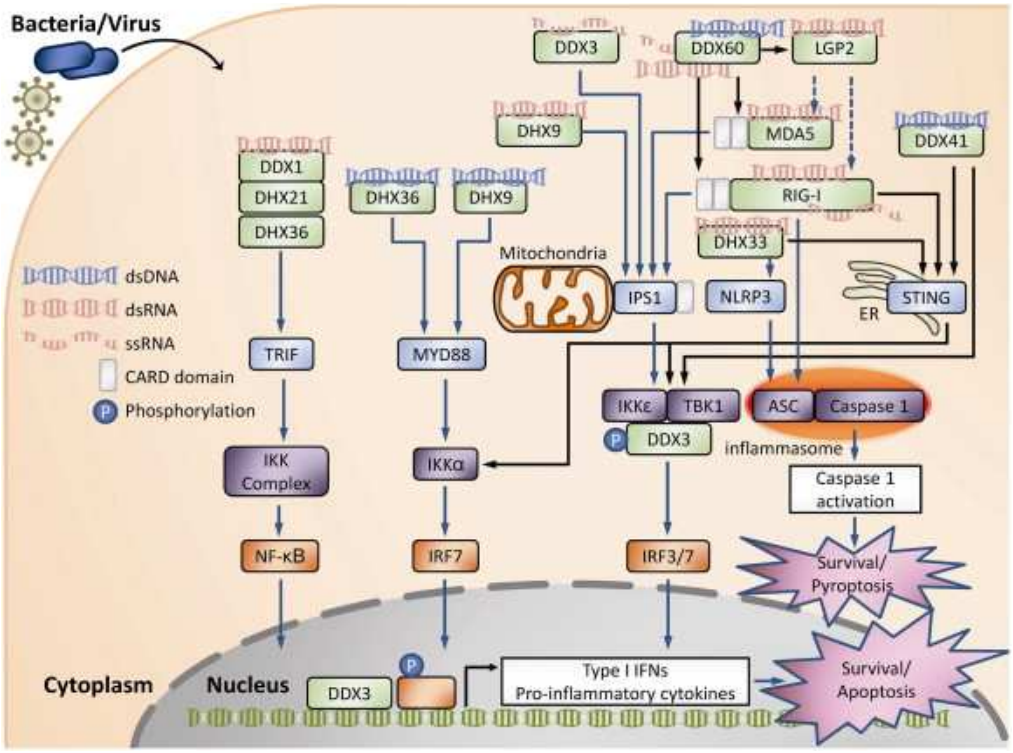


***Figure 1-5. DExD/H RNA helicases and their role in innate immune sensing.*** Schematic showing a broad overview of RNA helicases and their role in pathogen sensing. Image reproduced from Shih J-W, Lee Y-HW, 2013 [39].

Some of the non-RLR helicases that have been identified and characterized to have a role in innate immune sensing of RNA viruses are described below.

*DDX3:* DDX3 is ubiquitously expressed and was first identified as a helicase that associates with IKKε after virus infection. DDX3 interacts with IKKε and is phosphorylated at Ser-102, a key step that recruits IRF3 to the complex [119-120]. Knockdown of DDX3 resulted in lowered IFNβ promoter induction and decreased activation of IRF3/7 [119]. DDX3 has further been identified as a phosphorylation

substrate of the kinase, TBK-1 [121] and as a transcriptional regulator of IFN signaling [121]. In the context of VSV infection, DDX3 acts as a PRR and binds VSV RNA and enhances IFN induction in conjunction with RIG-I and MDA5 signaling in a MAVS-dependent mechanism [89].

*DHX9:* In myeloid dendritic cells, DHX9 senses dsRNA and works through a MAVS-dependent mechanism to act as a regulator of both NF-κB and IRF3 signaling. DHX9 acts as a PRR and uses the energy from hydrolysis of ATP to unwind RNA as well as RNA: DNA hybrids. DHX9 binds RNA through its N-terminus double-stranded RNA binding domain and binds CARD domain of MAVS through its C-terminus domain to drive signaling. DHX9 regulates proinflammatory cytokine production and type I IFN induction in response to influenza, reovirus infection and the synthetic PAMP, poly (I:C) [122]. DHX9 is interferon-inducible and has been identified as a substrate of RNA-activated protein kinase (PKR) that is phosphorylated in the context of HIV infection [123].

*DHX36:* DHX36 has been identified to be involved in augmenting the IFN induction in response to influenza A, Newcastle disease virus (NDV) infection and synthetic PAMP poly (I:C). DHX36 interacts with RIG-I irrespective of virus infection and facilitates dsRNA binding. On binding dsRNA, DHX36 forms a complex with PKR and drives its phosphorylation and activation through its ATPase and helicase activity. PKR activation has an essential role in antiviral stress granule formation. As DHX36 regulates PKR activation, the helicase indirectly regulates stress granule formation which serves as a

platform for recruiting signaling molecules enabling detection by the RIG-I like receptors [124].

*DDX1/DDX21/DHX36*: In myeloid dendritic cells, DDX1/DDX21/DHX36*,* the tri-partite complex is involved in sensing poly (I:C) and works through the adapter TRIF (TIR-domain containing adapter-inducing interferon-β) to establish an interferon response. DDX1 binds poly (I:C) through its helicase domain and DDX21 and DHX36 binds the TIR domain of TRIF and promotes IFN induction. The tri-partite complex has a role in antiviral response against influenza, reovirus infection and the synthetic PAMP, poly (I:C) [125].

*DDX60*: DDX60 localizes to the cytoplasm and is inducible upon virus infection. It binds viral ssRNA, dsRNA, dsDNA and interacts with RIG-I, MDA5 and LGP2 to act as a cofactor of RIG-I like receptor signaling [126]. DDX60 knockdown cells have compromised IFNβ production in response to poly (I:C) transfection, Polio virus, Sendai virus, VSV and HSV-1 infection [126].

*DHX33:* DHX33 is involved in binding dsRNA namely; synthetic PAMP, poly (I:C) and reovirus RNA in myeloid DCs through a MAVS-dependent manner to positively regulate both NF-κB as well as IRF3 signaling [127]. It also regulates NLRP3 inflammasome (NLR Pyrin-domain containing 3) formation in human macrophages [123].

*DDX24:* DDX24 is an IFN-inducible helicase that acts as a negative regulator of RLR signaling. It competes with RIG-I to bind RNA and promotes signaling through the adaptor proteins; Fas-associated death domain (FADD) and receptor interacting protein

1 (RIP1). This interaction inhibits IRF7 activity which is an essential transcription factor necessary for type I IFN induction [128].

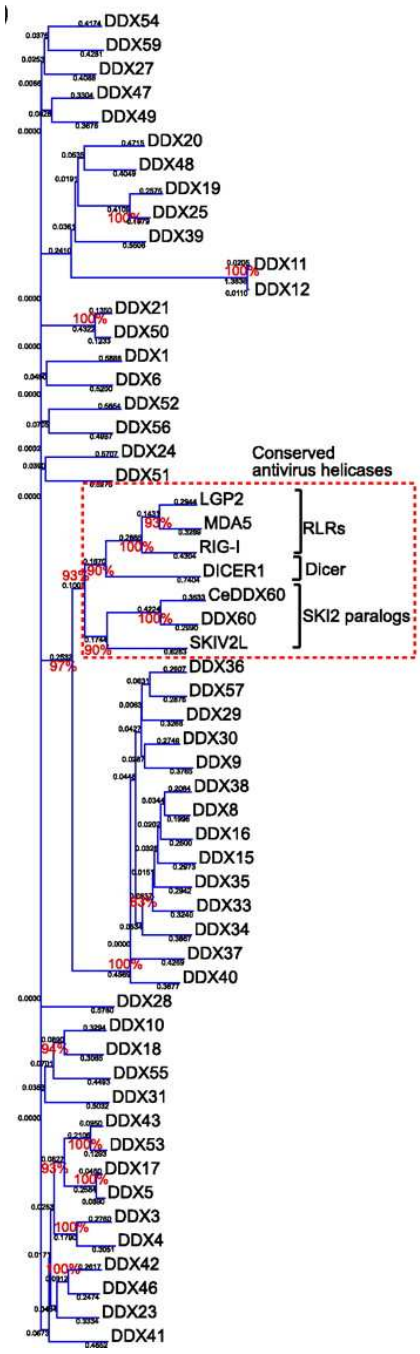


***Figure 1-6. Phylogenetic tree of DExD/H box RNA helicases from Caenorhabditis elegans.*** The genetic distances and boot strap probabilities are given in black and red. Reproduced from M. Miyashita et al., MCB, Sept. 2011, p. 3802–3819 [126].

## Multiple roles of non-RLR DExD/H box helicases.

The DExD/H box family of helicases are conserved (Figure 1-6) and the activity of approximately 57 RNA helicases has been identified and validated in humans [118]. DExD/H-box helicases have an essential role in antiviral immunity, pathogen sensing and further diversify the PRRs that are involved in innate immune sensing of viral RNA. The redundancy in PRRs may be a strategy evolved by the host to fight against the viral antagonism of the innate immune responses widely prevalent among many viruses [129].

Other than the role of DExD/H-box helicases in pathogen sensing and regulating the signaling cascades that establish innate immunity, the DExD/H box helicases are recruited by RNA viruses and play essential roles as host factors that assist with replicating viral genomes. The limited genome size of RNA viruses requires them to utilize several cellular host factors to complete their life cycle. For example, DDX1, DDX3 and DHX9 are host RNA helicases that are recruited by several viruses [116, 130]. The major human pathogens that cause chronic diseases such as, Hepatitis C virus (HCV) and HIV utilize host helicases for replicating their genomes, remodeling of RNA, and for viral gene expression [116, 131-133]. The recruitment of host helicases by viruses might be yet another mechanism of antagonism through which viruses evade innate immune detection. Recruitment of DExD/H-box helicases that serve as essential regulators of antiviral immunity and exploiting them towards replicating viral genomes can be an effective strategy in blunting the innate immune responses that control RNA viruses.

## Interferon-inducible antiviral genes that control RNA viruses

The viral PAMP sensing in an infected cell leads to activation of RLR signaling and results in expression of IRF3 and NF-κB dependent genes. These virus-responsive genes can confer antiviral immunity, induce the secretion of proinflammatory chemokines, cytokines and drive the recruitment of immune cells that can prime the adaptive immune response to infection. Subsets of these genes are induced in response to PRR activation through the activation of transcription factor IRF3, in an interferon-independent manner and are called IRF3-dependent genes [134-135]. The initial wave of antiviral response is further amplified by the secretion of type-I IFNs that bind cell surface IFNAR receptors, trigger JAK-STAT signaling and activate IFN-α/β-activated transcription factor complex, termed ISGF3 [interferon-stimulated gene factor 3 (ISGF3γ (IRF-9)/STAT1/STAT2)]. ISGF3 binds to a common enhancer element referred to as the ISRE (IFN-stimulated responsive element) to induce ISG expression. The ISGs that are induced by the interferon response are essential for limiting and controlling RNA virus infections. They work in multiple cell types at different stages of the viral life cycle like entry, egress, capsid assembly, replication and protein translation (Figure 1-7) [17-18, 136-137]. Several hundred ISGs are induced in response to viral infections, yet the function of only a select subset of ISGs have been delineated and characterized. Some of the well-characterized ISGs and their role in antiviral immunity will be described below.

*IFN-induced protein with tetratricopeptide repeats (IFIT) family, IFIT1, IFIT2, IFIT3 and IFIT5:* IFIT proteins are induced in response to IFN treatment, virus infection or PAMP

recognition and have upstream ISRE promoter elements that control their expression. IFIT1 and 2 genes are rapidly induced within 2 hours of exogenous IFN$\alpha$ treatment. Activation of PRRs like RIG-I, MDA5, TLR3 and TLR4 can induce the IFIT protein expression. Several different stimuli like LPS treatment, activation of transcription factors like IRF1, 3, 5, and 7 can induce IFIT gene expression. Rift Valley fever virus (RVFV), vesicular stomatitis virus (VSV), influenza A virus (IAV), West Nile virus (WNV) are some of the viruses that are very sensitive to the actions of IFIT proteins [138].

IFIT proteins are cytoplasmic and have tetratricopeptide repeats (TPR). These TPR motifs contain 34 amino acids and take helix-turn-helix structures and are usually involved in protein-protein interactions that regulate cell cycle, protein folding, protein transport and transcription. Most cell types do not express any IFIT proteins in the basal state except some of the myeloid subsets [139]. IFIT1 senses the presence of viral RNA in a 5'ppp dependent manner and forms an IFIT1-IFIT2-IFIT3 complex that inhibits viruses by sequestering viral RNA from the replicating pool or by degrading viral RNA [140]. Upon induction, IFIT1 and IFIT2 works through multiple mechanisms; inhibiting protein translation by blocking the action of the translation initiation factor EIF3, sequestering viral proteins, binding uncapped or incompletely capped RNA and regulating immune responses to infections [135].

*IFN-inducible transmembrane proteins IFITM1, IFITM2 and IFITM3:* IFITM1/2/3 proteins work as antiviral effectors that inhibit a broad range of enveloped viruses and modulate cellular tropism irrespective of the expression of viral receptors. These proteins are induced by IFNAR signaling and are involved in restricting entry and

endosomal fusion of IAV, WNV and dengue virus (DV) [141]. Other work has shown that they work to restrict Filoviruses like Ebola and Marburg virus, HIV-1, coronavirus and respiratory syncytial virus [19, 142-144]. In a recent study, the viral burden of dengue virus infected cells inversely correlated with the expression of IFITM3 protein levels. IFITM3 proteins were shown to be secreted out of the infected cell in extracellular exosomes. These exosomes were delivered from infected to non-infected cells thereby propagating the antiviral response through paracrine effect [145].

*Myxoma resistance proteins MX1, MX2:* These genes are induced by type I (IFN$\alpha$/$\beta$) and type III (IFN$\lambda$) IFNs. MX1 works in restricting a variety of RNA viruses namely; Orthomyxoviruses, Bunyaviruses, Rhabdoviruses, Togaviruses and DNA viruses. Human MX1 and MX2 have the broadest range of antiviral activity compared to other ISGs [146]. MX proteins are dynamin-like large GTPases. They oligomerize and form ring like structures that trap viral nucleocapsids and associated polymerases [19, 147-148]. Recently MX2 was shown to be an anti-retroviral factor that inhibits HIV-1 infection specifically and MX1 was shown to be highly specific in inhibiting influenza virus infection [149].

*Oligo-adenylate synthase OAS 1, OAS2, OAS3 and OASL:* The OAS family of genes are IFN-inducible and recognizes the presence of dsRNA. OASL is induced in response to virus infection and is an IRF3 dependent gene. The enzymatic activity of OAS results in the production of 2’-5’ oligoadenylates from ATP which polymerizes and activates the endoribonuclease RNase L to degrade viral and cellular RNA transcripts [19]. OAS genes have a role in the antiviral response against encephalomyocarditis virus (EMCV,

picornavirus) and alphaviruses like Chikungunya, Sindbis virus and Semliki forest virus. Polymorphisms in OAS gene is associated with susceptibility to flaviviruses like WNV, hepatitis C virus (HCV) and Coronavirus like SARS [150].

*RNA-activated protein kinase PKR:* PKR is a serine/threonine kinase that has N-terminal dsRNA binding domain and a C-terminal catalytic domain that is shared by eIF-2$\alpha$ kinases [151]. It is an IFN-inducible gene that binds both ssRNA and dsRNA with 5'ppp viral RNA. Viral RNA binding activates its kinase activity. Once activated PKR phosphorylates eIF2$\alpha$ to block cellular and viral protein synthesis, trigger cell death of infected cells and form stress granules (SGs) [19, 152].

There are several other antiviral genes that are induced like viperin and tetherin which prevents viral assembly and release, SAMHD1 (Sam-domain-and HD-domain containing protein 1) that depletes deoxynucleotides from the cellular pool and acts as retroviral restriction factor, ADAR1 (adenosine deaminase RNA-specific 1) and APOBEC3 (apolipoprotein B mRNA editing enzyme, catalytic polypeptide-like 3) that are adenosine and cytosine deaminases respectively that destabilize viral genomes by introducing mutations (Figure 1-7). Some of these ISGs are highly specific like tetherin or SAMHD1 to certain retroviruses whereas other ISGs like the IFIT, IFITM or OAS genes have broad spectrum antiviral effect against a wide range of viral families.

Understanding the antiviral activity of ISGs and characterizing novel ISG's is an active area of study. These studies can enable targeting ISGs that are most relevant to control specific viruses. Identifying and determining ISGs that have broad spectrum antiviral activity can facilitate development of antiviral therapies that can target a wide

range of viruses. Targeting the host innate immune genes provides an attractive alternative to treatment with direct-acting antivirals that target viral genes or viral gene products. This strategy targets the host and therefore minimizes the immune pressure on the viral genes to mutate and thus can prevent resurgence of drug resistance strains [19, 153].

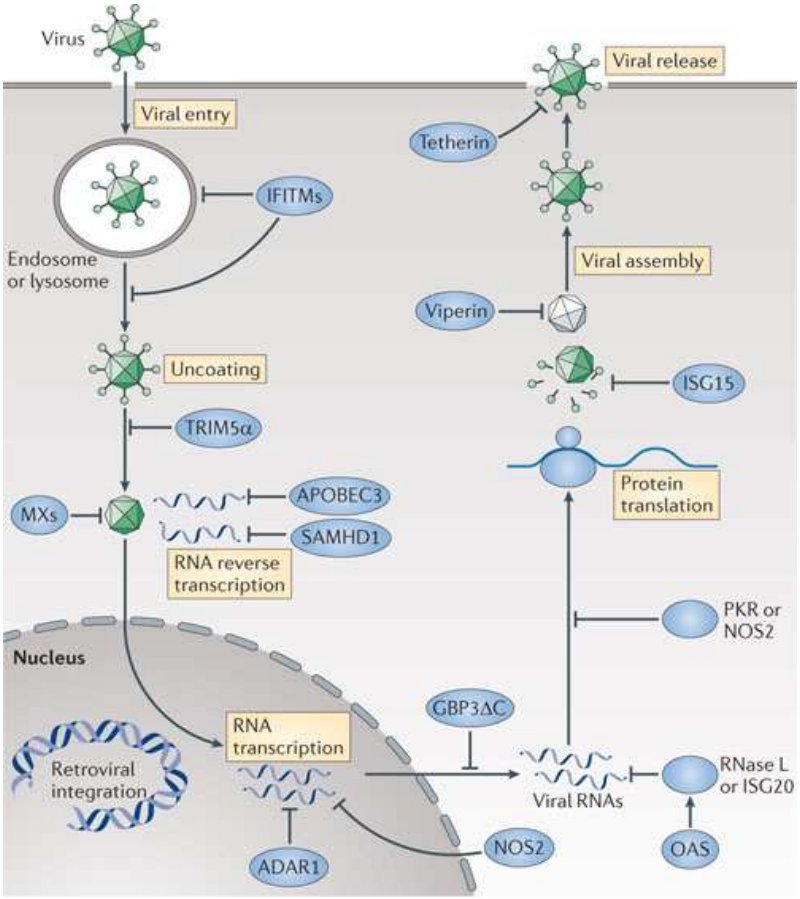


***Figure 1-7. Interferon-stimulated genes and their role in restricting viruses.*** ISGs work in multiple cell types and at different stages of the viral life cycle like entry, uncoating, replication, protein synthesis, assembly and release. Schematic shows ISGs; IFITMs, ADAR1, RNase L, PKR, MX1 etc. and their role in limiting viruses. Reproduced from MacMiking J. D., 12, 367-382, May 2012 [19].

## Viruses of the family Flaviviridae and the role of RLR signaling in restricting these viruses.

There are four main genera in the family *Flaviviridae*: *Flavivirus*, *Pestivirus, Pegivirus* and *Hepacivirus* [154]. The genus *Flavivirus* is the largest with 53 species of viruses. Some of the major human pathogens in this genus are: West Nile virus (WNV), dengue virus (DV), yellow fever virus (YF), Japanese encephalitis (JEV) and tick-borne encephalitis (TBE). All of the viruses that belong to the genus *Flavivirus* are classified as arboviruses as they are transmitted by arthropods. These viruses are transmitted through a mosquito-human transmission cycle except for WNV which is transmitted in an enzootic cycle where WNV remains in a mosquito-bird transmission cycle and humans and horses act as dead end hosts. WNV is primarily transmitted by the genus *Culex* sp. and YF by both *Aedes* sp. and *Haemogogus* sp. DV is transmitted by mosquitoes of the genus *Aedes aegypti* and to a lesser extent by *Aedes albopictus*. There has been an increase in incidence of arboviruses in recent decades [155-156]. These viruses cause a wide range of symptoms from mild fever to severe disease resulting in mortality. Vaccines that protects from severe disease are available for YF, JEV and TBE whereas human vaccines for preventing WNV and DV infections are not yet available. There are currently no chemotherapeutic agents available to treat infected people, alleviate symptoms and manage disease [157].

Hepatitis C virus is the sole species that belongs to the genus *Hepacivirus* and is a major human pathogen that in the majority of cases causes chronic hepatic disease that, unless treated with IFN therapy, can progress to hepatocellular carcinoma [158].

The genus *Pestivirus* has 4 species of viruses. These viruses are major pathogens that infect cattle and pigs. The fourth genus, *Pegivirus,* has 2 species of viruses. They are lymphotropic viruses and their pathogenicity in humans remain unknown [159-161].

The roles of RIG-I and MDA signaling in restricting *Flavivirus* and the role of RIG-I in limiting *Hepacivirus* are well established [20-21, 48, 153, 162-165]. RIG-I and MDA5 are essential PRRs that sense WNV and trigger IFN induction and ISG expression in response to WNV infection. The roles of the RLRs are well characterized in knockout murine cells and in murine model of WNV pathogenesis [20, 48, 63, 139, 166-167]. Similarly, studies on HCV detection, characterization of HCV PAMP (poly-U/UC) that can drive RIG-I specific signaling and HCV antagonism of the RIG-I pathway through the cleavage of MAVS has established the importance of RIG-I signaling in restricting HCV infections [12, 24, 49].

## Disease caused by viruses that belong to the Family Flaviviridae

### West Nile virus, disease, symptoms and current treatments.

WNV is classified into two distinct lineages based on the geographic distribution and severity of disease in humans. Lineage I viruses are the emerging viruses that cause outbreak of encephalitis and meningitis in Europe, North America and Middle East [168-169]. Lineage II viruses are non-emerging strains that are less virulent and remain geographically distinct to parts of Southern Africa, Madagascar and Cyprus [160].

West Nile virus is the least virulent of the genus *Flavivirus*. Many of the West Nile virus infected patients remain asymptomatic. One-fifth of those infected turn symptomatic with fever, headache, body ache, joint pain, vomiting, diarrhea or rash and about 1% of those have neurologic symptoms that can include headache, high fever, neck stiffness, disorientation, coma, tremors, seizures, or paralysis [170]. West Nile virus (WNV) infections were on the decline from 2008-2011 but saw a sudden increase in incidence in 2012. Among 5674 WNV disease cases as of december 2012, 2873 (51%) of the cases were neuro-invasive disease, resulting in 270 (9%) deaths [171] (CDC, 2012). There are currently no vaccines or antivirals available for treating symptomatic patients. Over-the-counter pain medication is given to provide relief from febrile symptoms. In very severe cases, patients are hospitalized and receive supportive treatment like intravenous fluids, pain medications and nursing care [157, 172].

**Dengue virus, disease, symptoms and current treatments.**

About 40% of the world's population are at risk from dengue (DV) and WHO reports an incidence of 50-100 million new cases of DV yearly including 500,000 dengue hemorrhagic fever (DHF) cases and 22,000 deaths, mostly among children [173]. DV comprises of five genetically related serotypes (DV 1-5) [174-175]. The disease symptoms can vary and can present as dengue fever (DF), Dengue shock syndrome (DSS) or dengue hemorrhagic fever (DHF). The primary symptoms of dengue fever are high fever, retro-orbital headache, arthralgia, myalgia, malaise, nausea and vomiting (CDC). DSS and DHF occur during secondary infection and are

characterized by very severe symptoms leading to death in 2.5% of the patients (WHO, 2012). In dengue hemorrhagic fever, the febrile phase lasts for 2-7 days, followed by a critical phase of 24-48 hours, during which capillaries become extremely permeable and fluid leaks from the blood vessels into the peritoneum or pleural cavity. This can result in low platelet counts, hemorrhage, internal bleeding, shock or death, unless supportive care is provided (WHO). There are no antivirals or vaccines available to treat or prevent dengue virus infection. Over-the-counter analgesics can help relieve pain and febrile symptoms. DHF patients have to be hospitalized and given fluid replacement therapy to prevent death [157, 175-176]. The five different serotypes and the antibody-dependent enhancement (ADE) (ADE is defined as non-neutralizing antibodies to one serotype which facilitates increased uptake of virus when infected with a different serotype and results in higher viremia) seen during secondary infection with a different serotype complicates treatment and has delayed vaccine development [174-175]

**Hepatitis C virus, disease, symptoms and current treatments.**

Hepatitis C virus is a blood borne pathogen that belongs to the family *Flaviviridae*, genus: *Hepacivirus*. There are 3-4 million new cases of hepatitis C virus (HCV) each year and about 150 million people are chronically infected with HCV and are at risk of developing liver cirrhosis or liver cancer. About 350,000 people die from HCV-related liver disease each year (CDC) [177]. The mainstay of treatment has been pegylated interferon and ribavirin for 24-48 weeks [158]. Sequence analysis of HCV divides the virus into 6 genotypes depending on the geographic distribution and

response to standard therapy with pegylated IFN-α and ribavirin [178]. Genotype 1 is the most prevalent in North America and is most resistant to the IFN therapy. Approximately 50% of the treated patients reach sustained virologic response which is defined as undetectable virus for at least 24 weeks after the end of treatment [179]. The addition of protease inhibitors to the standard IFN therapy has helped genotype 1 infected patients achieve better outcomes. With the development of NS5A and NS3 protease inhibitors, NS5B nucleoside and non-nucleoside inhibitors [180], the control of HCV seems to be an achievable goal in the next decade with combination drug therapy [164, 180].

HCV subverts the RIG-I pathway through cleavage of MAVS, a central signaling adapter that is essential for the interferon response [24, 162, 164]. WNV and DV antagonize the IFNAR signaling pathway as a way to establish infection [86, 153, 166, 175]. These viruses are highly sensitive to the IFN response and the viruses have evolved elaborate mechanisms to evade and antagonize the IFN pathway [129, 181-182]. This clearly attests to the efficiency with which induction of ISGs restricts viruses of the family *Flaviviridae*. The importance of the RLR pathway in controlling viruses that belong to the family Flaviviridae offers alternative methods to control these viruses. Developing agonists that drive the RLR signaling pathway to establish an antiviral state through the induction of innate immune genes offers an attractive alternative to conventional therapies. DAA that interfere with the viral life cycle and target viral gene products are well characterized and are widely used as therapeutic intervention strategies [183]. This approach, though highly effective and specific, has disadvantages. Viral drug resistance is still a major concern as RNA viruses have inherently unstable

genomes that rapidly mutate, creating quasispecies, and the immune pressure created by DAA on viral genes promotes viral escape through resistance mutations. This creates a problem for long-term use of DAA, as the mutations accumulated by the viral genomes eventually render DAA ineffective. The lack of vaccines and antivirals for WNV and DV and the concern about drug resistance strains that could arise from prolonged use of direct-acting antivirals (DAA) to clear HCV infection creates a real-time pandemic in need of alternative therapies and treatment regimens to control viruses of the family Flaviviridae [180].

## Chapter 2. DHX15 is a PRR that binds RIG-I like receptors and is a positive regulator of antiviral defense against RNA virus infections.

### Introduction

RIG-I and MDA5 are intracellular sensors that recognize and define viral RNA as non-self in an infected cell. They signal the host immune response to establish an antiviral program that limits and controls infection, and therefore play essential roles in controlling innate immunity. In the case of RIG-I, engagement of viral pathogen-associated molecular pattern (PAMP) RNA harboring a 5'-triphosphate with double-stranded (ds)RNA structure or polyuridine-rich single-stranded (ss)RNA sequence interspersed with cytosine bases (poly-U/UC) [40, 50, 165] induces RIG-I to hydrolyze ATP and assume an open, signaling competent conformation that permits its recruitment to the MAVS adaptor protein on the mitochondria-associated membranes (MAM) [28, 36, 71, 101]. RLR association with MAVS through their respective caspase activation and recruitment domains (CARDs) licenses the recruitment of signaling cofactors to MAVS and activation of key transcription factors including IRF3/7 and NF-κB that lead to the expression of antiviral genes, pro-inflammatory cytokines and chemokines that coordinately function to limit virus infection. These key steps that occur within minutes after viral RNA recognition defines the quality of the innate immune responses that in turn directs the development of adaptive immunity and the clearance of infection. RLR-dependent signaling to the innate immune response is critical for antiviral immunity, and when dysregulated can lead to inflammatory diseases [1-5, 11].

RIG-I is a DExD/H helicase that belong to the SF2 helicase super family and

functions as a molecular motor driven by ATP hydrolysis to engage and walk along a RNA ligand. This process supports scanning of RNA by RIG-I to identify PAMP motifs [184]. By this model, upon encountering a PAMP motif, RIG-I switches to its active conformation, and cofactors can then interact with MAVS to induce downstream signaling of innate immunity. There is increasing evidence supporting the involvement of non-RLR DExD/H helicases in regulating innate immune signaling pathways in controlling RNA and DNA virus infections. DDX3, DHX9, DHX29, DHX36, DDX60, DDX24 have been shown to regulate the RLR pathway [89, 122, 124, 126, 128, 185]. These observations indicate that non-RLR DExD/H box helicases can serve as cofactors in innate immune and inflammatory signaling programs. Moreover, a variety of proteins have been identified as RLR binding and signaling cofactors, revealing that cofactor activity is essential for RLR signaling [15, 36, 70, 186].

The current study focuses on identifying and characterizing novel regulators of RIG-I signaling. For this purpose, a proteomic analysis was carried out to identify factors that associate with constitutively active RIG-I mutant protein consisting of the tandem CARDs (N-RIG) [9, 12]. This screen identified DHX15 as a novel DExD/H box helicase that binds RIG-I and MDA5 to serve as an essential cofactor of RLR signaling. Mosallanejad et al. reported the identification of DHX15 as an activator of mitogen-activated kinase (MAPK) signaling in a gene misexpression screen with *Drosophila melanogaster* [187]. They found that DHX15 is required for poly (I:C)-dependent induction of NF-κB and MAPK transcriptional activities. Cells lacking DHX15 expression were defective in IFNβ, IL-6, TNFα and CxCl10 secretion and MAVS-mediated Caspase 3 activation in response to transfection of the dsRNA mimetic, poly (I:C), and showed

corresponding greater susceptibility to Sendai virus (SenV) and encephalomyocarditis virus (EMCV) infection. Lu et al. also identified DHX15 as a component of a protein complex bound to poly (I:C) within mouse cell extracts[188] In these studies, shRNA knockdown of DHX15 in the murine myeloid dendritic cell line D2SC resulted in defects in IFNβ, IL-6 and TNFα production in response to poly (I:C) transfection but not a synthetic dsDNA, and also in response to SenV and reovirus infection but not the DNA virus herpes simplex virus-1. Moreover, DHX15-deficient cells were shown to be defective in poly (I:C)-induced MAVS aggregation, and to reovirus activation of MAPK and transcription factors, IRF3 and NF-κB, thus implicating DHX15 in RLR-dependent antiviral signaling. This study is a third technically distinct screen that now identifies DHX15 as a cofactor of RLR signaling in human cells. This work demonstrates the essential roles for DHX15 in RLR-dependent signaling to the innate immune system in response to infection by a range of RNA virus genera in human cells. Importantly, this study is unique as it demonstrates DHX15 is a pathogen recognition receptor and signaling cofactor that associates with RIG-I and MDA5 to promote non-self RNA recognition and innate immune signaling.

## Materials and Methods

**Cell lines and viruses.** Huh7 (human hepatocyte) and HEK293 (human embryonic kidney epithelial) cell lines were cultured in Dulbecco's modified Eagle's medium (Cellgro) supplemented with 10% fetal bovine serum (FBS, HyClone), L-glutamine, sodium pyruvate and non-essential amino acids. THP-1 (human monocytic) cell line

was cultured in complete RPMI (invitrogen) supplemented with 10% heat-inactivated FBS, L-glutamine, sodium pyruvate and non-essential amino acids. THP-1 cells were differentiated into macrophage-like cells by culturing cells in complete RPMI media supplemented with 40 nM phorbol myristate acetate (PMA). Sendai virus (SenV, cantell strain) stocks were purchased from Charles River Laboratories. Encephalomyocarditis virus (EMCV) and vesicular stomatitis virus (VSV) have been described before and were titered by standard plaque assay on Vero cells [9]. Cells were inoculated with virus in serum free media at a multiplicity of infection (MOI) of 0.01 for EMCV or VSV and a concentration of SenV that ranged between 50-200 HAU/mL. Lentivirus particles for creating knockdown cells were purchased from the Sigma-Aldrich MISSION shRNA collection and express the following shRNA sequences: DHX15 (CCGGGTTGGTTCGATAATGGCCTTTCTCGAGAAAGGCCATTATCGAACCAACTTTTT, catalog# TRCN0000000006), MAVS (CCGGCAAGTTGCCAACTAGCTCAAACTCGAGTTTGAGCTAGTTGGCAACTTGTTTTTTG, catalog# TRCN0000148945), and the non-targeting shRNA control (NTV; CCGGCAACAAGATGAAGAGCACCAACTCGAGTTGGTGCTCTTCATCTTGTTGTTTTT, catalog# SHC002).

**Plasmids.** RIG-I, MDA5, MAVS, TBK1, IKKε, IRF3 expression constructs have been described [12, 21]. MAVS mutants lacking the N-terminal CARD (ΔCARD), the C-terminal transmembrane domain ΔTM, or both (ΔTMΔCARD) were created by using the Quikchange site-directed mutagenesis kit (Stratagene). DHX15 cDNA (Origene RC205914) was cloned into destination vector pCMV6 (Origene, PC00003, PC00005, PC00012, PC00014) for expression as N-terminally FLAG- or myc-tagged proteins.

DHX15 truncation and point mutants were created by using the Quikchange II XL lightning site-directed mutagenesis kit (Agilent technologies). Primer sequences are available upon request. Promoter luciferase reporter plasmids pIFNβ-luc, pIFIT1-luc and pCMV-*Renilla*-luc have been previously reported [189-190].

**Antibodies.** The following primary antibodies were used for immunoblot detection: Rabbit anti-RIG-I (969, raised in rabbit against a RIG-I CARD peptide sequence) [36], rabbit anti-MAVS (AT107, Enzo Life Sciences), rabbit anti-MDA5 ( AT113, Enzo Life Sciences), rabbit anti-DHX15 (AB70454, Abcam), rabbit anti-myc (AB9106, Abcam), and HRP-conjugated mouse anti-FLAG (A8592, Sigma). Monoclonal antibodies used for immunoprecipitation include: mouse anti-RIG-I (Alme-1, adipogen), mouse anti-MAVS IgG2b (Enzo Life Sciences), mouse anti-DDX15 IgG2a (E-6, Santa Cruz Biotechnology), mouse anti-FLAG M2 IgG1 (F3165, Sigma) and mouse anti-c-myc (9E10, Santa Cruz Biotechnology). HRP-conjugated secondary antibodies were obtained from Jackson ImmunoResearch.

**Real-time PCR (RT-PCR).** Cells were harvested in RLT buffer at the indicated times and total cellular RNA was purified using the RNeasy Mini kit (Qiagen). Total cDNA was synthesized from purified RNA using a combination of random oligo and oligo (dT) primers and the iScript cDNA synthesis kit (Bio-rad). Host and viral RNA levels were determined using SYBR Green (Applied Biosystems) and the 7300 RT-PCR system (Applied Biosystems). The relative expression level of host and viral genes were calculated as fold change over mock-infected controls, normalized to GAPDH using the

ΔΔCT method. RT-PCR primer sequences are listed in table 1 with the exception of the IL-6 primers, which were obtained from SA Biosciences.

| Primer | 5'-Sequence-3' |
|---|---|
| IFN-β F | AGTGTCAGAAGCTCCTGTGGC |
| IFN-β R | TGAGGCAGTATTCAAGCCTCC |
| IL-1β F | ATGATGGCTTATTACAGTGGCAA |
| IL-1β R | GTCGGAGATTCGTAGCTGGA |
| TNF-α F | GAGGCCAAGCCCTGGTATG |
| TNF-α R | CGGGCCGATTGATCTCAGC |
| MX1 F | GGTGGTCCCCAGTAATGTGG |
| MX1 R | CGTCAAGATTCCGATGGTCCT |
| IFIT1 F | GCGCTGGGTATGCGATCTC |
| IFIT1 R | CAGCCTGCCTTAGGGGAAG |
| RIG-I F | TGTGCTCCTACAGGTTGTGGA |
| RIG-I R | CACTGGGATCTGATTCGCAAAA |
| MAVS F | ATGCCGTTTGCTGAAGACAAG |
| MAVS R | AGGGCAGGTAAGGCAGAATCT |
| IFIT2 F | CACATGGGCCGACTCTCA |
| IFIT2 R | CCACACTTTAACCGTGTCCAC |
| GAPDH F | GAAGGTGAAGGTCGGAGT |
| GAPDH R | GAAGATGGTGATGGGATTTC |
| SenV F | GACGCGAGTTATGTGTTTGC |
| SenV R | TTCCACGCTCTCTTGGATCT |

**Table 2-1. Real-time PCR primer sequences used in gene expression studies**

**Measuring infectious virus particles.** Huh7 and HEK293 cells were infected at an MOI of 0.01 with EMCV for 18 hours or VSV for 12 hours. Cell culture supernatant was

collected at the indicated time points post-infection. Infectious viral particles in the supernatant were measured by standard plaque assay with agar overlay on Vero cells. Plaques were stained with neutral red and counted 24 hours after infection.

**Immunoprecipitation and immunoblot analyses.** Cell lysates were collected in RIPA buffer (50 mM Tris-Cl pH 7.5, 150 mM NaCl, 5mM EDTA, 1% NP-40, 0.5% sodium deoxycholate, 0.1% SDS) supplemented with a mammalian protease inhibitor cocktail (Sigma-Aldrich), phosphatase inhibitor cocktail (Calbiochem) and okadaic acid and clarified by centrifugation at 15,000 x g for 10 minutes at 4 ℃. Cell lysates were quantified by BCA (Thermo Scientific) and a standard amount of protein taken across samples for each immunoprecipitation. Immunoprecipitations were performed using the antibody of choice and Protein G Dynabeads (GE Life Sciences) in RIPA buffer. Beads were washed three to five times with RIPA buffer before the proteins were eluted in SDS-PAGE sample buffer. Proteins were detected by immunoblot analyses and visualized using the ECL prime substrate (GE life sciences)**.**

**Immunoprecipitation and mass spectrometry.** The FLAG-tagged N-terminus of RIG-I (N-RIG) was overexpressed in HEK293 cells and immunoprecipitated with anti-FLAG M2 antibody. The eluted proteins were trypsin-digested and separated on an nano-HPLC using a 5 cm Magic C18 Column (Michrom Bioresources, Auburn, CA) using a buffer system of (A) water + 0.1% formate and (B) acetonitrile + 0.1% formate (Avantor Performance Materials, Phillipsburg, NJ) in a 60 min gradient from 98% A/2% B to 5% A/95% B. The peptides were analyzed on a linear ion trap mass spectrometer (LTQ, Thermo Fisher Scientific) based on their mass to charge ratio and the peptide sequence

was determined. The predicted sequence was searched against human IPI v3.28 database using SEQUEST to identify and match sequences present in the database. The results of these searches were analyzed using PeptideProphet [191] and ProteinProphet [192]. Proteins with at least 2 unique peptides or more and a probability score of 0.99-1 were considered positive hits [36].

**ATPase assay.** DHX15 recombinant protein was expressed in *Escherichia coli* using expression vector E3 and purified from inclusion bodies to approximately 95% purity as estimated by densitometric analysis of the Coomassie blue-stained SDS-PAGE gel (GenScript). RIG-I recombinant protein was a gift from Joe Marcotrigiano and was previously described [49-50]. The synthetic dsRNA poly (I:C) was purchased from Invivogen. The hepatitis C virus xRNA and poly-U/UC RNA were in vitro transcribed from synthetic DNA oligonucleotide templates (Integrated DNA Technologies) using the T7 MEGAshortscript kit (Ambion) and the ATPase assays were performed as previously described [50] . Briefly, various amounts of RNA (0-1 pmol) were mixed with 5 pmol purified DHX15 or RIG-I protein in a total of 25 uL ATPase reaction buffer (20mM Tris-HCl pH 8.0, 1.5 mM $MgCl_2$, 1.5 mM DTT). Reactions were incubated at 37℃ for 15 minutes, ATP (Sigma) was added to a final concentration of 1 mM, and the reactions incubated at 37℃ for 15 minutes. Absorbance of eac h sample in BIOMOL Green reagent (Enzo Life Sciences) was measured at $OD_{630nm}$ in microplate format and the free phosphate concentration calculated based on the standard curve.

***In vitro* binding RNA ELISA.** RIG-I alone, DHX15 alone or RIG-I and DHX15 mixed together (3 pmol) were coated on nunc plates in 50 mM tris pH 7.5, 150 mM NaCl, 1

mM DTT for 2 hours at room temperature. The plates were blocked with 5% BSA in tris-buffered tween 20 (0.1%) for 1 hour. Plates were washed in PBS tween 20 (0.1%). Following the wash, increasing picomoles of biotinylated poly (I:C) (Invivogen) or xRNA (5-0 pmol) diluted in water containing RNAase inhibitor (1:300) (Ambion) were added to the plate and incubated for 1.5 to 2 hour. The plates were washed before addition of a horse radish peroxidase labeled neutravidin antibody (Thermo scientific, 1:10,000) for 1 hour. TMB substrate was added and incubated for 5 minutes. The enzyme reaction was stopped with acid and the absorbance was measured at OD 450nm and 570 nm in microplate format. The $OD_{450nm}$ 450 nm was plotted as a function of picomoles of RNA to assess binding of RNA to protein.

**Filter binding assay.** Various amounts of RNA(0-4 pool), hepatitis C virus xRNA or poly-U/UC RNA were mixed with 5 picomoles of purified DHX15 protein or alternatively fixed concentrations of RNA were mixed with increasing concentrations of DHX15 protein (0-10 pmol) in a total of 25uL reaction buffer (20mM Tris-HCl pH 8.0, 1.5mM $MgCl_2$, 1.5mM DTT). Reactions were incubated at 37℃ for 15 minutes and spotted on pre-wet nitrocellulose membrane assembled on a Bio-dot SF microfiltration apparatus (Bio-rad) according to manufacturer's instructions. The membrane was washed, blocked with Licor blocking buffer (Licor, 927-40100) and incubated with streptavidin 800 (1:10,000, Licor, 926-32230) for 1 hour and then the fluorescence intensity read on Licor odyssey CLx.

**Statistical analysis.** All statistical analyses were performed using the GraphPad Prism 5.0. software using 2-way ANOVA with Bonferroni post-tests or one-way ANOVA

analysis. The interaction between cell types (DHX15, RIG-I, MAVS, NTV stable knockdown cells) at different time points or multiplicity of infection were compared. The RNA binding and ATPase analysis were evaluated by linear regression analysis. GraphPad Prism was used to compare slopes of two or more regression lines to test whether the slopes were significantly different.

## Results

**DHX15 is a RIG-I binding protein.** To identify signaling cofactors that associate with RIG-I, an approach combining immunoprecipitation and proteomics approach was used. For this purpose, a FLAG-tagged RIG-I construct consisting entirely of the two N-terminal tandem CARDs (N-RIG) that mediates constitutive signaling through MAVS was ectopically expressed in HEK293 cells. Proteins that associate with the activated RIG-I-MAVS complex were recovered through FLAG-N-RIG immunoprecipitation and identified by mass spectrometry. In this way, a total of 244 cellular factors were identified with a probability score of 0.99 or greater. The score is based on the probability that the peptides from a sample reliably match those in the protein database [193]. Elimination of factors that were present in control immunoprecipitations (using a construct expressing 2x FLAG alone) then revealed potential RIG-I cofactors. Among the identified proteins were several proteins known to associate with and regulate RLR signaling including DDX3X, ISG15 and DDX58 (Table 2-2). Another RIG-I binding protein was identified as a novel DExD/H helicase, DHX15. While this report was in final preparation Mosallanejad et al. identified DHX15 interacted with MAVS and was an

activator of NF-κB and MAP kinase pathways, but its role in RIG-I signaling was not evaluated [187].

To determine if DHX15 is involved in RLR signaling, we assessed whether cells lacking DHX15 retain RLR signaling and induce IFNβ promoter activity during virus infection of human cells. For this purpose, we created stable Huh7 and THP-1 cell lines harboring short hairpin RNA (shRNA) to knock down DHX15 expression. RNA expression analysis showed 50-60% knockdown of DHX15 (Figure 2-1A). Using similar methods, we also created cell lines with 80% and 50% knockdown of MAVS or RIG-I expression, respectively. As a control, we created a cell line that stably expressed a non-targeting shRNA (non-targeting vector, NTV) that will activate the RNAi pathway but does not target any human or mouse genes (Sigma-Aldrich MISSION Lentiviral control). Infection of the NTV control cells with SenV (a paramyxovirus that potently triggers RIG-I signaling) resulted in robust induction of the IFNβ promoter as compared to mock-infected cells in luciferase-reporter assays (Figure 2-1B). In contrast, SenV infection of cells with knockdown of DHX15 or MAVS resulted in little or no induction of the IFNβ promoter. Thus, DHX15 supports SenV-induced RIG-I-dependent signaling to the IFNβ promoter. DHX15 expression in the shRNA knockdown cells was reconstituted using a DHX15 construct that cannot be targeted by the shRNA. Reconstitution of DHX15 expression in these cells restored SenV-induced RIG-I-dependent signaling to the IFNβ promoter (Figure 2-1C), confirming that DHX15 is required for RIG-I signaling triggered by SenV infection.

| Protein | protein probability | No. unique peptides | Entrez No. | Entrez name | Reference |
|---|---|---|---|---|---|
| DEAH_(Asp-Glu-Ala-His)_box_polypeptide_15 | 1 | 3 | 1665 | DHX15 | |
| ATP-dependent_RNA_helicase_DDX3X | 1 | 3 | 1654 | DDX3X | Oshiumi H, 2010 |
| Interferon-induced_17_kDa_protein_precursor | 0.99 | 1 | 9636 | ISG15 | Krug R. M., 2005 |
| ATP-dependent_RNA_helicase_DDX58 | 1 | 3 | 23586 | DDX58 | Saito T., 2007 |

**Table 2-2. DHX15 associates with a signaling complex that co-precipitates with a constitutively active RIG-I mutant.** A FLAG-tagged RIG-I construct that consists of only the tandem CARDs (aa1-228, N-RIG) and is signaling-competent was over-expressed in HEK293 cells. Proteins that associate with N-RIG were enriched by FLAG immunoprecipitation and identified by LC-MS/MS.

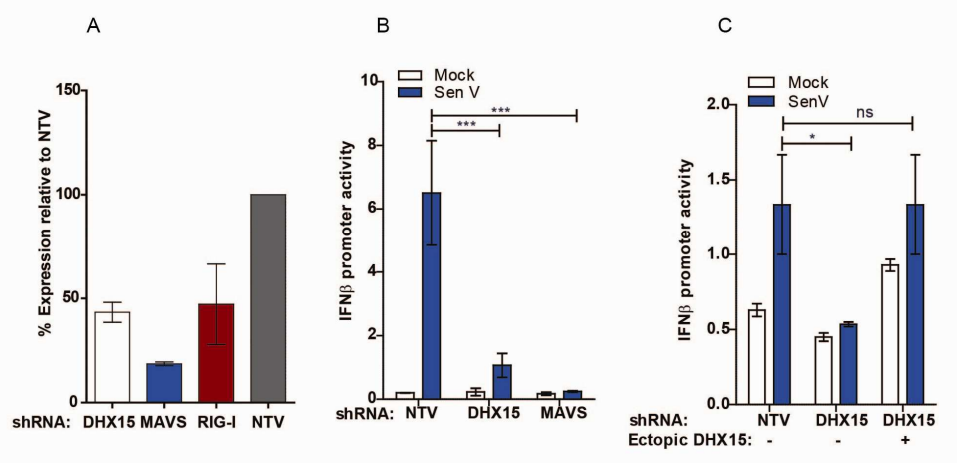


***Figure 2-1. DHX15 is a positive regulator of interferon induction.*** (A) The relative gene expression levels (%) of the genes DHX15, MAVS and RIG-I in Huh 7 or THP-1 cells that stably express shRNA to DHX15, MAVS, RIG-I or a control sequence not found in human or mouse cells (non-targeting vector, NTV) as measured by RT-PCR analysis. (B) Huh7 knockdown cells that stably express shRNA to DHX15, MAVS or NTV were co-transfected with an IFNβ promoter-driven firefly luciferase reporter plasmid and a CMV promoter-driven *Renilla* luciferase reporter plasmid. Cells were either mock-infected or infected with SenV for 24 hrs and analyzed for dual luciferase activity. The results are expressed as relative luciferase activity showing average ratio firefly over *Renilla* from two independent experiments. Error bars represent standard deviations calculated from two independent experiments. 2-way ANOVA with Bonferroni post-test show the P value to be ***< 0.001. (C) Huh7 knockdown cells were co-transfected with

an IFNβ promoter-driven firefly luciferase reporter plasmid, a CMV promoter-driven *Renilla* luciferase reporter plasmid and either a vector-control plasmid or a plasmid that ectopically-expressed DHX15. Cells were mock-infected or infected with SenV for 24 hours and then analyzed for dual luciferase activity. The results are expressed as relative luciferase activity showing average ratio firefly over *Renilla* from a representative experiment out of 3. Error bars represent standard deviations. 2-way ANOVA with Bonferroni post-test show the P value to be *< 0.05, ns = not significant.

**DHX15 is not required for cellular response to type I IFN.** To define DHX15's role in RLR signaling, the knockdown cells were assessed for their ability to respond to type I IFN. For this purpose, the control NTV cells and cells lacking DHX15 were tested for induction of IFIT1 promoter activation (Figure 2-2A) after treatment with 100 IU/ml of IFNβ. IFIT1 is an innate immune response gene whose expression is potently induced by RLR signaling of IRF3 activation or upon cell exposure to type I IFNs [135]. These data indicate that cells lacking DHX15 expression retain the ability to induce IFIT1 promoter activation similar to NTV cells upon treatment with IFN, indicating that DHX15 is not required for the type I IFN response. Furthermore, DHX15 is not itself an interferon-stimulated gene (ISG) because we found that the expression level of DHX15 remains relatively unchanged in cells after treatment with 100 IU/ml of IFNβ under conditions when the IFIT1 mRNA is expressed more than 1000-fold over non-treated cells (Figure 2-2B). These studies show that ectopic expression of DHX15 by itself can drive IFNβ promoter induction (Figure 2-2C) and correspondingly drive the expression of IFNβ mRNA. RT-PCR analysis shows that overexpression of DHX15 triggers IFNβ mRNA levels to be 5-fold higher levels compared to cells expressing vector construct alone (Figure 2-2D). Taken together, this set of data suggests that DHX15 functions

upstream of the type I IFN receptor and within a virus-responsive innate immune signaling cascade that drives IFN induction.

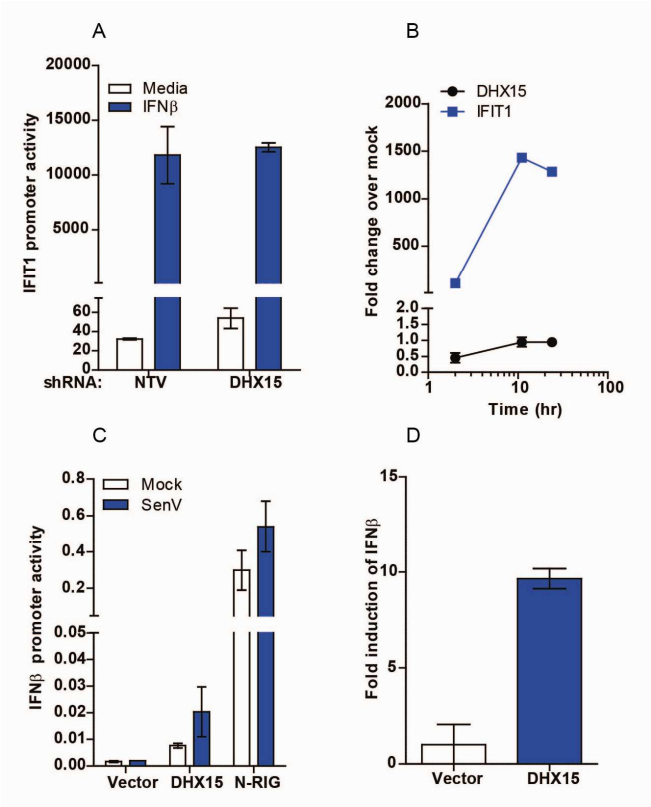


***Figure 2-2. DHX15 expression regulates IFN signaling.*** (A) Huh7 knockdown cells were co-transfected with an ISG56/IFIT1 promoter-driven firefly and CMV promoter-driven *Renilla* luciferase reporter plasmids. Cells were mock-treated or treated with exogenous IFNβ in the media for 24 hours and analyzed for dual luciferase activity. Results are expressed as relative luciferase activity (average ratio firefly over *Renilla*) from a representative experiment out of 4. Error bars represent standard deviations. (B) Huh7 cells were treated with IFNβ (100 IU/ml). Cells were collected at 2, 12 or 24 hours and the relative expression of the ISG56/IFIT1 and DHX15 genes were measured by RT-PCR, normalized to GAPDH and expressed as fold-induction over the mock-treated control. The results are from a representative experiment out of 2 and error bars represent standard deviation. (C) HEK293 cells were co-transfected with the IFNβ promoter-driven firefly and CMV promoter-driven *Renilla* luciferase reporter plasmids along with either a control vector or a plasmid that permitted ectopic expression of a FLAG-tagged DHX15. Cells were collected 24 hours post-transfection and measured for dual luciferase activity. Data represents relative luciferase activity and error bars represent standard deviations from a representative experiment out of 2. (D) HEK293 cells were co-transfected with either a control vector or a plasmid that expressed a

FLAG-tagged DHX15. At 24 hrs post-transfection, IFNβ gene expression in total cellular RNA was measured by RT-PCR, normalized to GAPDH and expressed as fold-induction over the vector transfection.

**DHX15 is required to signal the innate immune response to virus infection.** To define the processes of innate immune signaling that are subject to DHX15 control, the expression of a variety of known RLR signaling-responsive genes of innate immunity in NTV control cells or cells with knockdown of DHX15, MAVS or RIG-I over a time course of SenV infection was measured. Huh7 cells (human hepatoma) and THP-1 (human monocyte/macrophage) cells lacking DHX15 expression exhibited a severe defect in SenV-induced signaling that translated to delayed and/or abrogated expression of IRF3-responsive genes and ISGs including IFIT1, IFIT2, MX1 and RIG-I, IFNβ, and NF-κB-responsive pro-inflammatory cytokines IL-1β, TNFα and IL-6 (Figures 2-3A and 2-3B). A similar outcome was observed in cells with reduced MAVS or RIG-I expression. Correspondingly, cells lacking DHX15 or MAVS/RIG-I expression were increasingly susceptible to SenV infection and supported increased viral RNA load compared to NTV control cells (Figure 2-3C). The signaling defect observed in DHX15 and MAVS knockdown cells also correlated with reduced IFIT1 protein levels following SenV infection (Figure 2-3D). Thus, DHX15 is a signaling cofactor of RIG-I that imparts induction of IFN-β and onset of innate immune defenses to control RNA virus infections.

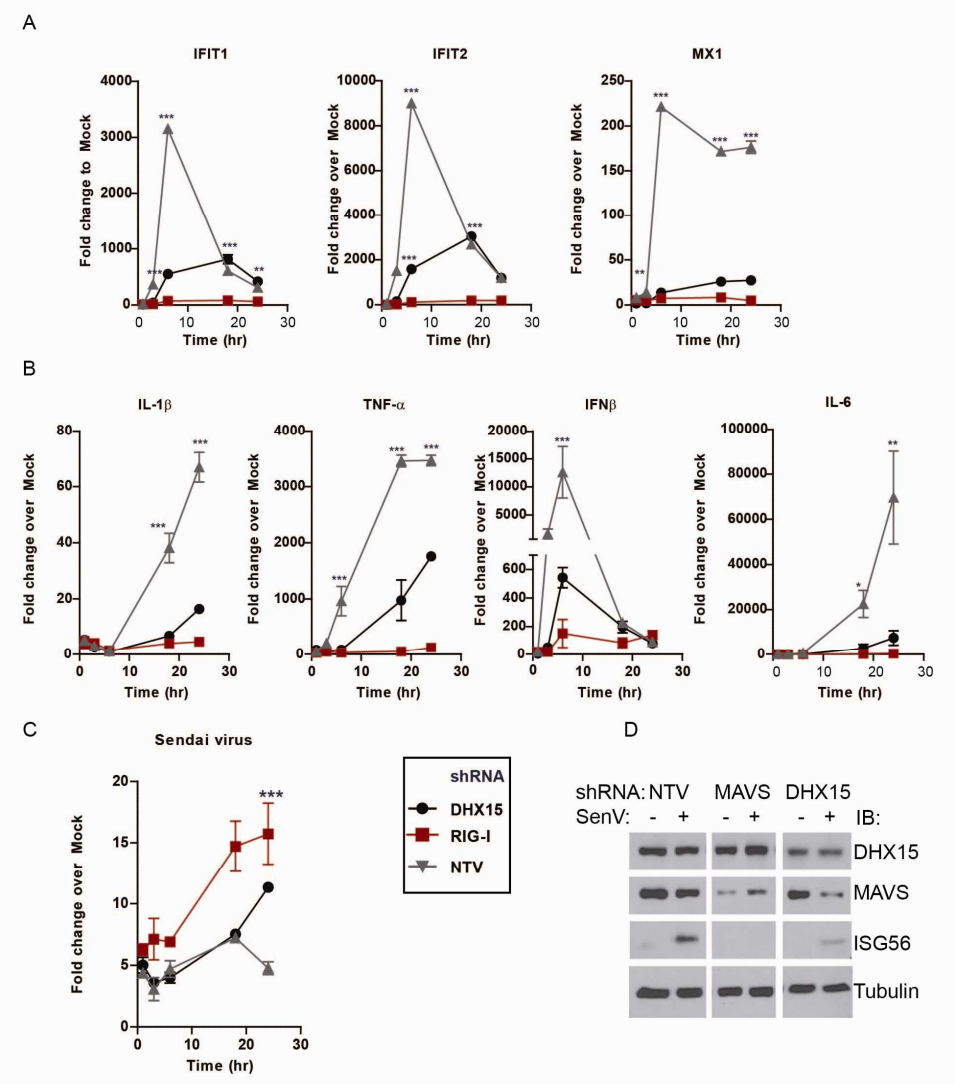


***Figure 2-3. DHX15 regulates innate immune and inflammatory gene expression in response to RNA virus infection.*** PMA-differentiated macrophage-like THP-1 knockdown cells were mock-infected or infected with SenV. Total cellular RNA were collected at 0, 1, 3, 6, 18 and 24 hours post-infection. (A) The expression of innate immune genes ISG56/IFIT1, IFIT2, and MX1 were measured by RT-PCR, normalized to GAPDH and expressed as fold-induction over the mock-infected control. Results shown are from a representative experiment out of 3 and error bars represent standard deviation. 2-way ANOVA with Bonferroni post-tests show the P value to be *< 0.05, ** < 0.01, *** < 0.001. (B) The type I IFN and proinflammatory cytokine expression of IFNβ, IL-1β, TNF-α and IL-6 genes were measured by RT-PCR, normalized to GAPDH and expressed as fold-induction over the mock-infected control. Results shown are from a representative experiment out of 3 and error bars represent standard deviation. 2-way ANOVA with Bonferroni post-test show the P value to be *< 0.05, ** < 0.01, *** < 0.001. (C) Huh7 knockdown cells were mock-infected or infected with SenV and total cellular RNA

collected at 0, 6, 12, 18, 24 hours post-infection analyzed for SenV genomic RNA by RT-PCR, normalized to GAPDH and expressed as fold-induction over the mock-infected control. Two-way ANOVA with Bonferroni post-tests show the P value to be *** < 0.001 (D) Huh7 knockdown cells were mock-infected or infected with SenV for 24 hrs and analyzed by SDS-PAGE. ISG56/IFIT1, MAVS and DHX15 expression relative to tubulin was determined by western blot using respective antibodies.

**DHX15 is a component of the RLR-MAVS signaling complex.** Co-immunoprecipitation studies were done to define DHX15 interactions with components of RLR signaling. As shown in Figure 2-4A, myc-tagged DHX15 forms a stable complex with FLAG-RIG-I when co-expressed in human cells, showing that DHX15 can interact with full length RIG-I. To determine if the interaction between RIG-I and DHX15 can be enhanced by RLR signaling activation, endogenous immunoprecipitation studies were done with lysates that were mock-infected or infected with SenV to activate RIG-I signaling (Figure 2-4B). In this study, RIG-I is not associated with DHX15 in resting cells when RIG-I is in its signaling-off state [29-30]. In resting cells, the RLRs are expressed at low levels but are induced to high level expression upon virus infection or interferon treatment [7-9]. The lack of interaction in the endogenous immunoprecipitation experiments from mock-infected cells could be due to the low expression levels of RIG-I in uninfected cells (Figure 2-4A). In contrast, abundant RIG-I was in a stable complex with DHX15 after SenV virus infection wherein RIG-I is in a signaling-on and active state (37), indicating that the DHX15/RIG-I interaction can be enhanced by RIG-I activation. Notably, the immunoprecipitation studies identified the presence of MAVS within this RIG-I-DHX15 complex after virus infection, suggesting a three-way interaction between RIG-I, DHX15 and MAVS in a manner driven by RIG-I signaling activation.

To determine whether DHX15 can also associate with MDA5 and/or MAVS in similar manner to RIG-I, the interaction of FLAG-DHX15 was tested with myc-RIG-I, myc-MDA5 or myc-MAVS in the presence or absence of SenV infection. DHX15 binds MDA5 when co-expressed regardless of virus infection (Figure 2-4C). Previous studies have shown that MDA5 is subject to less stringent auto-regulation than RIG-I such that ectopic expression of MDA5 can drive signaling activation independently of virus infection [9, 63], consistent with DHX15 association to signaling-active MDA5. Similarly, MAVS ectopic expression in cells can drive innate immune signaling regardless of virus infection [24, 26-27]. DHX15 can interact with MAVS when the proteins are co-expressed (Figure 2-4C). Thus, DHX15 is an RLR binding protein that interacts with signaling-competent RIG-I, MDA5, and MAVS.

To define DHX15's placement in the RLR-signaling pathway, epistasis (overexpression) experiments were conducted in DHX15 knockdown cells. Signaling-competent molecules like MAVS, the IRF3 kinases; TBK1 and IKK$\varepsilon$ [23-24, 107], active mutants encoding tandem CARDs of RIG-I (N-RIG) or MDA5 (N-MDA5), and an active IRF3 mutant (IRF3-5D) were tested [9, 12, 24, 194]. Expression of TBK1, IKK$\varepsilon$ and IRF3-5D in DHX15-knockdown cells each restored signaling to the IFN$\beta$ promoter to levels of NTV control cells whereas expression of N-RIG, N-MDA5 and MAVS did not (Figure 2-4D). Thus, DHX15 regulates innate immune signaling actions within the RLR pathway above the level of MAVS but at the level of RIG-I and MDA5.

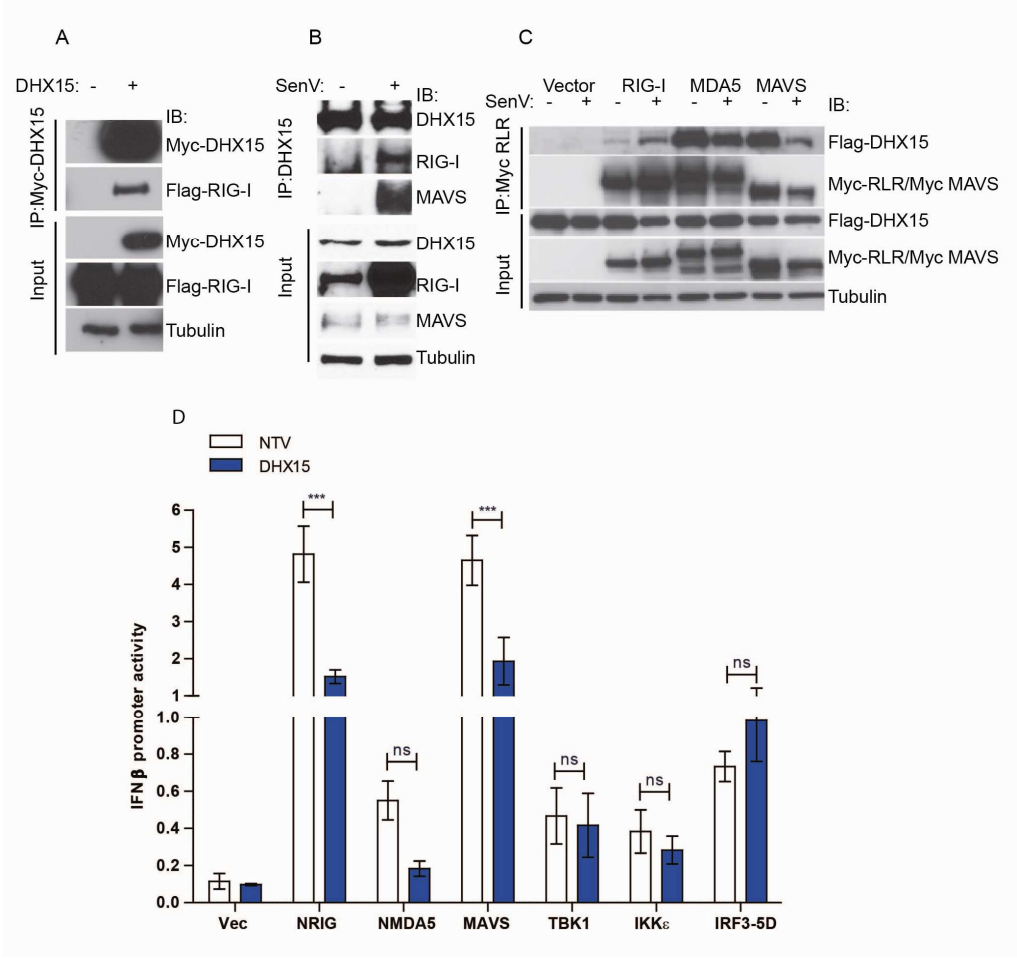


***Figure 2-4. DHX15 interacts with RIG-I, MDA5 and MAVS.*** (A) HEK293 cells were co-transfected with FLAG-RIG-I and either a control Myc-vector or a plasmid expressing Myc-DHX15. The same amount of total protein between 500 μg-2000 μg was used in each immunoprecipitation. Myc-DHX15 was immunoprecipitated from total cell lysine using an anti-Myc mouse monoclonal antibody and protein G magnetic beads. Myc-DHX15 and co-precipitating proteins were eluted in SDS-PAGE sample buffer and analyzed by western blot analysis using anti-FLAG and anti-myc antibodies. 20 μg of total cell lysine was analyzed on SDS-PAGE western blot to evaluate expression levels of the constructs and is labeled as input. (B) HEK293 cells were mock-infected or infected with SenV for 7 hours. Cell lysates were prepared from which endogenous DHX15 was immunoprecipitated using an anti-DHX15 mouse monoclonal antibody and protein G magnetic beads. DHX15 and co-precipitating proteins were eluted using SDS-PAGE sample buffer, and analyzed by western blot analysis for RIG-I, MAVS, DHX15 and tubule. 20 μg of total cell lysine was analyzed on SDS-PAGE western blot to evaluate expression levels of the constructs and is labeled as input. (C) HEK293 cells were co-transfected with FLAG-DHX15 along with an empty Myc-vector or plasmids expressing Myc-RIG-I or Myc-MDA5 or Myc-MAVS. Cells were either mock-infected or infected with SenV for 24 hours. The respective Myc-tagged proteins were

immunoprecipitated using an anti-Myc mouse monoclonal antibody bound to protein G dynabeads. Co-precipitating proteins were eluted in SDS-PAGE sample buffer and analyzed by western blot for FLAG-DHX15. 20 μg of total cell lysate was analyzed on SDS-PAGE western blot to evaluate expression levels of the constructs and is labeled as input. (D) Huh7 knockdown cells (NTV control or DHX15 knockdown cells) were co-transfected IFNβ promoter-driven firefly luciferase reporter plasmid, a CMV promoter-driven *Renilla* luciferase reporter plasmid and either a vector-control plasmid or a plasmid that ectopically-expressed constitutively-active signaling factors of the RLR pathway: N-RIG, N-MDA5, MAVS, TBK-1, IKKε and IRF3-5D. Lysates were collected 24 hours after transfection and analyzed for dual luciferase reporter activity. The results are expressed as relative luciferase activity showing average ratio firefly over *Renilla* from a representative experiment out of 3. Error bars represent standard deviations. 2-way ANOVA with Bonferroni post-test show the P value to be *** < 0.001, ns = not significant.

**DHX15 interacts with the CARDs of RIG-I and MAVS.** To define the protein domains that are important for the observed interactions, co-immunoprecipitation studies with truncation mutants of DHX15, RIG-I, and MAVS were conducted. In the case of RIG-I, only full-length RIG-I and N-RIG (consisting of the tandem CARDs) but not C-RIG (consisting of the helicase and repressor domain) associated with Myc-DHX15 (Figure 2-5A), suggesting that DHX15 associates with RIG-I through its N-terminal CARDs. Alternatively, DHX15 could be associating with the signaling-competent N-RIG through its oligomerization with endogenous full-length RIG-I. However, this possibility seems unlikely as a similar interaction was not observed with C-RIG, which also oligomerizes with endogenous full-length RIG-I but is dominant negative for signaling [12]. Ectopically overexpressed FLAG-DHX15 associated with full-length MAVS (Figure 2-5B), consistent with a recent report (46). DHX15 could also associate with MAVS lacking the transmembrane domain in the C-terminus albeit not quite to levels of full-length MAVS. DHX15 did not associate with MAVS lacking the aa 10-77 encoding the signaling-

competent CARD (neither MAVS ΔCARD nor MAVS ΔCARDΔTM can bind to DHX15), indicating that MAVS interacts with DHX15 through its N-terminal CARD in a manner requiring MAVS placement on the MAM [28].

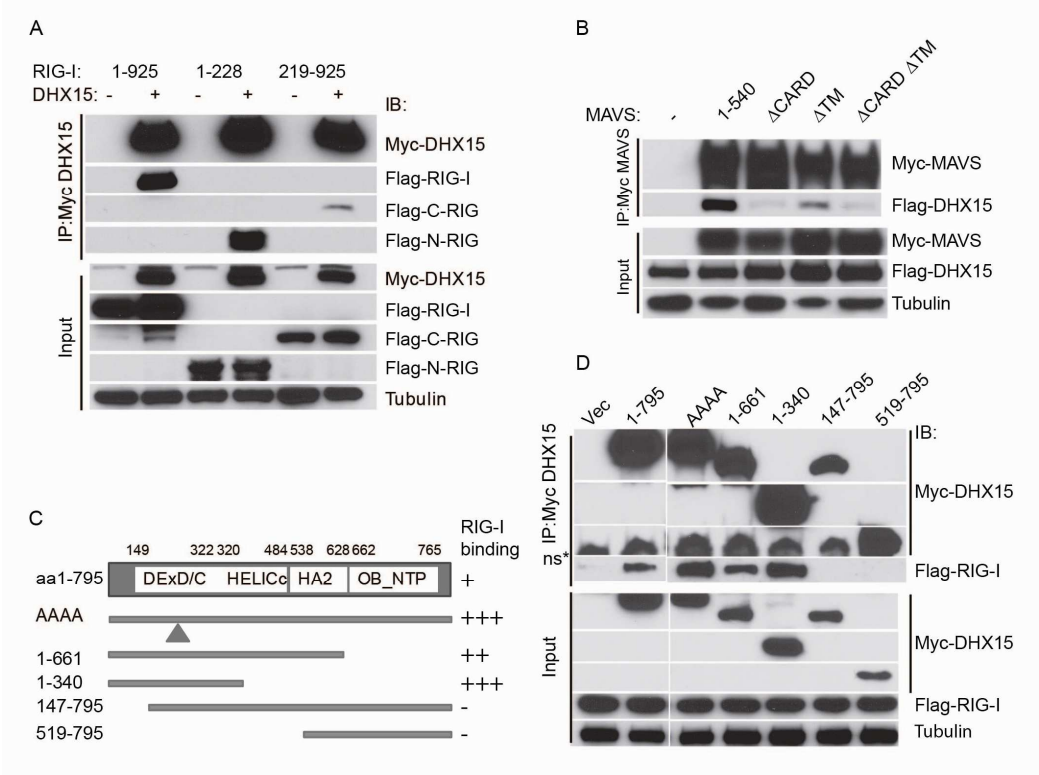


***Figure 2-5. The N-terminus of DHX15 binds the CARD domains of RIG-I and MAVS.*** (A) HEK293 cells were co-transfected with either a control Myc vector or a plasmid expressing Myc-DHX15 along with FLAG-RIG-I constructs that express full-length RIG-I (aa1-925), the constitutively-active N-RIG (aa1-228), or the dominant negative C-RIG (aa219-925). Myc-tagged proteins were immunoprecipitated from cell lysates using an anti-Myc mouse monoclonal antibody and protein G-coated magnetic beads. Co-precipitating proteins were eluted from the beads in SDS-PAGE sample buffer and analyzed by Western blot analysis for Myc-DHX15 and various FLAG-tagged RIG-I proteins. 20 μg of total cell lysate was analyzed on SDS-PAGE Western blot to evaluate expression levels of the constructs and was labeled as input. (B) HEK293 cells were co-transfected with either a control Myc vector or a plasmid expressing Myc-MAVS or MAVS truncations Δ CARD, Δ TM, Δ CARD Δ TM, and FLAG-DHX15. Myc-tagged proteins were immunoprecipitated from cell lysates using an anti-Myc mouse monoclonal antibody and protein G-coated magnetic beads. Co-precipitating proteins were eluted from the beads in SDS-PAGE sample buffer and analyzed by Western blot analysis for Myc-MAVS constructs and FLAG-DHX15. 20 μg of total cell lysate was

analyzed on SDS-PAGE western blot to evaluate expression levels of the constructs and is labeled as input. (C) Schematic of DHX15 protein and conserved motifs as determined by NCBI Reference Sequence: NP_001349.2. Also represented are the various DHX15 truncation mutants created to define interactions with RIG-I by immunoprecipitation, the results of which are summarized on the right. (D) HEK293 cells were co-transfected with either a control Myc vector or a plasmid expressing Myc-DHX15 (1-795) or its N-terminal truncations 147-795 and 519-795 or C-terminal truncations 1-661 and 1-340 or DEAH box mutant, AAAA and FLAG-RIG-I. Cell lysates were prepared from which Myc-tagged proteins were immunoprecipitated using an anti-Myc mouse monoclonal antibody and protein G-coated magnetic beads. Co-precipitating proteins were eluted from the beads in SDS-PAGE sample buffer and analyzed by western blot analysis for Myc-DHX15 and FLAG-RIG-I. 20 μg of total cell lysate was analyzed on SDS-PAGE western blot to evaluate expression levels of the constructs. *ns represents non-specific band.

Almost the entirety of the DHX15 protein consists of motifs and protein domains that are typical of a DExD/H box helicase (Figure 2-5C), a highly conserved DEAH motif (aa 149-322), a helicase C-terminal domain (HELICc, aa 320-484), an oligonucleotide-binding motif (OB NTP bind, aa662-765) and a helicase-associated domain (HA2, aa 538-628) (NCBI, CCDS33966.1). The DHX15 N-terminus contains a less characterized region that was previously shown to be important for nucleolar targeting (aa 1-62) and nuclear entry (aa 63-152) associated with pre-mRNA splicing activities of DHX15 [195]. Mutant constructs lacking these various regions of DHX15 as well as a DHX15 mutant with all the residues within the DEAH motif II mutated to alanine that abrogates ATPase activity and inhibits helicase activity were cloned [196]. RIG-I binding was retained by DHX15 aa 1-340, while DHX15 mutants lacking the protein's N-terminus all failed to bind RIG-I (Figure 2-5D). The DHX15 C-terminus was not essential for binding to RIG-I nor did alanine substitution of the DEAH box motif disrupt RIG-I binding (Figure 2-5C and 2-5D). These results demonstrate that the N-terminal 340 aa region of DHX15 imparts binding to RIG-I. Taken together, these results indicate that the DHX15 N-terminal region can bind to the CARD(s) of RIG-I and MAVS.

**DHX15 hydrolyzes ATP constitutively promotes synergistic binding of dsRNA by RIG-I, and binds HCV PAMP with high affinity.** DHX15 is a DEAH RNA helicase and as such presumably has the ability to hydrolyze ATP towards biological activities that may include RNA-binding, translocation on RNA or RNA unwinding. The role of the ATPase activity of DHX15 was evaluated in the presence of RNA ligands known to activate RIG-I activation: the ssRNA, hepatitis C virus (HCV) poly-U/UC RNA, dsRNA poly (I:C) RNA, and a control ssRNA HCV xRNA which, although it induces Toll like receptor (TLR) 7-dependent activation of the NLRP3 inflammasome in macrophages, does not activate RIG-I signaling of innate immunity [197]. As expected, purified recombinant RIG-I protein hydrolyzed ATP to release free phosphate in a concentration-dependent manner when incubated with poly-U/UC RNA but not xRNA (Figure 2-6A) [49]. In contrast, purified recombinant DHX15 hydrolyzed ATP to release high levels of free phosphate regardless of the RNA species and even did so alone in the absence of RNA, suggesting that DHX15 hydrolysis of ATP at least in a cell-free system occurs constitutively without the requirement for an RNA ligand (Figure 2-6A, B). Note that in Figure 2-5D, the DHX15 mutant that is defective in ATPase activity interacts with RIG-I to wildtype levels. Lu et al. and Mossallanejad et al. additionally show that DHX15 point mutants that are defective in ATP hydrolysis, signal as effectively as wildtype DHX15 to induce MAPK and NF-κB signaling in response to dsRNA [187-188]. Similarly, DHX15 appears to hydrolyze ATP constitutively and the ATP hydrolysis activity is not required for RLR signaling to innate immunity. The RNA binding ability of RIG-I alone, DHX15 alone and equal moles of RIG-I and DHX15 mixed together were evaluated by in vitro binding RNA ELISA. RIG-I binds poly (I:C) with lower affinity than DHX15. DHX15 binds

poly (I:C) with higher affinity than RIG-I. RIG-I and DHX15 combined together synergistically bind poly (I:C) better than either protein alone suggesting the PAMP binding ability is greatly enhanced when the two helicases are present together (Figure 2-6C). A linear regression analysis comparing RNA binding of RIG-I, DHX15 and the two proteins mixed together results in a RNA binding curve that has significantly different slopes suggesting a synergistic effect in RNA binding (RIG-I, slope represented by m = 0.01284 ± 0.002839, DHX15, m =0.05755 ± 0.01282, RIG-I +DHX15 = 0.2836 ± 0.06095), (Figure 2-6C).

DHX15 was tested for purity by Coomassie staining and the protein was observed as a single band with purity of ≥ 95% (Figure 2-6D). To test the PAMP recognition by DHX15 with a RIG-I specific agonist, the HCV PAMP (poly-U/UC region, 0-4 pmol) and a control xRNA that are both ssRNA found in the 3' UTR region of HCV were tested for binding to DHX15. The HCV PAMP triggers RIG-I specific signaling whereas xRNA is inactive and serves as a negative control. DHX15 (5 pmol) binds HCV PAMP in a dose dependent manner (0-4 pmol of RNA, Figure 2-6E). The fluorescence intensity was measured and plotted as a function of RNA concentration and confirmed that DHX15 binds increasing concentrations of PAMP RNA but not xRNA (Figure 2-6F). Fixed concentrations of RNA (0.125, 0.25, 0.5 pmol) were titrated with increasing concentrations of DHX15 (0-10 pmol). DHX15 binds with very high affinity and specificity to HCV PAMP but not the xRNA (Figure 2-6G). The fluorescence intensity was plotted as a function of picomoles of DHX15 and shows a dose dependent effect in binding to PAMP RNA but not the xRNA (Figure 2-6H). DHX15 can thus bind both

dsRNA and ssRNA PAMPs with high specificity and therefore acts as a PRR that is involved in innate immune sensing of non-self RNA.

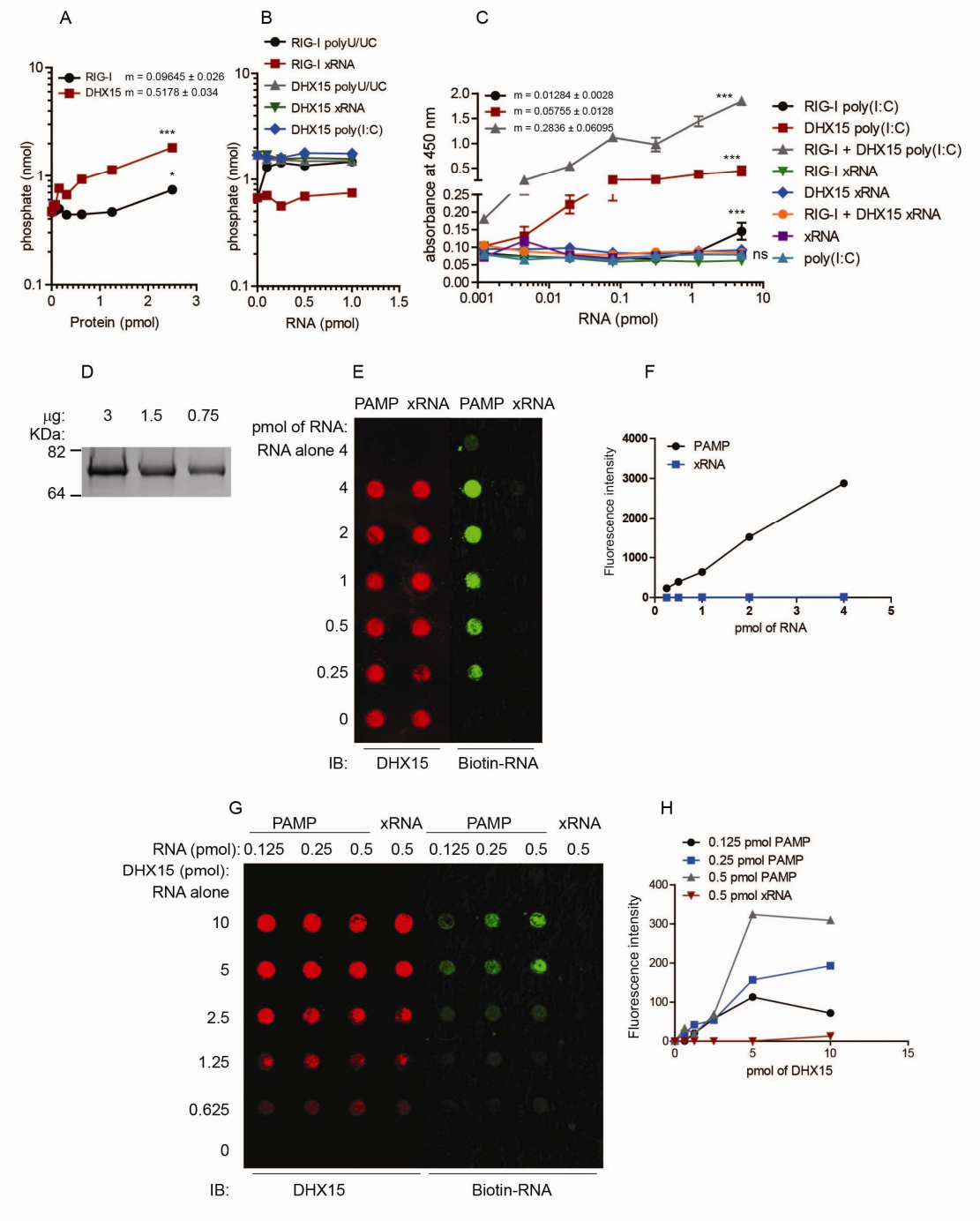


***Figure 2-6. DHX15 has constitutive ATPase activity and binds dsRNA poly (I:C) and ssRNA HCV PAMP RNA.*** (A) Increasing concentrations of DHX15 and RIG-I (0.25 pmol-

0) protein was tested for its ability to hydrolyze ATP. The nano moles of free phosphate released is plotted over picomoles of protein. The slopes of the curves were compared and found to be significantly different by linear regression analysis p value * <0.05, *** < 0.0001. (B) Sub-optimal dose of DHX15 (0.3 pmol) and RIG-I (5 pmol) were tested in the presence of increasing concentration (0.01-1 pmol) of HCV PAMP, X-RNA and poly (I:C). The nano moles of free phosphate released is plotted over picomoles of RNA. (C) The RNA binding ability of RIG-I , DHX15, or equal picomoles of both mixed together (3 pmol) were measured for its interaction with increasing picomoles of biotinylated poly(I:C) RNA or biotinylated xRNA (5 -0 pmol) as measured by ELISA. The plot shows absorbance measured at 450 nm as a function of increasing picomoles of RNA. The slopes of the curves were compared and found to be significantly different by linear regression analysis p value *** < 0.0001, ns = not significant and the slopes are represented by "*m*" (D) Fixed concentration of DHX15 (5 pmol) was tested for its ability to bind increasing concentration of HCV PAMP and xRNA (0-4 pmol) by filter binding assay. The image represents the amount biotinylated RNA bound to DHX15. (E) The fluorescence intensity of the nitrocellulose membrane in panel D was measured and plotted as a function of picomoles of RNA concentration. (F) The ability of increasing concentrations of DHX15 (0-10 pmol) to bind fixed concentration of RNA (0.125, 0.25, 0.5 pmol of HCV PAMP and 0.5 pmol of xRNA) were tested by filter binding assay. The image represents the amount biotinylated RNA bound to increasing concentrations of DHX15. (G) The fluorescence intensity of the nitrocellulose membrane in panel F was measured and plotted as a function of picomoles of DHX15.

**Role of DHX15 in RNA virus infection.** Since DHX15 restricts SenV infection (see Figure 2-3C) the role of DHX15 in restricting infection by other RNA viruses, including vesicular stomatitis virus (VSV) and encephalomyocarditis virus (EMCV) were evaluated. Notably, VSV is recognized specifically by RIG-I while EMCV is recognized by MDA5 *in vitro* and *in vivo* [11, 13, 47]. The Huh7 DHX15 knockdown cells were tested for their ability to control infection by either virus. Cells were mock-infected or infected with VSV or EMCV, and infectious virus production was subsequently measured by plaque assay of culture supernatant. Lack of DHX15 expression associated with an increase in infectious viral particles of VSV (Figure 2-7A) and EMCV (Figure 2-7B) compared to the NTV control cells. Thus, DHX15 is a positive regulator and cofactor of RLR signaling

that when absent, results in defective innate immune signaling and increased virus burden. This study reveals that DHX15 is an essential RLR cofactor of innate immune signaling and response to control infection by diverse RNA viruses.

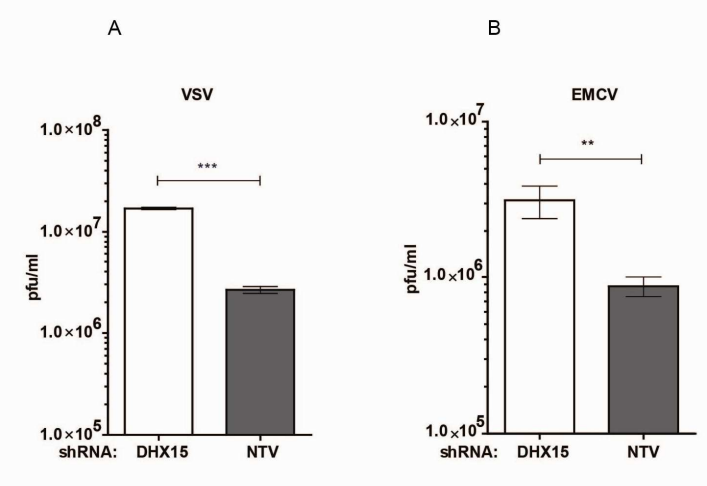


***Figure 2-7. DHX15 is required for antiviral immunity against RNA viruses.*** Huh7 knockdown cells were mock-infected or infected with (A) vesicular stomatitis virus at an M.O.I. of 0.01 for 12 hours or (B) encephalomyocarditis virus at an M.O.I. of 0.01 for 18 hours. Cell culture supernatants were clarified by centrifugation (removal of cell debris) and the infectious virus particles measured by plaque assay on Vero cells at 24 hours post-infection. Results shown are average infectious virus particles calculated per milliliter cell culture supernatant, and analyzed for statistical significance by 2-way Anova with Bonferroni posttests. * represents $p<0.01$ and ** represents $p<0.001$.

## Discussion

Pathogen recognition and signaling are tightly controlled processes that when aberrantly regulated result in immune dysfunction [1-5]. RLR signaling is regulated by the dynamic recruitment of signaling cofactors that assemble as a complex on MAVS filaments. The complex is then licensed for signaling to initiate transcriptional programs that drive the innate immune response. The results indicate that DHX15 is a component

of the RLR signaling pathway through interaction with RIG-I, MDA5, and MAVS. Moreover, DHX15 can regulate MAP-kinase and NF-κB signaling that is initiated by RLR signaling [187-188]. Importantly, this study demonstrates that DHX15 is an RLR-binding protein that regulates RLR signaling through its interaction with the CARDs of RIG-I in the steady-state. Upon virus infection, active RIG-I translocates from the cytosol to membrane compartments in the cell to bind to MAVS on the MAM [28, 36]. This study identifies that DHX15 can bind to RIG-I in resting cells and is present as a low abundance complex but that the DHX15/RIG-I complex increases in abundance under conditions of RIG-I signaling activation. DHX15 can bind to PAMP RNA including the HCV PAMP 5'ppp poly-U/UC RNA and the dsRNA PAMP poly(I:C) [49]. I propose that this RNA PAMP-binding activity and RIG-I interaction serve to support and enhance PAMP recognition and signaling by RIG-I. Moreover, DHX15 can be found in a complex with ectopic MDA5 and MAVS, both of which are signaling-competent under these expression conditions. Thus, DHX15 is a RLR-binding protein that can also bind to MAVS upon RLR activation, possibly mediating a higher ordered complex to facilitate the RLR/MAVS interaction that drives downstream signaling (Figure 2-8).

Biochemical analysis identified that the N-terminal region of DHX15 is responsible for mediating its interactions with RIG-I. This region of DHX15 encodes the DEAH motif that defines this protein family and has been functionally implicated in the U-12 spliceosome [196, 198] as well as in interacting with the human La protein (SS-B), an RNA-binding phosphoprotein that has been implicated in RNA processes including pre-mRNA splicing, transcription, RISC activation and even viral RNA replication and translation that is driven by the internal ribosome entry sites present in viral genomes

[195, 199-202]. This region of DHX15 might therefore function in protein interactions to support a variety of biological processes.

My observations are consistent with the model that DHX15 functions as a co-receptor for RLRs for PAMP RNA detection that can function by (1) sensitizing RLR detection of viral RNA, perhaps by assisting in the unwinding of RNA or the presentation of PAMPs for RLR detection, (2) stabilizing RLR engagement of PAMP RNA for sustained signaling and/or (3) facilitating efficient translocation of the activated RLR complex to MAVS to signal innate immunity. DHX15 constitutively hydrolyzes ATP even in the absence of RNA ligands (Figure 6A), and DHX15 mutants that are defective in ATPase activity interacts with RIG-I to promote signaling suggesting that the ATPase activity of DHX15 is not involved in PAMP recognition and innate immune signaling [187-188]. DHX15 is essential for RIG-I or MDA5-dependent signaling by VSV and EMCV, respectively, suggesting that DHX15 may serve as a cofactor to either RLR to facilitate signaling to MAVS. This notion is further supported by the data showing DHX15 interacts with MAVS through the MAVS CARD and requires the MAVS TM domain both of which are essential for RLR/MAVS interaction and RLR signaling via the MAM [28]. Thus, the data supports a model in which once the DHX15 facilitates RIG-I PAMP binding through its basal interaction through the RLR CARDs, it facilitates RIG-I interaction with MAVS to render a stable signaling complex and induction of the innate immune response.

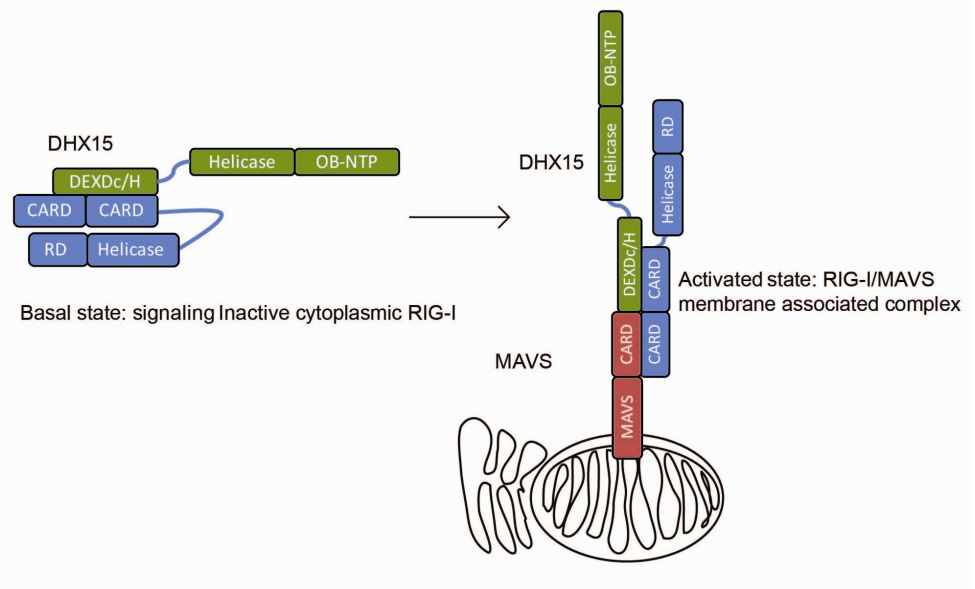


***Figure 2-8. DHX15 interacts with RIG-I in the steady-state and upon virus-induced activation DHX15 binds RIG-I and MAVS.*** DHX15 is an RNA helicase that interacts through its N-terminus DEXD/H domain to RIG-I CARDs. DHX15 may act as a RIG-I co-receptor and facilitate RNA PAMP recognition. During virus infection, PAMP-engagement to DHX15 and RIG-I facilitates RIG-I activation and translocation of the two-helicase complex to MAVS.

Several helicases including DDX60, DDX3X, DHX36, DHX29, DDX24, and DHX9 have been identified to regulate the RLR pathway [89, 122, 124, 126, 128, 185]. Non-RLR helicases, DDX3X, DHX9, DDX60, DHX33, and the tri-partite complex of DDX1/DDX21/DHX36 have all been identified as RNA sensors involved in non-self RNA recognition [39, 89, 122, 125-127]. This study now extends this list to include DHX15 as an RLR signaling cofactor. A key observation of this study is that DHX15 can bind to both 5'ppp HCV PAMP RNA and to poly (I:C) dsRNA to enhance PAMP RNA binding by RIG-I. Given that DHX15 is abundantly and ubiquitously expressed, I speculate that DHX15 facilitates PAMP RNA recognition by the RLRs which are less abundantly expressed in the steady-state. RLR expression levels increase either in response to IRF3 activation or type I IFN induction. Further studies on how DHX15 can differentiate

between cellular versus viral RNA will be essential in understanding the role of DExD/H box helicases in pathogen recognition and how they cooperate with other nucleic acid sensing pathways.

## Acknowledgments

This work was supported by National Institutes of Health grants (NIAID R01AI060389, 1R01AI098943, U19AI03019, 5R01AI104002) and the University of Washington/Fred Hutchinson Cancer Research Center Viral Pathogenesis Training Grant (T32AI083203). I would further like to thank Alison Kell, Tien-Ying Hsiang, Matthew K. Muramatsu, Ran Dong and Aimee McMillan for technical assistance, Nanette Crochet for microscopy and Gregory Zornetzer for mass spectrometry assistance.

# Chapter 3. Targeting innate immunity through RIG-I agonists and their role as broad-spectrum antivirals.

## Introduction

The RLR family of cytoplasmic sensors are germ line encoded pathogen recognition receptors that detect PAMP within viral RNA. Signaling through the RLRs is essential for the innate immune response to many RNA viruses, the absence of which renders cells and mice highly susceptible to virus infection [11, 20, 167]. Upon engagement to PAMP-containing viral RNA, RIG-I and MDA5 induce the expression of many innate immune genes, pro-inflammatory cytokines, chemokines and type I IFNs through homotypic CARD-CARD interactions with their common adaptor MAVS protein. These products of RLR signaling act in concert to suppress and control virus infection. The inflammatory cytokines and chemokines recruit and program immune cells for viral clearance, and the secreted type I IFNs signal through cell surface IFNAR1/2 to trigger signaling through the JAK-STAT pathway to activate ISGF3, which directly results in the expression of hundreds of genes with direct antiviral activity. Type I IFNs thus has an amplification effect and its signaling is essential for limiting and controlling viral infections in the host [15, 203].

The importance of RLR signaling for antiviral immunity is most evident in mice deficient in either RIG-I, MDA5 or MAVS that despite intact Toll like receptors and other PRRs exhibit greater susceptibility to RNA and DNA virus infection. Importantly, RLR signaling is so critical to the control of virus infection that viruses including members of the *Flaviviridae*, *Orthomyxoviridae*, *Coronaviridae*, *Filoviridae* and *Retroviridae* have

evolved to encode viral proteins that can directly antagonize or compromise RLR signaling function or have developed elaborate mechanisms to hide their viral genomes or replication intermediates from RLR detection [18, 162, 181-182, 204-209]. Whether by means of escaping RLR detection or antagonizing RLR signaling, these viruses subvert or compromise host immune defenses to promote viral replication and propagation. Therapeutic agonists that can activate RLR signaling may therefore be an effective strategy to control virus infections by promoting or modulating the host innate immune antiviral responses. Such agents would have the added benefit of being broadly-effective against different viruses. These immune-modulating agents would exert a broad immune response that cannot be easily overcome by individual virus or the accumulation of viral mutations.

RNA viruses pose a significant public health problem worldwide and are the frequent cause of emerging and re-emerging viral infections. There has been an increased incidence of disease caused by arthropod-borne members of the *Flaviviridae* in recent decades. The World Health Organization reports a increased incidence, morbidity and mortality caused by both WNV and DV and declared these pathogens as emerging viruses of public health concern that call for more effective therapy. Another member of the *Flaviviridae,* the hepatitis C virus (HCV) is transmitted through the blood. HCV is another virus of global public health concern. With the development of DAA including NS5A- and NS3-specific protease inhibitors and NS5B nucleoside and non-nucleoside inhibitors used in combination with conventional IFN and ribavirin therapies, control of HCV appears to be an achievable goal in the next decade, but drug resistance is still a concern with prolonged use of these DAA. Additionally, these DAA,

though highly effective, can add upwards of USD$50,000 to the cost of treating HCV and have therefore been cost-prohibitive to many patients, inviting the design of alternative therapies to control HCV. The *Filoviridae* Ebola virus (EBOV) outbreak that started in December 2013 in the West African country of Guinea has now spread to Liberia, Sierra Leone, and Nigeria. With a total of 4555 deaths reported as of October 2014, this epidemic is the deadliest and largest EBOV outbreak in recorded history. Despite foreign aid and the use of the experimental drug ZMapp [210], the epidemic remains largely uncontained, and the Centers for Disease Control and prevention (CDC) confirmed the first case of Ebola in the United States while the Democratic Republic of Congo reports a second EBOV outbreak that started in August 2014 that is apparently unrelated to the ongoing West African epidemic [211]. These incidences of epidemics impart an urgent need for therapeutic interventions.

Previous work from Kineta Inc. (Small bio-tech involved in developing RIG-I agonists as adjuvants and antivirals), reported a high throughput cell-based screening approach in which small, drug-like molecules that target the RLR pathway and drive IRF3 activation were identified. Among them were a group of isoflavone compounds that exhibited potent antiviral activity against HCV and influenza A virus in cultured cells [212] and benzothiazoles that had potent activity against respiratory syncytial virus (RSV) infections in cultured cells (Wang et al., under review) . Here, I report the identification of a third family of small molecule compounds, hydroxyquinolines that can target the RLR pathway to drive IRF3 activation. These compounds induce pro-inflammatory cytokines and chemokines, and importantly, the expression of antiviral genes in treated cells. Prophylactic and therapeutic treatment of cell cultures

significantly decreased the viral RNA load of cells infected with WNV, DV, HCV and EBOV and concomitantly suppressed the production of infectious virus. This study thus identifies a novel class of immune-modulating molecules that function as innate immune agonists of RLR signaling to suppress infection by members of the *Flaviviridae* and *Filoviridae*. This body of work reveals the strong potential of developing these RLR agonists as broad-spectrum antiviral agents to control RNA virus infections and provides proof of principle for targeting RLR signaling for innate immune induction as a viable approach for antiviral therapies.

## Material and Methods

**Cell lines and viruses.** Huh7, human hepatocyte and HEK293 cells, embryonic kidney epithelial cell lines were cultured in Dulbecco's modified Eagle's medium (Cellgro) supplemented with 10% fetal bovine serum (FBS, HyClone), L-glutamine, sodium pyruvate and nonessential amino acids. THP-1 (human monocytic) cell line was cultured in complete RPMI (invitrogen) supplemented with 10% heat-inactivated FBS. THP-1 cells were differentiated in complete RPMI supplemented with 40nM PMA for 30 hrs prior to their use in experiments. Huh7-K2040 replicon cells that contain variants of the Con1 HCV (genotype 1B) subgenomic replicon RNA were cultured in cDMEM with 400ug/ml of G418 selection [189]. Normal primary human umbilical vein endothelial cells (HUVECs) were obtained from Clonetics, Inc. (San Diego, CA), and maintained in endothelial cell growth medium (Clonetics), which was supplemented with human recombinant epidermal growth factor, hydrocortisone, fetal bovine serum, gentamicin,

and bovine brain extract (Clonetics). The WNV isolate TX 2002 (WNV-TX) was described previously [166] and titered by standard plaque assay on Vero cells. DV, serotype-2 (DV2) was a gift from Alec J. Hirsch. DV2 was grown on the C636 mosquito cell line and titered by standard plaque assay on Vero cells. Cell culture adapted HCV was produced from pJFH-1 encoding the JFH-1 genotype 2A infectious clone and *in vitro* transcribed as described previously [213]. Zaire Ebola virus (ZEBOV, Kikwit 199510621) was used for infections. All ZEBOV infections were done by Chad Mire at the University of Texas Medical Branch (UTMB), Galveston in a BSL4 facility.

**Antibodies.** The following primary antibodies were used for immunoblot detection: Rabbit anti-RIG-I (969, raised in rabbit against a RIG-I CARD peptide sequence) [36], rabbit anti-MDA5 ( AT113, Enzo Life Sciences), HCV rabbit anti-NS5A (K03HQ), rabbit anti-IFIT1, rabbit anti Mx1. HRP-conjugated secondary antibodies were obtained from Jackson ImmunoResearch.

**Compounds.** Compounds were synthesized by Life Chemicals Inc. and KINETA, Inc. and were solubilized in 100% DMSO and kept frozen as 10 mM stocks. The compounds were stored in small aliquots to prevent multiple freeze-thaws and were step-wise diluted to reach the desired concentration in 0.5% DMSO for all drug treatments [212].

**Real-time PCR (RT-PCR) quantitation of viral RNA.** Cells were harvested in RLT buffer and total cellular RNA was purified using the RNeasy kit (Qiagen). cDNA was synthesized from the purified RNA by both random and oligo (dT) priming using the iScript cDNA synthesis kit (Bio-rad). WNV and DV2 RNA levels were measured using SYBR Green method (Applied Biosystems) on RT machine (Applied Biosystems, 7300

RT-PCR) using the relative quantitation method. The samples were normalized by subtracting out the CT values of GAPDH. The fold induction of ISG or viral RNA over either DMSO treatment control or mock-infected cells was calculated. RT-PCR primer sequences are available upon request. The HCV RNA for the standard curve was generated by *in vitro* transcription assay using the pSJ plasmid that contains the full length JFH-1 genotype 2a clone [86]. A standard curve of HCV RNA was generated by serially diluting the *in vitro* transcribed HCV RNA from $10^7$ to $10^0$ copies/μL. HCV RNA levels were measured using taqman assay (EZ RT-PCR core reagents, Applied Biosystems) through the absolute quantitation method. The HCV standard curve was used to extrapolate the copies/μl of HCV RNA present in each sample.

| Primer | 5'-Sequence-3' |
|---|---|
| IFN-β F | AGTGTCAGAAGCTCCTGTGGC |
| IFN-β R | TGAGGCAGTATTCAAGCCTCC |
| IFN-λ1 F | CACGCGAGACCTCAAATATGTG |
| IFN-λ1 R | AGGGTGGGTTGACGTTCTCA |
| IFN-λ2/3 F | GCCACATAGCCCAGTTCAAGTC |
| IFN-λ2/3 R | GGCATCTTTGGCCCTCTTAAA |
| IL-1β F | ATGATGGCTTATTACAGTGGCAA |
| IL-1β R | GTCGGAGATTCGTAGCTGGA |
| TNF-α F | GAGGCCAAGCCCTGGTATG |
| TNF-α R | CGGGCCGATTGATCTCAGC |
| IFIT-1 F | TTGATGACGATGAAATGCCTGA |
| IFIT-1 R | CAGGTCACCAGACTCCTCAC |
| MX1 F | GGTGGTCCCCAGTAATGTGG |
| MX1 R | CGTCAAGATTCCGATGGTCCT |

| | |
|---|---|
| GAPDH F | ACAACTTTGGTATCGTGGAAGG |
| GAPDH R | GCCATCACGCCACAGTTTC |
| IFIT1 F | GAGCTGGGTATGCGATCTC |
| IFIT1 R | CAGCCTGCCTTAGGGGAAG |
| IFITM1 F | TACTCCGTGAAGTCTAGGGACAG |
| IFITM1 R | AACAGGATGAATCCAATGGTCA |
| RIG-I F | TGTGCTCCTACAGGTTGTGGA |
| RIG-I R | CACTGGGATCTGATTCGCAAAA |
| MAVS F | ATGCCGTTTGCTGAAGACAAG |
| MAVS R | AGGGCAGGTAAGGCAGAATCT |
| IFIT2 F | CACATGGGCCGACTCTCA |
| IFIT2 R | CCACACTTTAACCGTGTCCAC |
| GAPDH F | GAAGGTGAAGGTCGGAGT |
| GAPDH R | GAAGATGGTGATGGGATTTC |
| SenV F | GACGCGAGTTATGTGTTTGC |
| SenV R | TTCCACGCTCTCTTGGATCT |
| EMCV F | GACGCTTGAAGACGTTGTCTTCTTA |
| EMCV R | CCCTACCTCACGGAATGGGGCAAAG |
| WNV 5'UTR F | CGCCTGTGTGAGCTGACAAAC |
| WNV 5'UTR R | CATAGCCCTCTTCAGTCC |
| DENV2 F | TGTTGGTGCAACTCTACGTCCACA |
| DENV2 R | TGTGGAACGAGTGCCACTGATCTT |

**Table 3-1. Real-time PCR primer sequences used in gene expression studies**

**Measuring infectious WNV and DV2 particles.** Huh7 and HEK293 cells were treated with compounds 24 hours before or 2-24 hours after virus infection. Supernatants were collected at 24 and 48 hours post-infection and the infectious viral particles in the supernatants were measured by standard plaque assay using agar overlay on Vero

cells. The plaques were counted on day 2 for WNV using neutral red and day 8 for DV2 using crystal violet staining.

**HCV Focus forming unit (FFU) assay.** Huh7 cells were compound treated at 20 µM for 24 hours before virus infection. The 48 hour supernatants were collected and the infectious viral particles produced were titered on Huh7.5 cells by serial dilution. The focus forming unit/ml of supernatants was counted on a microscope to determine the HCV titer [50].

**Immunoblot analyses**. Cells were trypsinized and collected in RIPA buffer (50 mM Tris-Cl pH 7.5, 150 mM NaCl, 5mM EDTA, 1% NP-40, 0.5% sodium deoxycholate, 0.1% SDS) supplemented with a cocktail of protease inhibitors (Sigma) and phosphatase inhibitors (Calbiochem) and okadaic acid (Calbiochem). Following cell lysis, nuclear material was removed by centrifugation at 15,000 x g for 10 minutes at 4 ℃. Cell lysates were quantified by BCA (Thermo sci entific), analyzed on a denaturing Tris-HCl polyacrylamide gel and transferred onto nitrocellulose membranes. Cellular and viral proteins of interest were detected by immunoblot analysis using specific primary antibodies described earlier and HRP-conjugated secondary antibodies (Jackson Laboratory) and visualized by chemiluminescence on x-ray film.

**Infection studies.** ***Pre-treatment with compounds.*** HEK293 or Huh7 cells were used for WNV infection and Huh7 cells were used for HCV and DV2 infection. Cells were pre-treated with compounds at 20, 10, 2, 0.2 µM in 0.5% DMSO background diluted in cDMEM for 24 hours and infected at a MOI of 1 in serum free media at 37℃. The cells were exposed to virus for 2-4 hours before replacing with cDMEM. Cells were harvested

in RLT buffer for RNA purification and supernatants at 24 and 48 hours were collected for plaque assays. IFN-β at 100 units/ml was used as a positive control and 0.5% DMSO was used as a negative control.

***Post-infection treatment with compounds.*** Cells were seeded and infected with virus at a MOI of 0.1 (HCV and WNV) or 1 (DV) in serum free media. The cells were exposed to virus for 2-4 hours after which compounds were added at 20, 10, 2, 0.2 µM in 0.5% DMSO background diluted in cDMEM. Cells were harvested in RLT buffer for RNA purification and supernatants were collected for measuring infectious viral particles produced at 24 and 48 hours post-infection. IFN-β at 100 IU/ml was used as a positive control and 0.5% DMSO was used as a negative control.

**Infection studies with Ebola virus.** Human umbilical vein endothelial cells (HUVECs) were plated in 24 well plates and allowed to grow to confluency. Once the monolayer was confluent, cells were either mock treated or treated with 5µM or 1µM of KIN 1408. Twenty two hours post treatment (22 p.t.), the treatment medium was removed and the cells were treated again with 5µM or 1µM of KIN 1408. Two hours post the additional treatment (22 + 2 p.t.), HUVECs were infected with *Zaire ebola virus* (ZEBOV, Kikwit 199510621) MOI of 0.5 for 1 hour at 37$^{\circ}$C with rocking every 15 minutes. The inoculum was then removed and replaced with medium containing no drug or 5µM or 1µM of KIN 1408. Samples were collected at 96 hours post infection and were analyzed by conventional plaque assay on Vero E6 cells. Briefly, increasing 10-fold dilutions of the samples were adsorbed to Vero E6 monolayers in duplicate wells (200µl); the limit of detection was 25 PFU/ml.

**Infection studies with Influenza.** HEK293 cells were infected at a multiplicity of infection (MOI) of 0.1 and then treated with a range of compound concentrations. Infections were allowed to proceed for 24 hours, after which the supernatant was harvested and used to infect MDCK cells at an appropriate dilution. MDCK cell monolayers were fixed in the wells for 6.5 hours. Immunostaining was performed using a FITC-coupled monoclonal antibody directed against the Influenza A NP protein. Viral foci were quantified via ArrayScan and measured as focus forming unit per ml of supernatant.

**Infection studies with respiratory syncytial virus.** HeLa cells were infected at a multiplicity of infection (MOI) of 0.1 and then treated with a range of compound concentrations. Infections were allowed to proceed for 48 hours, after which the supernatant was harvested and used to infect HeLa cells at an appropriate dilution. HeLa cell monolayers were fixed to the well plate after 24 hours. Immunostaining was performed using a mouse monoclonal antibody directed against the 47-49 kDa Fusion Protein of RSV (Millipore MAB8262) as the primary antibody, and a goat anti-mouse FITC conjugated secondary antibody. Viral foci were quantified via ArrayScan and measured as focus forming unit per ml of supernatant.

**Microarray analysis.** The genomics studies were conducted by Labcorp, Seattle, WA (previously called Covance). Differentiated THP-1 cells treated with 10, 2.5 and 0.625 μM of KIN 1400, 1408 and 1409 were compared to HCV PAMP poly-U/UC 2 μg/ml, XRNA 2 μg/ml, IFNβ 25 U/ml, SenV (Sendai virus) 25 HAU/ml and 0.5% DMSO. Cells were harvested at 20 hours in RLT buffer. RNA was purified using Qiagen RNeasy kits

and RNA expression was assessed by microarray using Agilent Sure Print G3 Human Genome Microarrays (version 2). Array data was processed using R/Bioconductor (R Development Core Team (2012) R: A Language and Environment for Statistical Computing. Vienna, Austria: R Foundation for Statistical Computing) [214]. Raw data were quantile normalized followed by linear modeling using the limma package [215](Smyth GK (2004) Linear models and empirical bayes methods for assessing differential expression in microarray experiments. Stat Appl Genet Mol Biol 3: Article3.). Genes with significant changes following treatment were defined by those with a > 2-fold increase or decrease over DMSO or XRNA controls with a Benjamini-Hochberg corrected p-value < 0.01. The gene expression heatmap was clustered using correlation distances, and Gene Ontology Biological Processes enriched in lists of genes mapping to such clusters were determined using Enrichr [216]

**In vivo experiment and flow cytometry.** C57/BL6 mice were injected with 20 mg/Kg of compound dissolved in 100% DMSO and injected through intra-peritoneal injection. The cells recruited to the peritoneal cavity were collected by peritoneal lavage. Cells were counted and stained for the markers; CD11b, CD11c, Ly6C and MHC class II using respective antibodies (BD scientific). The percentage of CD11b, CD11c and double positive cells and their activation states ($Ly6C^{+}$, $MHC\text{-}II^{+}$) were determined using BD LSRII on BD FACS Diva software. The absolute numbers of cells were calculated from the cell counts. All the analysis were done using FlowJo software.

# Results

## KIN1400 triggers IRF3-dependent antiviral genes and IFNβ expression.

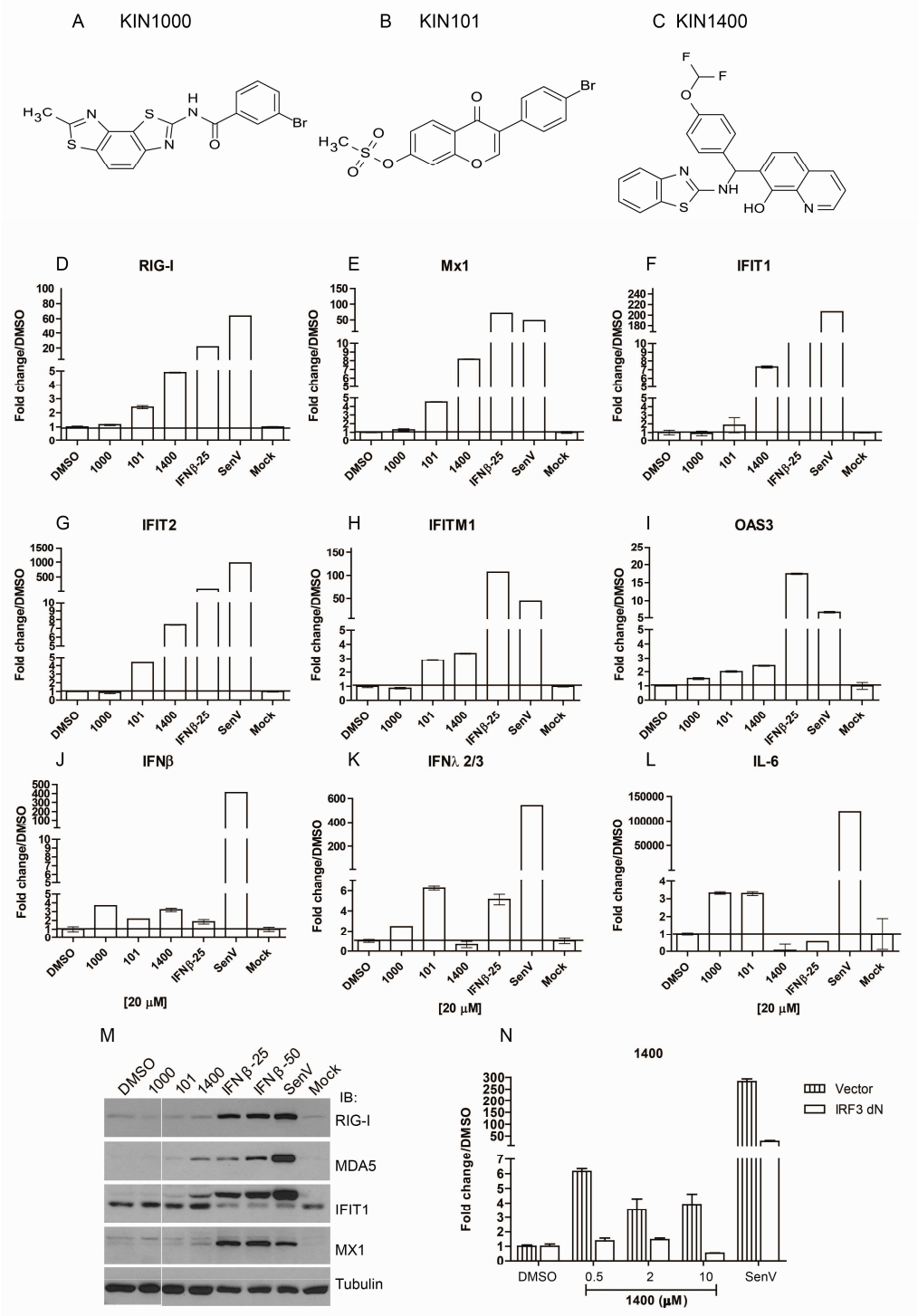

***Figure 3-1: Innate immune genes induced by the compounds.*** Structures of (A) KIN1000 that belongs to the benzothiozole family, (B) KIN101 that belongs to the isoflavone and (C) KIN1400 that belongs to the hydroxyquinoline family. PMA-differentiated THP-1 cells were treated with 20 μM of compounds for 20 hours and the total cellular RNA was purified. The expression of innate immune genes (D) DDX58 (RIG-I), (E) MX1, (F) IFIT1, (G) IFIT2, (H) IFITM1, (I) OAS3, (J) IFNβ, (K) IFNλ2/3 and (L) IL6 were measured by RT-PCR, normalized to GAPDH and expressed as fold-induction over 0.5% DMSO treatment. (M) Western blot analyses of total protein lysates collected from differentiated THP-1 cells treated with 20 μM of compounds for 20 hours. The protein expression of the genes RIG-I, MDA5, ISG56 (IFIT1), MX1 relative to tubulin was determined by western blot using respective antibodies. (N) HEK293 cells were transfected with either a vector-control plasmid or a plasmid that ectopically-expressed constitutively-active IRF3-dN (dominant negative that abolishes signaling) for 16-24 hours and then treated with 20 μM of KIN1400 for 20 hours and the expression of innate immune gene IFIT2 was measured by RT-PCR, normalized to GAPDH and expressed as fold-induction over 0.5% DMSO treatment.

A cell-based screen was conducted in which small molecule compounds were identified from a diversity library, and these compounds activated RLR-dependent IRF-3 activation leading to IFIT1, IFIT2 or IFNβ transcription [212], (Wang ML et al., under review). Kineta Inc. ( Small Bio-tech based in Seattle, WA ) has previously reported the identification of two classes of small molecules with potent antiviral activity: a group of isoflavone-like compounds (represented here by KIN101 [212]) that potently suppressed HCV and influenza A virus growth in cultured cells and a second group of small molecules with a benzothiazole core (represented here by KIN1000, Wang ML et al., under review) that potently suppressed respiratory syncytial virus (RSV) growth in cultured cells. Here, I report the identification of a third class of IRF3-activating compounds KIN1400, which belong to the class of hydroxyquinolines. KIN1400 has a completely distinct chemical structure as compared to KIN1000 and KIN101. (Figure 3-1A-C).

Previous work confirmed that KIN101 and KIN1000 treatment of cells promotes IRF3-dependent expression of many innate immune and interferon-dependent genes. To define the innate immune signaling pathways induced by KIN1400, I first surveyed whether KIN1400 can induce the expression of RLR-dependent antiviral genes was tested. THP-1 macrophage-like cells were treated with 0.5% DMSO or 20 μM KIN1000, KIN101 or KIN1400 and the RLR-dependent gene expression was evaluated by real-time qPCR. As control, cells were treated with exogenous IFNβ, infected with Sendai virus (SenV; known activator of RIG-I-dependent signaling) or mock-infected. Real-time qPCR showed that KIN1400 potently induced the expression of innate immune genes DDX58 (RIG-I), Mx1, IFIT1, IFIT2, IFITM1 and OAS3 as compared to the vehicle, DMSO (Figure 3-1D-I). KIN1400 induction of innate immune gene expression was also demonstrated at the protein level by immunoblot analysis, which showed greater RIG-I, MDA5, IFIT1 and MX1 expression in cells treated with KIN1400 as compared to DMSO (Figure 3-1M). Real time qPCR showed that KIN1400 also potently induced the expression of IFNβ but did not induce any detectable levels of type III IFN (IFNλ 2/3) or the pro-inflammatory cytokine IL-6 (Figure 3-1J-L). At this dose, KIN1400 appears to be more potent than either KIN1000 or KIN101 at inducing the expression of innate immune genes. Although KIN1400 induces IFNβ to levels equivalent to KIN1000 and greater than KIN101 (Figure 3-1J), KIN1000 and KIN101 is better than KIN1400 at inducing expression of IFNλ 2/3 and IL-6 (Figure 3-1K and 3-1L). Although KIN1400, KIN1000 and KIN101 were all identified in similar screens that selected for small molecules that activated RLR-dependent signaling, the three compounds induce gene

expression patterns that are clearly distinct, suggesting that the three compounds may have biological activities that may impart each with different antiviral activities.

To confirm whether IRF-3 is required for KIN1400 induction of innate immune gene expression, cells that were transiently-transfected to express an IRF-3 mutant (IRF3 dN) that acts as a dominant negative molecule were assessed for its ability to express IFIT2 after treatment with KIN1400. At 0.5, 2 and 10μM KIN1400, cells expressing IRF3 dN did not induce IFIT2 expression as compared to the vector-transfected control cells (Figure 3-1N). Although IRF3 dN expression was not sufficient to completely block IFIT2 expression that is induced by the more potent SenV infection, signaling is significantly reduced. These data verify that KIN1400 signals through IRF-3 to drive innate immune gene expression. Taken together, these data verify that KIN1400 to be a small molecule that can drive IRF3-dependent innate immune gene and IFNβ expression that drives the potent antiviral action that is distinct from KIN101 or KIN1000.

**KIN1400 potently suppresses WNV in cultured cells.** The compounds KIN101, KIN1000 and KIN1400 were tested for their ability to protect cultured cells from WNV infection. The compounds were added to HEK293 cells for 24 hrs before the cells were infected with WNV at a multiplicity of infection (MOI) of 1. Total cellular RNA and cell culture supernatant was collected 24 hrs after infection and evaluated for intracellular WNV RNA levels relative to GAPDH by real-time qPCR or for infectious WNV particle count by standard plaque assay, respectively. At 20μM, KIN101 had little apparent effect while

KIN1000 moderately suppressed intracellular WNV RNA levels in comparison to DMSO treatment control as measured by real-time qPCR (Figure 3-2A). In contrast, KIN1400 potently suppressed intracellular WNV RNA to levels greater than even that achieved with 100 IU/mL IFNβ treatment. Additionally, KIN1400 suppression of WNV RNA levels was dose-dependent, and 2μM KIN1400 was sufficient to achieve a 50% or greater inhibition of WNV RNA levels (Figure 3-2B). The pre-treatment of cells with KIN1400 also led to an approximately log reduction in infectious WNV particle production as compared to cells that were treated with DMSO at 48 hours (Figure 3-2C). These data show KIN1400 to be effective at controlling WNV infection in cultured cells when the compound is administered prior to infection.

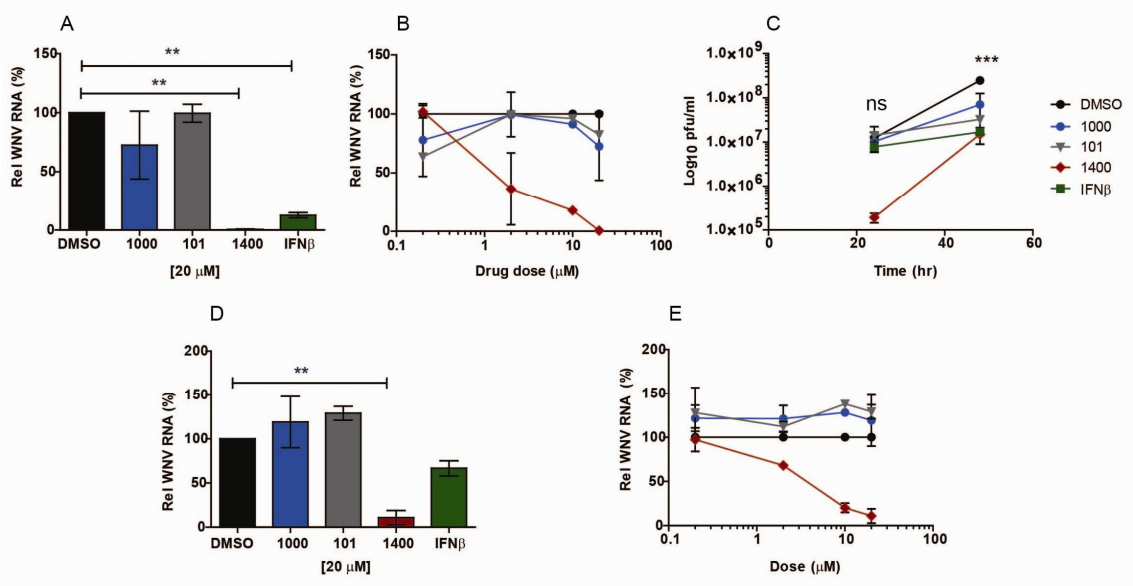


***Figure 3-2. Effect of compounds on inhibiting WNV infection.*** (A) Pre-treatment of HEK293 cells with 20 μM of 1000, 101 and 1400 for 24 hours before infection with WNV (MOI 1) and the relative decrease in WNV RNA levels (%) measured 24 hours after infection. (B) HEK293 cells were pre-treated with a dose range of 20, 10, 2, 0.2 μM of 1000, 101 and 1400 for 24 hours before infection with WNV (MOI 1) and the relative decrease in WNV RNA levels (%) measured 24 hours after infection by RT-PCR. (C) Pre-treatment of HEK293 cells with 20 μM of 1000, 101 and 1400 for 24 hours before

infecting with WNV (MOI 1) and the cell culture supernatants were collected 24 and 48 hours after infection and the infectious virus particles measured by plaque assay on Vero cells. Results shown are average infectious virus particles at 24 and 48 hours calculated per milliliter cell culture supernatant. (D) HEK293 cells were infected with WNV (MOI 0.1) for 2 hours and were treated with 20 μM of compounds, 2-4 hours after infection and the relative decrease in WNV RNA levels(%) was measured at 24 hours after infection by RT-PCR. (E) HEK293 cells were infected with WNV (MOI 0.1) for 2 hours and were treated with a dose range of 20, 10, 2 and 0.2 μM of compounds, 2-4 hours after infection and the relative decrease in WNV RNA levels(%) was measured at 24 hours after infection by RT-PCR. The relative levels of virus were calculated by RT-PCR as fold change over DMSO-treated controls, normalized to GAPDH using the ΔΔCT method. Results are average of two independent experiments. Error bars represent standard deviations. Statistical test used was one-way with Dunnett's multiple comparison test or Two-way ANOVA with Bonferroni posttests *** represents $p < 0.001$, ** $p< 0.01$, * $p<0.05$, ns not significant.

KIN101, KIN1000 and KIN1400 were also tested for their ability to inhibit WNV when the compounds were administered post-infection. In this case, WNV virus-infected HEK293 cells (MOI 0.1) were treated with compounds at 2 or 4 hours after infection. Total cellular RNA and cell culture supernatant was collected 24 hrs after infection and evaluated as before. When administered post-infection, IFNβ treatment resulted in a moderate suppression of intracellular WNV RNA levels as compared to DMSO (Figure 2D). This is consistent with reports that this strain of WNV encodes viral proteins that can antagonize and overcome type I IFN-induced JAK-STAT signaling [166]. Among the compounds, only KIN1400 was able to potently suppress WNV RNA levels at 20μM. When administered post-infection, KIN1400 suppression of WNV RNA levels is also dose-dependent although a concentration approaching 15μM is required to achieve 50% suppression. Our data shows KIN1400 as a compound that exhibits potent antiviral activity against WNV infection whether it is administered before or after WNV infection.

**KIN1400 potently suppresses DV infection.** In addition to WNV, the compounds were evaluated for their ability to inhibit DV, another member of the *Flaviviridae* of the genus *Flavivirus*.

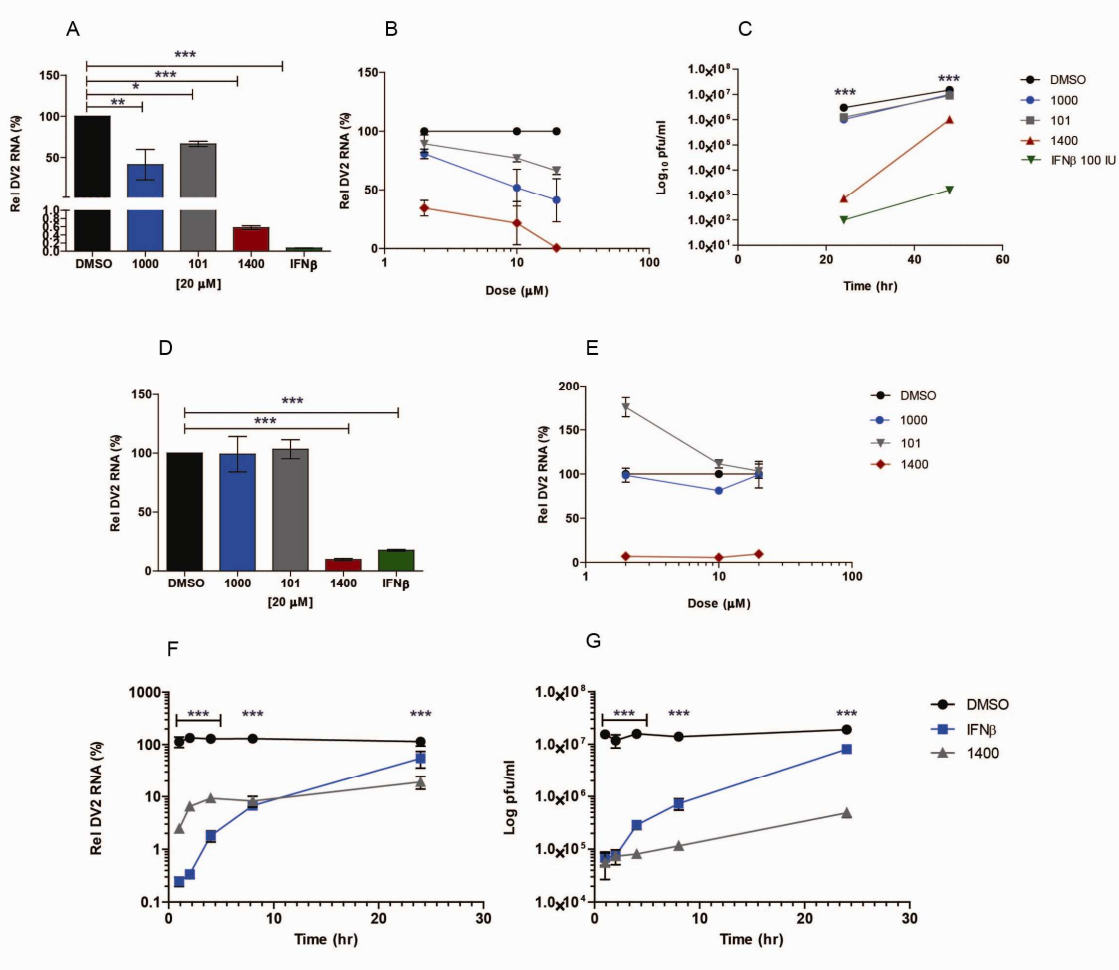


***Figure 3-3. Effect of compounds in inhibiting DV2 infection.*** (A) Pre-treatment of Huh7 cells with 20 μM of 1000, 101 and 1400 for 24 hours before infecting with DV2 (MOI 1) and the relative decrease in DV2 RNA levels (%) measured 24 hours after infection by RT-PCR. (B) Huh7 cells were pre-treated with a dose range of 20, 10, 2 μM of 1000, 101 and 1400 for 24 hours before infection with DV2 (MOI 1) and the relative decrease in DV2 RNA levels (%) measured 24 hours after infection by RT-PCR. (C) Pre-treatment of Huh7 cells with 20 μM of 1000, 101 and 1400 for 24 hours before infecting with DV2 (MOI 1) and the cell culture supernatants were collected 24 and 48 hours after infection and the infectious virus particles measured by plaque assay on Vero cells. Results shown are average infectious virus particles at 24 and 48 hours calculated per milliliter

cell culture supernatant. (D) Huh7 cells were infected with DV2 (MOI 0.1) for 2-4 hours and were treated with 20 μM of compounds, 2-4 hours after infection and the relative decrease in DV2 RNA levels(%) was measured at 24 hours after infection by RT-PCR. (E) Huh7 cells were infected with DV2 (MOI 0.1) for 2-4 hours and were treated with a dose range of 20, 10, and 2 μM of compounds, 2-4 hours after infection and the relative decrease in DV2 RNA levels(%) was measured at 24 hours after infection by RT-PCR. The relative levels of virus were calculated by RT-PCR as fold change over DMSO-treated controls, normalized to GAPDH using the ΔΔCT method. Results are average of two independent experiments. Error bars represent standard deviations. Statistical test used was one-way with Dunnett's multiple comparison test or Two-way ANOVA with Bonferroni posttests *** represents $p < 0.001$, ** $p< 0.01$, * $p<0.05$, ns not significant.

In this case, 20μM of each compound was administered to human hepatoma Huh7 cells 24 hrs prior to infection with DV serotype 2 (DV2) at an MOI of 1. KIN1000 and KIN101 treatment both resulted in moderate reduction in intracellular DV2 RNA levels as determined by real-time qPCR and compared to DMSO treatment control, whereas treatment with 100 IU/mL IFNβ or KIN1400 potently suppressed viral RNA levels (Figure 3-3A). Although all KIN compounds demonstrate dose-dependent suppression of DV2 RNA levels in cells, KIN1400 is by far the most potent among the compounds tested, demonstrating a greater than 50% decrease in viral RNA levels at 2μM concentration (Figure 3-3B). This corresponded to an almost 4-log drop in infectious DV2 particle production at 24 hrs post-infection, in contrast to the 5-log drop that was achieved with IFNβ treatment relative to DMSO treatment control (Figure 3-3C). When administered at 2-4 hrs post-infection, only KIN1400 reduced intracellular DV2 RNA levels and its effects at 20μM is equivalent or better than that achieved with 100 IU/mL IFNβ treatment (Figure 3-3D, E).

Taken together, this work identifies KIN1400 as a compound that can potently inhibit flaviviruses WNV and DV2 in cultured cells, whether administered prophylactically prior to infection or therapeutically at times post-infection. To define the kinetics of KIN1400 antiviral action, a time-of-addition study was conducted to determine the duration of time after DV2 infection when KIN1400 could potently suppress DV2 replication. For this purpose, cells infected with DV2 at an MOI of 1 were treated with 20μM 1400 at 1, 2, 4, 8 and 24 hours. The DV2 viral RNA levels in cells and infectious viral particle numbers in cell culture supernatant after 48 hrs post-infection were measured. As control, DV2 infected cells were similarly treated with DMSO or IFNβ at 100 IU/mL. KIN1400 at 20 μM and IFNβ at 100 U/ml were both effective in reducing viral RNA levels in cells (Figure 3-3F) and infectious DV2 particle production (Figure 3-3G) when administered at all time points even 24hrs post-infection. However, as expected, the sooner KIN1400 and IFNβ were administered after DV2 infection, the greater their antiviral effect. These data indicate that KIN1400 can inhibit viral replication and infectivity even when administered at times approaching peak viral replication (24 hrs). These data demonstrates KIN1400 is a potent antiviral agent against two different flaviviruses of public health concern.

**KIN1400 potently inhibits HCV replication.** WNV and DV are both mosquito-borne members of the *Flaviviridae* belonging to the genus *Flavivirus*. To assess whether the compounds have antiviral activity against other viruses of the *Flaviviridae,* KIN 1400 was tested for its efficacy in inhibiting HCV, which belongs to the genus *hepacivirus*.

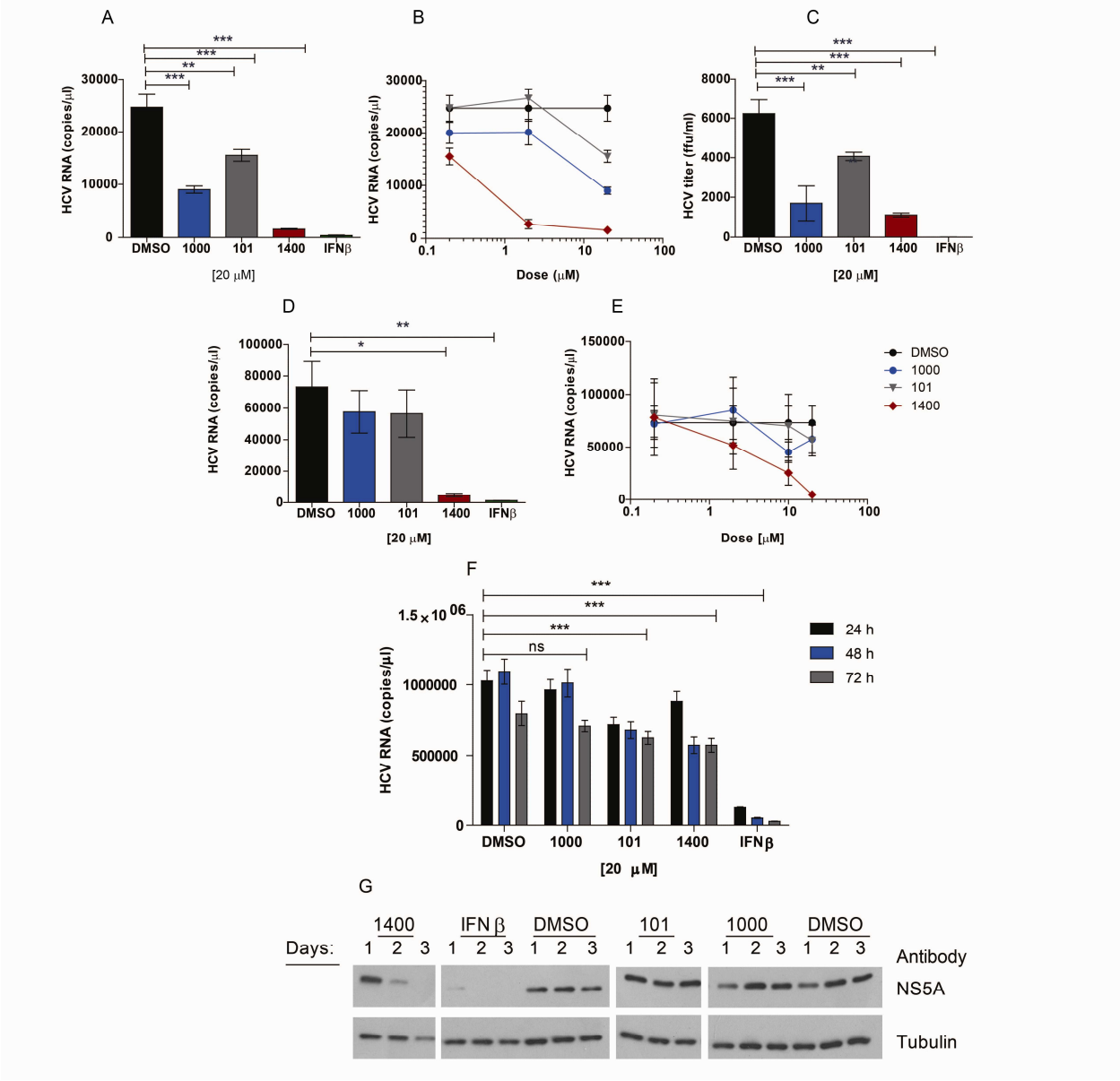


***Figure 3-4. Effect of compounds on HCV (JFH-1) infection.*** (A) Pre-treatment of Huh7 cells with 20 µM of 1000, 101 and 1400 for 24 hours before infecting with HCV (MOI 1) and the relative decrease in HCV RNA (copies/ml) measured at 24 hours post-infection by taqman RT-PCR assay. (B) Huh7 cells were pre-treated with a dose range of 20, 2, 0.2 µM of 1000, 101 and 1400 for 24 hours before infection with HCV (MOI 1) and the relative decrease in HCV RNA levels (%) measured 24 hours after infection by taqman RT-PCR assay. (C) Pre-treatment of Huh7 cells with 20 µM of 1000, 101 and 1400 for 24 hours before infecting with HCV (MOI 1) and the cell culture supernatants were collected at 48 hours after infection and the infectious virus particles measured by focus forming unit assay on Huh7.5 cells. Results shown are average focus forming unit at 48 hours calculated per milliliter cell culture supernatant. (D) Huh7 cells were infected with

HCV (MOI 0.1) for 2-4 hours and were treated with 20 μM of compounds, 2-4 hours after infection and the relative decrease in HCV RNA (copies/ml) measured at 24 hours after infection by taqman RT-PCR assay. (E) Huh7 cells were infected with HCV (MOI 0.1) for 2-4 hours and were treated with a dose range of 20, 10, 2 and 0.2 μM of compounds, 2-4 hours after infection and the relative decrease in HCV RNA (copies/ml) was measured at 24 hours after infection by taqman RT-PCR assay. (F) K2040 HCV replicon cells were treated with 20 μM of compound for 24, 48 and 72 hours and the HCV RNA (copies/ml) was measured at 24, 48 and 72 hours after infection by taqman RT-PCR assay. (G) K2040 HCV replicon cells were treated with 20 μM of compound for 24, 48 and 72 hours and the total cell lysates collected at various time points were loaded on a SDS-PAGE to evaluate HCV NS5A protein levels relative to tubulin. Results are average of two independent experiments. Error bars represent standard deviations. Statistical test used was one-way with Dunnett's multiple comparison test or Two-way ANOVA with Bonferroni posttests *** represents $p < 0.001$, ** $p< 0.01$, * $p<0.05$, ns not significant.

When administered to Huh7 cells at 20μM, 24hrs prior to infection, KIN1000 more so than KIN101 moderately inhibited HCV JFH1 RNA levels whereas KIN1400 potently suppressed HCV RNA to levels approaching that achieved with 100 IU/mL IFNβ treatment (Figure 3-4A). KIN1400 also had a dose-dependent effect in reducing HCV viral RNA (Figure 3-4B). This translated to corresponding reductions in infectious HCV released into the cell culture supernatant (Figure 3-4C). When administered 2-4 hrs post-infection, only treatments with 100 IU/mL IFNβ or KIN1400 significantly inhibited HCV RNA levels in cells as compared to DMSO treatment control (Figure 3-4D). KIN1400 effect on HCV is dose-dependent, demonstrating an EC50 of < 2 μM and ~ 2-5 μM when administered 24hrs before or 2-4 hrs after infection, respectively (Figure 3-4E).

The efficacy of the compounds in suppressing HCV in a cell culture model of HCV persistence was evaluated. K2040 replicon cells which maintain self-replicating copies of the HCV Con1 RNA [217-218] were treated with 20 μM of compounds or 100

IU/mL IFNβ and the effect they had on viral RNA as compared to DMSO treatment control was evaluated by RT-PCR at 24, 48 and 72 hrs after compound treatment. These data demonstrate that compound treatment moderately decreased HCV RNA levels in the replicon cells whereas consistent with previous reports, IFNβ at 100 IU/mL potently reduced HCV RNA levels at all time points (Figure 3-4F). Correspondingly, IFNβ more potently than KIN1400 but not KIN101 nor KIN1000 can reduce HCV NS5A protein levels in K2040 cells as measured by immunoblot analyses (Figure 3-4G). This data suggests that KIN1400 can be used to control HCV infection in cultured cells in both an acute infection as well as a chronic infection model.

**Analogs KIN1408 and 1409 retain activities similar to the KIN1400 parent.** This study identified KIN1400 as a compound that inhibited multiple members of the *Flaviviridae*, regardless of whether the compound was administered prophylactically prior to infection or therapeutically at time points after infection has been established in cells. The KIN1400 compounds belong to the class of “hydroxyquinolines”. Structural analogs of KIN1400 were designed to identify chemical modifications that can increase the drug potency as measured by IRF3 activation, enhance antiviral activity or solubility. The analogs 1407, 1408, 1409, 1410 were synthesized (Figure 3-5 A-D). All the analogs share an “aminothiazole” portion. The thiazole was substituted with benzene (KIN1400, 1407, 1408) or a phenyl group (KIN1409 and KIN1410). All the analogs also had a substituted phenyl group with side chain groups such as trifluoromethyl-, difluoromethoxy-, or methoxy- group (Figure 3-5 A-D). When administered to

macrophage-like THP-1 cells, KIN1407, KIN1408 and KIN1409 induced innate immune genes IFIT1, IFIT2, RIG-I and Mx1 expression to levels similar to the KIN1400 parent in comparison to DMSO treatment control (Figures 3-5E). Although KIN1410 induced expression of these genes moderately, levels remained low in comparison to the other analogs.

KIN1400 analogs were also assessed in comparison to KIN1400 for their ability to cause IRF-3 nuclear translocation as a measurement of IRF-3 activation. Measurements by the ArrayScan show that KIN1400 and analogs KIN1407, 1408, 1409 and 1410 drive IRF-3 translocation into the nucleus in dose-dependent manner (Figure 3-5F) suggesting that the analogs retain the ability to activate IRF-3 similar to their parent compound KIN1400. Among the analogs tested, KIN1409 alone appears to be more potent at inducing IRF-3 activation than KIN1400 at equivalent concentrations. KIN1407 exhibits IRF-3 activity similar to KIN1400 while KIN1409 and KIN1410 demonstrate less potent activity in Huh7 cells. The analogs were evaluated for their ability to suppress DV2 infection in cultured cells. Huh7 cells were infected with DV2 at an MOI 1 and the compounds were administered to cells at the indicated concentrations 24 hrs post-infection. Total cellular RNA was collected at 48 hrs post-infection and assessed by RT-PCR for relative DV2 RNA levels as compared to DMSO treatment control. As with KIN1400 before, treatment with all four analogs resulted in similar dose-dependent reduction in DV2 RNA levels (Figure 3-5G). Consistent with its lower potency at inducing innate immune gene expression, KIN1410 demonstrate the lower potency at reducing DV2 RNA levels. These data identifies 3 analog molecules, KIN1407, KIN1408 and KIN1409 that retain the ability to drive IRF-3 activation and induce innate immune

gene expression and concomitantly suppressed DV2 RNA levels similarly to or better than the KIN1400 parent.

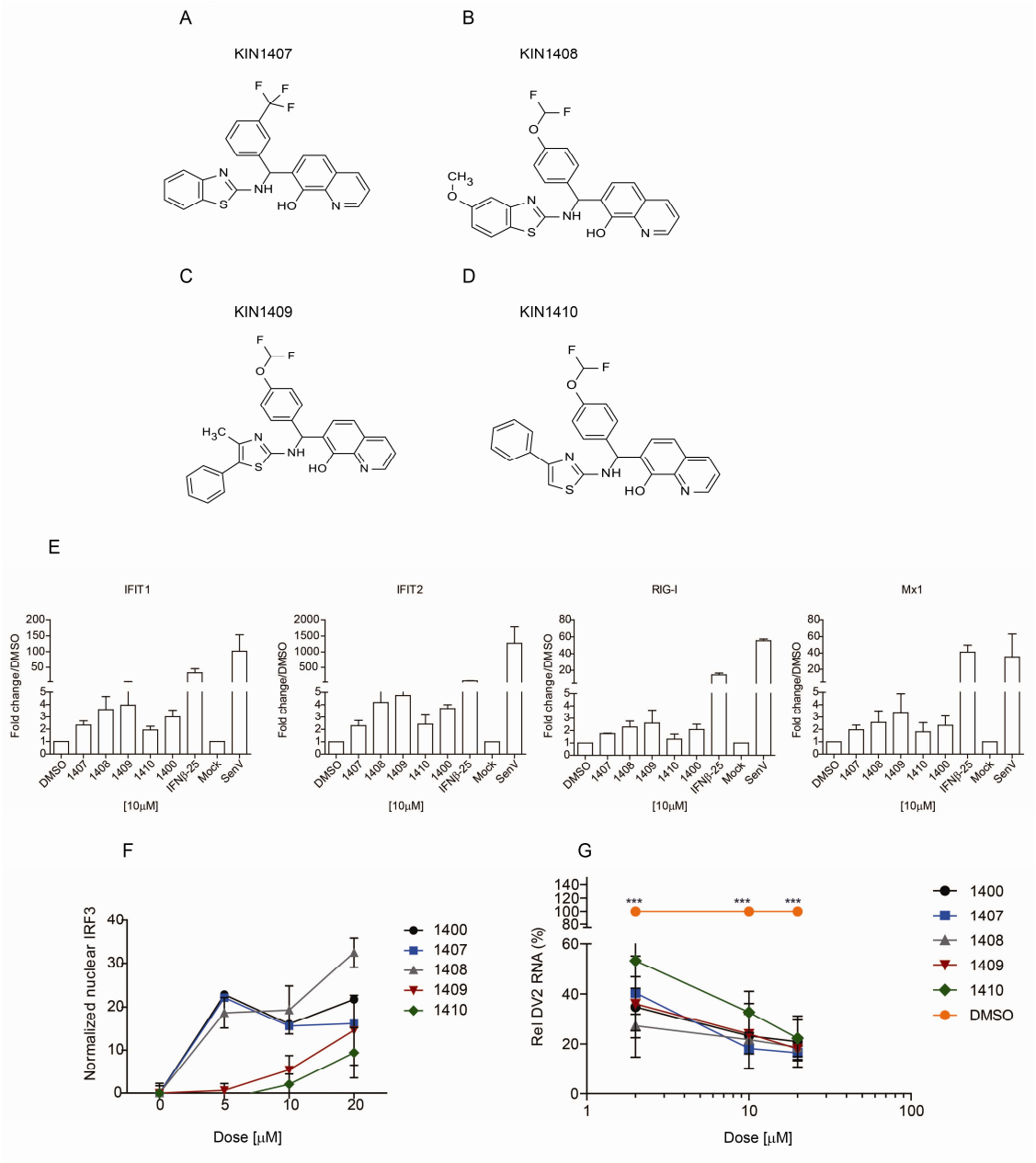


***Figure 3-5. Structure-activity relationship of 1400 and analogs.*** Structures of 1400 analogs with the side chain substitution. The analogs share an aminothiazole with either benzene (A) KIN1407, (B) KIN1408 or phenyl (C) KIN1409 (D) KIN1410 substitution. All analogs share a phenyl group and the phenyl could be substituted with trifluoromethyl-, difluoromethoxy-, fluoro-, bromo-, or methoxy- groups. (E) PMA-differentiated THP-1

cells were treated with 10 μM of compounds 1400, 1407, 1408, 1409, 1410 and the total cellular RNA was collected 20 hours after treatment and the expression of innate immune genes IFIT1, IFIT2, DDX58 (RIG-I) and Mx1was measured by RT-PCR, normalized to GAPDH and expressed as fold-induction over 0.5% DMSO treatment Results shown are from a representative experiment out of 2 and error bars represent standard deviation. (F) Huh7 cells were treated with 20, 10, 5 μM of 1400 or the analogs 1407, 1408, 1409 and 1410 and the relative amounts of nuclear IRF-3 was measured by array-scan and plotted over concentration of compound (μM). (G) Huh7 cells were infected with DV2 (MOI 1) for 2-4 hours and were treated with a dose range of 20, 10, and 2 μM at the 24 hour time point, post-infection with compounds 1400, 1407, 1408, 1409, 1410 and the relative decrease in DV2 RNA levels(%) were measured at 48 hours after infection by RT-PCR, normalized to GAPDH and expressed as fold-induction of viral RNA (%) over 0.5% DMSO treatment. Results are average of two independent experiments. Error bars represent standard deviations. Statistical test used was one-way with Dunnett's multiple comparison test or Two-way ANOVA with Bonferroni posttests *** represents $p < 0.001$, ** $p< 0.01$, * $p<0.05$, ns not significant.

**KIN1408 and KIN1409 induce a more selective gene expression profile.** Without further formulation, KIN1408 and KIN1409 appear to be more readily soluble than the KIN1400 parent and also show to be most potent in inducing an innate immune response. Therefore these two analogs were tested in gene expression analyses in comparison to the KIN1400 parent. Macrophage-like THP-1 cells were treated with KIN1400, 1408 or 1409 at 0.625, 2.5 or 10μM. Total cellular RNA was collected 20 hrs after compound treatment and analyzed for genome-wide alterations in gene expression by microarray. For control, cells were also treated with 0.5% DMSO or 25 IU/mL IFNβ. Cells infected with 25 HAU/mL SenV and cells that had been transfected with a RIG-I-specific agonistic RNA from the HCV genome, poly-U/UC (PAMP RNA) or HCV xRNA which cannot activate RIG-I signaling were also used as controls. Differential gene expression was defined as at least a 2-fold change in expression and a Benjamini-Hochberg

corrected p-value < 0.01 as compared to the appropriate negative control (XRNA for PAMP RNA and DMSO alone for all other samples).

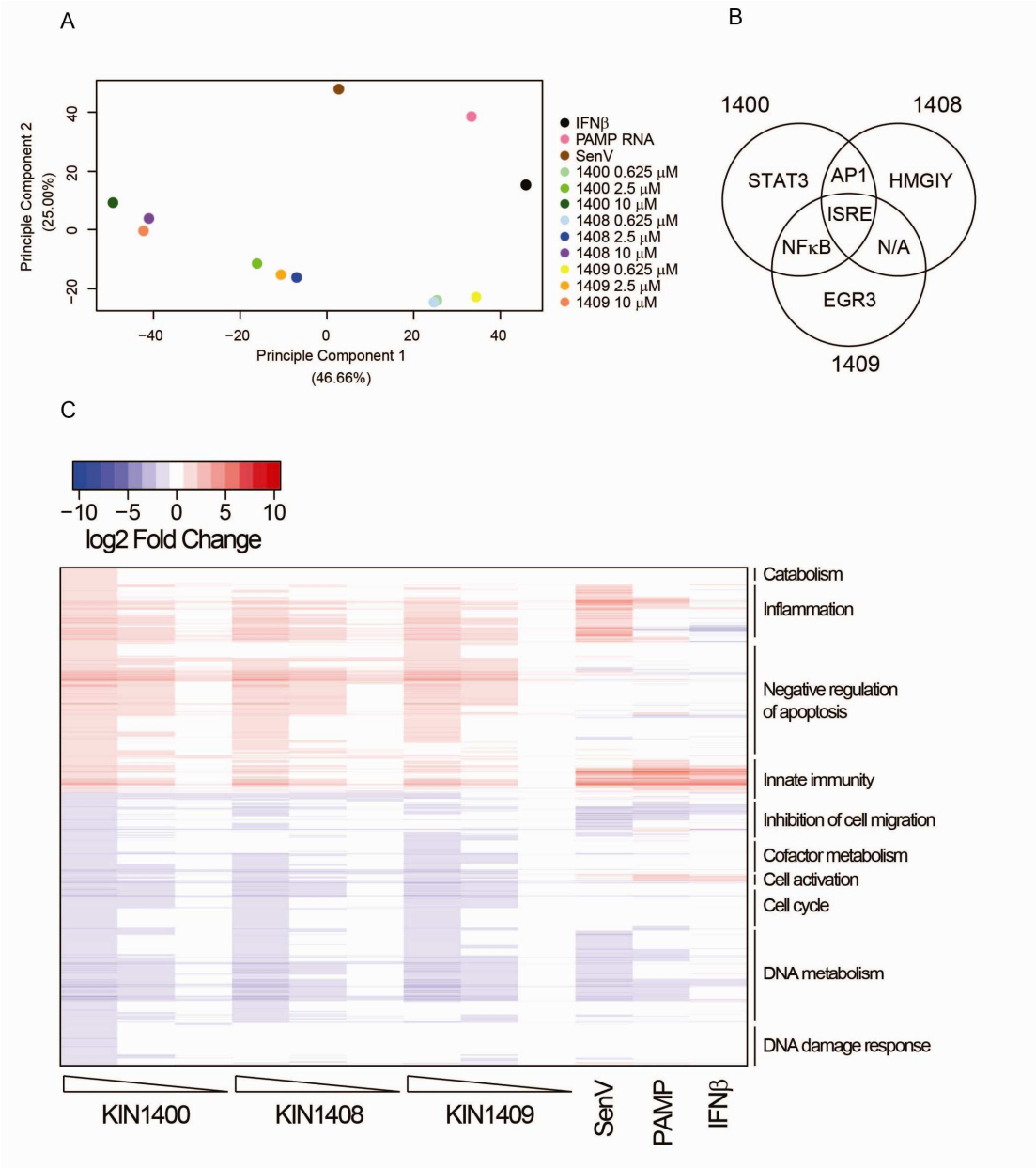


***Figure 3-6. Genomics analysis of 1400, 1408 and 1409 treatment.*** PMA-differentiated THP-1 cells were treated with 10, 2.5 and 0.625 μM of compounds 1400, 1408 and 1409 for 20 hours. (A) Two-dimensional principle components analysis shows patterns among gene expression profiles across SenV, IFNβ, HCV PAMP, 1400, 1408 and 1409 treatments. (B) Transcription factors up-regulated and enriched that are unique and

common to 1400, 1408 and 1409 treatments from the microarray data analysis (C) Heatmap showing differentially expressed genes sorted based on hierarchical clustering using correlation as a distance measure. Gene clusters were classified by the most highly enriched gene ontology biological process.

Two-dimensional principle components analysis was used to identify patterns among gene expression profiles across treatments (Figure 3-6A). Expression profiles of the KIN1400 family of compounds showed a dose-dependent change across the 3 doses tested, and the 3 compounds grouped together at each dose. Furthermore, the expression profile of cells treated with the KIN compounds was distinct from that of IFNβ treatment, HCV PAMP transfection or SenV infection. This result demonstrated that the KIN1400 series of compounds induced a unique profile of gene expression. The transcription factors that were up-regulated by KIN1400, 1408 and 1409 were analyzed and a Venn diagram was used to identify the transcription factors that are unique and common to all three compounds. All three compounds drive IRF3 activation, defined as ISRE in the Venn diagram (Figure 3-6B). Next, all genes differentially expressed in at least one treatment were plotted in a heatmap (Figure 3-6C). The rows of the heatmap were sorted based on hierarchical clustering using correlation as a distance measure. Gene clusters were classified by the most highly enriched gene ontology biological process. Patterns of gene expression across doses demonstrate that the three compounds induce comparable changes in gene expression. Additionally, many genes regulated by the KIN compounds are also differentially expressed during IFNβ treatment, PAMP RNA transfection or SenV infection, consistent with shared induction of innate immune antiviral responses. Finally, the parental KIN1400 compound primarily differs from the analogs in its induction of a set of genes involved in catabolism and its

repression of a set of genes involved in the DNA damage response. This result may explain the increased cytostatic effect of the KIN1400 parent compound as compared with the KIN1408 and KIN1409 analogs (data not shown). Importantly, the KIN1408 and KIN1409 analog compounds are highly comparable to the parental 1400 compound in their induction of innate immune and inflammatory-related genes, supportive of their comparable antiviral profiles against a number of viruses.

**KIN1400 analogs have broad-spectrum antiviral activity and can recruit immune cells in vivo.** KIN1408 was tested for its ability to suppress EBOV (Zaire). Human endothelial HUVEC cells were pre-treated with 0.5% DMSO or KIN1408 at 1 or 5μM for 24 hours before infection with EBOV at an MOI of 0.5 for 1 hour and post-infection treated with media supplemented with DMSO or KIN1408 and kept on cells for the remainder of the experiment. Infectious viral particles in the cell culture supernatants at 96 hrs post-infection were measured by plaque assay. Treatment of cells with 5μM KIN1408 was sufficient to cause a 1.5 log decrease in infectious virus particles produced in the 96 hour supernatant as compared to the treatment with DMSO, clearly confirming that 1408 is inhibitory against EBOV (Figure 3-7A). Similarly the inhibitory effect of 1400 and analogs; 1408 and 1409 were tested on other RNA viruses from different families. The antiviral activity of the KIN1400 and analogs were tested in controlling IAV infection. A titration of 10, 2.5 and 0.6 μM of KIN1400, 1408 and 1409 were tested after infection with IAV at a MOI 0.1. The 24 hour supernatants had significant decrease in infectious viral particles at all the doses tested confirming that KIN1400 and analogs are antiviral

against IAV that belongs to the family *Orthomyxoviridae* (Figure 3-7B). To test the antiviral activity of the KIN1400 family against *Paramyxoviridae* a titration of 3, 0.3, 0.1, 0.03 μM of KIN1400 and analogs were tested in controlling RSV infections. HeLa cells were infected with RSV at a MOI 0.1 and a dose titration of the compounds was added to the cells after infection. There was a log decrease in the infectious virus particles produced in the 48 hour supernatant when treated with KIN1400, 1408 or 1409 at a concentration of > 3 μM (Figure 3-7C). This data confirms that in addition to numerous members of the *Flaviviridae*, KIN1400 family compounds can also suppress infection by the families *Filoviridae*, *Orthomyxoviridae* and *Paramyxoviridae* in cultured cells, suggesting the potential for this class of molecules as novel antiviral agents that can broadly target many RNA viruses.

Finally, to test the ability of the compounds to trigger immune cell recruitment *in vivo,* the absolute numbers of cells recruited to the peritoneal cavity at 72 hours and the activation states of these cells were compared after intra-peritoneal injection with1408 or 1409 or DMSO administration. KIN1409 efficiently triggered immune cell recruitment of $CD11b^{+}/CD11c^{+}$ double positive cells. The immune cells that were recruited by 1409 had significantly higher upregulation of the activation marker Ly6C as well as MHC class II molecules compared to DMSO treatment (Figure 3-7 D). KIN1409 also triggered significantly more recruitment of $CD11b^{+}$ cells in the peritoneal cavity at 72 hours compared to the DMSO control. The immune cells recruited were more activated as represented by the activation marker Ly6C compared to DMSO control (Figure 3-7 D). This *in vivo* study confirms that KIN1409 can drive immune cell recruitment of

macrophages represented by $CD11b^+$ cells as well myeloid dendritic cells $CD11b^+/CD11c^+$ double positive cells after compound administration. Thus KIN1409 once formulated can be tested for its antiviral efficacy *in vivo* in murine model of WNV pathogenesis. These compounds are well positioned as they are able to recruit antigen presenting cells as well as are able to drive RLR-responsive antiviral genes that are necessary for controlling RNA viruses.

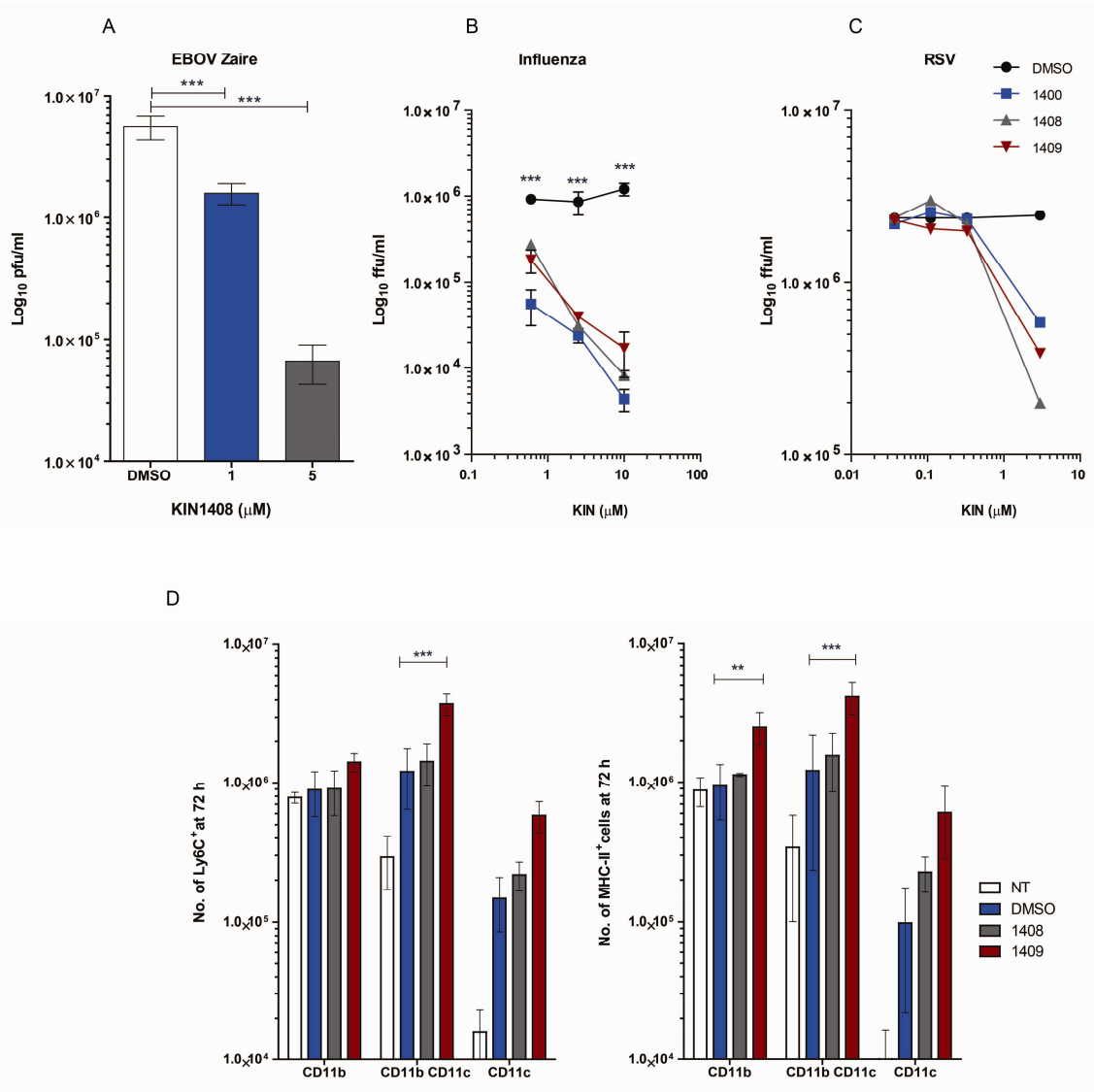

***Figure 3-7. Broad-spectrum antiviral effect and invivo immune cell recruitment by of KIN1400 analogs.*** (A) Normal primary human umbilical vein endothelial cells (HUVECs) were treated with 5 and 1 μM of 1408 or culture media for 22 hours and then infected with EBOV (MOI 0.5) for 1 hour and then replaced with media containing the compound. The cell culture supernatants were collected at 96 hours after infection, clarified by centrifugation (removal of cell debris) and the infectious virus particles measured by plaque assay on Vero cells. Results shown are average infectious virus particles at 96 hours calculated per milliliter cell culture supernatant, and analyzed for statistical significance by two-way Anova with Bonferroni posttests. *** represents $p<0.001$. (B) HEK293 cells were infected with Influenza A H3N2 strain, A/Udorn/72 at a MOI 0.1. The supernatants were collect at 24 hours and titered on MDCK cells and immunostained with FITC-coupled influenza A NP monoclonal antibody and the focus forming unit per ml was measured on array scan. (C) HeLa cells were infected with RSV, ATCC #VR-1540 (A2 strain) at a MOI 0.1. The 48 hours supernatants were collected and tittered on HeLa cells and immunostained with antibody to 47-49 kDa Fusion Protein of RSV as the primary antibody, and goat anti-mouse FITC conjugated secondary antibody and the focus forming unit per ml was measured on array scan. Statistical significance was tested by two-way Anova with Bonferroni posttests. *** represents $p<0.001$. (D) C57BL/6 mice were injected with 20 mg/kg of compound dissolved in 100% DMSO through intra-peritoneal injection and the immune cells recruited at 72 hours were collected by peritoneal lavage and the cells were counted and stained with Ly6C and MHC Class II antibodies among the $CD11b^+$, $CD11b^+/CD11C^+$ double positive and $CD11c^+$ population of cells. Statistical significance was tested by two-way Anova with Bonferroni posttests. *** represents $p<0.001$, ** $p<0.01$.

## Discussion

The RLRs are essential PRRs that are triggered in response to sensing RNA viruses in the cytoplasm. Subsequent signaling induces innate immune gene expression and establishes an antiviral state that is necessary for controlling RNA virus infections. This work was focused on developing novel therapeutics that can target this pathway as an intervention to limit and control RNA virus infections. A small molecule diversity library designed based on the RIG-I binding pocket was used to screen for compounds that can trigger IRF3 activation and nuclear translocation in Huh7 reporter cells in a dose-dependent manner [212]. The innate immune response of these compounds were

tested using differentiated THP1 cells and identified that the KIN 1400 induces a broad-spectrum antiviral profile. KIN 1400 induces RLR-dependent genes: RIG-I (DDX58), IFIT1, IFIT2, MX1, OAS1 and IFITM1 expression. The innate immune genes control viruses at different stages of their lifecycle. The antiviral gene OAS3 binds and degrades viral and cellular RNA, IFIT1 and 2 inhibit protein synthesis, MX1 wraps around viral nucleocapsids to prevent intracellular trafficking, and RIG-I and OAS induce secretion of IFN α/β to establish an antiviral state that can limit viral replication and spread [136]. Though the compounds were selected based on their IRF3 activation, the KIN compounds differentially induce a discrete sub-set of antiviral genes and proinflammatory cytokines suggesting that different compounds could be targeted for different viruses depending on the essential genes required for controlling specific viruses. Correspondingly, 1400 was most effective in controlling viruses of the family Flaviviridae and Filoviridae at concentrations ≥ 2 μM when pre-treated 24 hours prior to virus infection. Compound 1000 was effective in inhibiting DV2 RNA levels at concentrations ≥ 10 μM and compounds 1000 and 101 were effective in inhibiting HCV RNA levels at concentrations ≥ 0.2 μM and ≥ 20 μM respectively, when pre-treated 24 hours before infection. Upon post-infection treatment at 2-4 hours after infection, 1400 at concentrations ≥ 2 μM was effective in decreasing WNV, DV and HCV replication. A time of addition analysis of 1400 after DV2 infection confirmed that 1400 could be used to control viral infections even after viral replication has peaked. The HCV replicon K2040 system was used to study the antiviral effect of the compounds. The concerns about entry and egress of the virus is negated with the replicon system and the direct effect of the compound on decreasing viral RNA replication or inhibiting viral protein

synthesis can be evaluated in this system. Compounds 101 and 1400 (20 μM) effectively decreased viral RNA replication at 24, 48 and 72 hour time points and compounds 1400 (20 μM) at 48/72 hours effectively inhibited NS5A viral protein synthesis. It is difficult to discern from these experiments if the compounds have a direct effect on inhibiting viral protein synthesis or whether the decrease in availability of viral RNA transcripts resulted in a concomitant decrease in NS5A protein levels.

This study identifies 1400 as a broad spectrum antiviral that is effective prophylactically and therapeutically against viruses of the *Flaviviridae* and *Filoviridae* family. Structural analogs of 1400 increase IRF3 nuclear translocation, antiviral potency, solubility and evaluate the effect of side change substitution. This led us to identify compounds 1408 and 1409 that could potently drive IRF3 activation in a dose-dependent manner and were effective at a concentration of ≥ 2 μM in inhibiting WNV and DV replication even when treated at 24 hours after infection, once the peak of viral replication has been reached.

To better understand the signaling pathways essential for the KIN 1400 to drive an antiviral effect, HEK293 were transfected with dominant negative IRF3 (IRF3-DN) and the induction of IFIT2 expression by KIN 1400 was measured. The IFIT2 expression was completely abolished in the presence of dominant negative IRF3 confirming the requirement for IRF3 activation for KIN 1400 to signal the innate immune response. Binding studies with tagged compounds can identify molecules that directly interact with the compounds and narrow down the pathways involved in antiviral signaling.

This study was designed as a proof-of-concept to establish that activation of IRF3 and triggering RLR-specific innate immune genes can be an effective approach in controlling RNA virus infections through small-molecule intervention. The importance of the RLR pathway in controlling RNA viruses is highlighted by the viral antagonism of the pathway by RNA viruses, WNV, DV, HCV, influenza, Ebola and HIV. Compounds that drive a RLR response can overwhelm the virus with a robust innate immune response and therefore assist in early clearance of the virus. This approach has several advantages that make it more desirable than conventional intervention strategies. The compounds target the host genes instead of the viral genes and therefore could prevent viral resistance mutations that are common in RNA viruses. Additionally, the compounds induce germ-line encoded host innate immune genes that are antiviral and therefore could be effectively used as a first line of defense in controlling newly emerging RNA viruses, even when little information about the virus is available. The compounds could be broad-spectrum, pan-genus or pan-family inhibitors as the host innate immune genes are targeted by the small molecules. The innate immune genes induced by the compounds target a wide variety of antiviral genes that work at inhibiting viruses at different stages of the viral life cycle and therefore could be effective against viral quasispecies widely prevalent among RNA viruses.

Testing the compounds in the *in vivo* murine model of West Nile virus pathogenesis can help understand the role of these compounds in prophylactically and therapeutically controlling viral replication in an infection setting. The animal study can help evaluate if the compounds are able to prevent neuroinvasion of the virus into the blood-brain barrier. Formulating the compounds to increase their bioavailability and

optimizing the routes of delivery may be crucial before the drugs can be tested in an *in vivo* model.

## Acknowledgements

This work was supported by National Institutes of Health (NIH/NIAID #1R01AI098943-01, Innate Immune Antivirals for Biodefense) and University of Washington/Fred Hutchinson Cancer Research Center Viral Pathogenesis Training Grant (T32AI083203). I would like to thank Ran Dong, Megan L. Knoll for assisting with animal studies, Courtney R. Wilkins for microarray analysis, Chad Mire (UTMB) for Ebola infection studies, Shari Kaiser for influenza and RSV infection studies, Jeff Posakony and Kerry Fowler, Kineta Inc. for designing and synthesizing compounds, Sunil Thomas, Matthew K. Muramatsu, Aimee McMillan and Gabriele Blahnik for technical assistance and Renee Ireton for antiviral project management. I would finally like to thank Alison Kell, Amy stone, Tien-Ying Hsiang and Amina Negash for reading this thesis and giving me constructive feedback.

## Chapter 4. Future work and conclusion

### DHX15 is a PRR that works as a PAMP co-receptor and RLR interacting protein

I have identified a novel DExD/H box RNA helicase, DHX15, as a positive regulator of interferon induction in response to RNA virus infections. My work identifies DHX15, as a RIG-I and MDA5 interacting protein that works as a PRR and facilitates viral RNA binding. DHX15 is constitutively expressed and ubiquitously present in multiple cell types, whereas RIG-I is expressed at very low levels in the steady-state and is induced on sensing viral RNA. The complex of RIG-I bound to DHX15 synergistically bind poly (I:C) than either protein alone suggesting that the presence of DHX15 dynamically alters the affinity of RIG-I for viral RNA. DHX15 also binds the HCV PAMP (poly-U/UC) with greater affinity than RIG-I and with high specificity as DHX15 is able to discriminate between the HCV PAMP and the HCV xRNA. Therefore the model that I propose is that DHX15 binds viral RNA, both ssRNA as well as dsRNA with high affinity and triggers the first round of low-level interferon induction which leads to the upregulation of RLRs, sensitization of the RLRs for PAMP recognition and binding and RLR activation.

The role of DHX15 in RNA metabolism and pre-mRNA splicing is well established [195-196, 198]. DHX15 binds cellular RNA in the context of mRNA splicing. My data suggest that DHX15 has a dual role and can differentiate between signaling competent (HCV poly-U/UC) and signaling-incompetent RNA (HCV xRNA). The central question of DExD/H box helicases in innate immune signaling is how these RNA helicases discriminate between cellular and non-self viral RNA? Does the discrimination

of self versus non-self RNA occur through the recruitment of a distinct set of co-factors or are these functions compartmentalized to different organelles, thereby separating the innate immune sensing function from its role in cellular RNA metabolism or splicing? DHX15 is alternatively spliced at the mRNA level and this creates 6 or more isoforms of DHX15 at the mRNA level. Identifying whether different isoforms of DHX15 could be regulating different functions could identify specific isoforms that regulate innate immune signaling and RNA metabolism.

This work suggests that DHX15 interacts with the RLRs (RIG-I and MDA5) and MAVS. The RLRs form a signaling complex on the intracellular membranes called the MAM, which facilitates the recruitment of signaling factors that amplify the initial response. Evaluating whether DHX15 has a role in stabilizing the complex of RLRs and MAVS at the MAM will delineate whether DHX15 has a role in the formation of the "signalosome" complex at the intracellular membranes. My data also suggest that DHX15 is a CARD interacting protein that can bind RIG-I, MDA5 and MAVS. Validating the presence of RIG-I, DHX15 and MAVS as a complex in a virus-infected cell through either microscopy or tandem immunoprecipitation will confirm the presence of a virus-inducible ternary complex of RIG-I, DHX15 and MAVS. RIG-I translocation to the MAM has been reported through membrane fractionation studies [28, 36]. Given that DHX15 interacts with RIG-I basally, evaluating whether DHX15 translocates with RIG-I to the MAM upon RIG-I activation will narrow down the functional role of DHX15 as a RIG-I interacting protein.

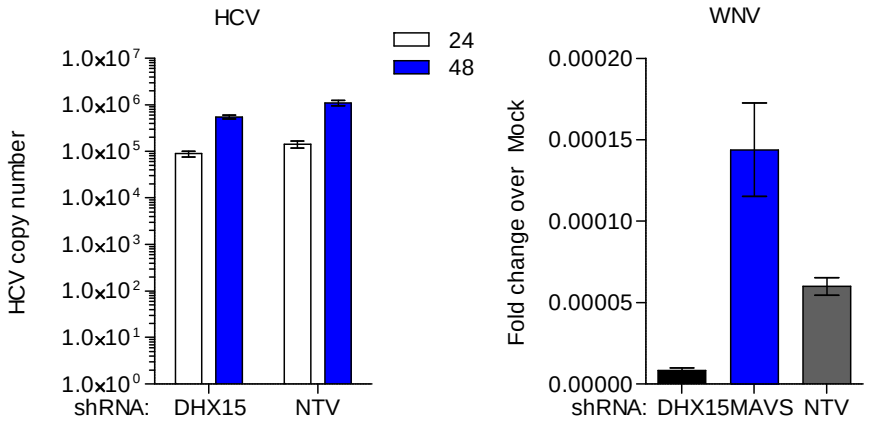


***Figure 4-1. DHX15 is necessary for the replication of viruses of the family Flaviviridae.*** The DHX15 knockdown and control NTV Huh7 cells were infected with HCV (JFH-1, MOI 0.25) and WNV (Madagascar strain, MOI 0.1). The viral RNA was measured at 24 and 48 hour by qRT-PCR using absolute quantitation taqman assay for HCV and at 48 hour time point using relative quantitation sybr green assay for WNV, normalized to GAPDH and expressed as fold-induction over Mock infection.

DHX15 knockdown cells were tested with a variety of RNA viruses like West Nile virus and hepatitis C virus. My data suggests that DHX15 is a RNA helicase that is required for the replication of both WNV and HCV viral genomes. The pro-viral role of DHX15 in assisting dengue and WNV replication has been reported previously in a high through-put screen that was conducted to identify host cellular factors that are essential for viral replication [219]. In my studies, the lack of DHX15 resulted in a significant reduction in viral RNA levels compared to the control NTV cells, suggesting that DHX15 is an essential RNA helicase that is required for replication of WNV and HCV genome (Figure 4-1) [219]. The dual role of DExD/H in antiviral immunity and in assisting with viral replication has been reported with DDX1, DDX3 and DHX9 [116, 130]. So it is not surprising, that DHX15 is yet another helicase that has a dual role in antiviral immunity and as a host factor that is recruited to replicate viral genomes of the family Flaviviridae.

This may be another mechanism by which these viruses antagonize the innate immune signaling cascade. Recruiting helicases that are necessary for antiviral immunity and blunting the innate immune responses can be a powerful approach in utilizing host factors favorably to replicate viral genomes. DHX15 is an enzyme that has both ATPase activity as well as helicase activity and could be easily targeted for antiviral therapies. Given the importance of DHX15 in replicating viral genomes, inhibiting the ATPase and helicase activity of DHX15 through enzyme inhibitors could be effective against controlling WNV, DV and HCV.

In conclusion, my work identifies DHX15 as a PRR that interacts with RIG-I and MDA5 and acts as a PAMP co-receptor potentiating RLR signaling to establish innate antiviral immunity against RNA virus infections.

**RIG-I agonists as broad-spectrum antivirals**

In the second part, I have characterized small molecule agonists that belong to the class of hydroxyquinolines as broad-spectrum antivirals. These compounds drive IRF3 activation and induce the host innate immune response and are effective in controlling and restricting RNA viruses. My work identifies KIN 1400 as a lead compound and KIN 1408 and 1409 as analogs that work against a broad range of viruses namely, WNV(Tx2002), HCV(JFH-1), DV2, Ebola (Zaire), IAV (Udorn strain, H3N2) and RSV (A2 strain). Pathway mapping of the compounds identify that IRF3 activation is required for KIN 1400 to signal. Target validation with tagged compounds may be essential to understand the exact mechanism through which the compounds are

able to inhibit the viruses. Characterizing the interaction of the compounds with the RLR's or the signaling molecules downstream of RLR activation will identify if the compounds are truly RLR agonists that specifically target the pathway. The compounds once formulated can be used in animal studies. Testing KIN 1408 and 1409 in the *in vivo* WNV pathogenic mouse model in a prophylactic or therapeutic treatment setting will characterize the in vivo potency of the compounds and identify if the compounds can increase the survival of mice infected with WNV. The ability of the compounds to prevent neuro-invasive disease can also be tested in the WNV mouse model of pathogenesis.

Formulation of the compounds can increase its solubility, bioavailability and prevent adverse effects like precipitation. An effective formulation that can deliver the compound optimally can facilitate immune cell recruiting, allow for uptake of the compounds to the lymph nodes and spleen by the antigen presenting cells. Timing the administration of the compounds and optimizing the route of administration so that the compounds reach the lymph nodes around the same time as the viral peak can promote early clearance of the virus.

## References


1. Imaizumi, T., et al., *Involvement of retinoic acid-inducible gene-I in inflammation of rheumatoid fibroblast-like synoviocytes.* Clin Exp Immunol, 2008. **153**(2): p. 240-4.
2. Imaizumi, T., et al., *Retinoic acid-inducible gene-I (RIG-I) is induced by IFN-{gamma} in human mesangial cells in culture: possible involvement of RIG-I in the inflammation in lupus nephritis.* Lupus, 2010. **19**(7): p. 830-6.
3. Imaizumi, T., et al., *Expression of retinoic acid-inducible gene-I (RIG-I) in macrophages: possible involvement of RIG-I in atherosclerosis.* J Atheroscler Thromb, 2007. **14**(2): p. 51-5.
4. Kitamura, H., et al., *Cytokine modulation of retinoic acid-inducible gene-I (RIG-I) expression in human epidermal keratinocytes.* J Dermatol Sci, 2007. **45**(2): p. 127-34.
5. Tsugawa, K., et al., *Expression of mRNA for functional molecules in urinary sediment in glomerulonephritis.* Pediatr Nephrol, 2008. **23**(3): p. 395-401.
6. Kato, H., et al., *Cell type-specific involvement of RIG-I in antiviral response.* Immunity, 2005. **23**(1): p. 19-28.
7. Kang, D.C., et al., *Expression analysis and genomic characterization of human melanoma differentiation associated gene-5, mda-5: a novel type I interferon-responsive apoptosis-inducing gene.* Oncogene, 2004. **23**(9): p. 1789-800.
8. Yoneyama, M., et al., *Shared and unique functions of the DExD/H-box helicases RIG-I, MDA5, and LGP2 in antiviral innate immunity.* J Immunol, 2005. **175**(5): p. 2851-8.
9. Yoneyama, M., et al., *The RNA helicase RIG-I has an essential function in double-stranded RNA-induced innate antiviral responses.* Nat Immunol, 2004. **5**(7): p. 730-7.
10. Yount, J.S., T.M. Moran, and C.B. Lopez, *Cytokine-independent upregulation of MDA5 in viral infection.* J Virol, 2007. **81**(13): p. 7316-9.
11. Loo, Y.M., et al., *Distinct RIG-I and MDA5 signaling by RNA viruses in innate immunity.* J Virol, 2008. **82**(1): p. 335-45.
12. Sumpter, R., Jr., et al., *Regulating intracellular antiviral defense and permissiveness to hepatitis C virus RNA replication through a cellular RNA helicase, RIG-I.* J Virol, 2005. **79**(5): p. 2689-99.
13. Yoneyama, M. and T. Fujita, *Function of RIG-I-like receptors in antiviral innate immunity.* J Biol Chem, 2007. **282**(21): p. 15315-8.
14. Johnson, C.L. and M. Gale, Jr., *CARD games between virus and host get a new player.* Trends Immunol, 2006. **27**(1): p. 1-4.
15. Loo, Y.M. and M. Gale, Jr., *Immune signaling by RIG-I-like receptors.* Immunity, 2011. **34**(5): p. 680-92.
16. West, A.P., G.S. Shadel, and S. Ghosh, *Mitochondria in innate immune responses.* Nat Rev Immunol, 2011. **11**(6): p. 389-402.
17. Sen, G.C., *Viruses and interferons.* Annu Rev Microbiol, 2001. **55**: p. 255-81.
18. Wang, B.X. and E.N. Fish, *The yin and yang of viruses and interferons.* Trends Immunol, 2012. **33**(4): p. 190-7.
19. MacMicking, J.D., *Interferon-inducible effector mechanisms in cell-autonomous immunity.* Nat Rev Immunol, 2012. **12**(5): p. 367-82.
20. Suthar, M.S., M.S. Diamond, and M. Gale, Jr., *West Nile virus infection and immunity.* Nat Rev Microbiol, 2013. **11**(2): p. 115-28.
21. Saito, T., et al., *Regulation of innate antiviral defenses through a shared repressor domain in RIG-I and LGP2.* Proc Natl Acad Sci U S A, 2007. **104**(2): p. 582-7.

22. Cui, S., et al., *The C-terminal regulatory domain is the RNA 5'-triphosphate sensor of RIG-I.* Mol Cell, 2008. **29**(2): p. 169-79.
23. Kawai, T., et al., *IPS-1, an adaptor triggering RIG-I- and Mda5-mediated type I interferon induction.* Nat Immunol, 2005. **6**(10): p. 981-8.
24. Loo, Y.M., et al., *Viral and therapeutic control of IFN-beta promoter stimulator 1 during hepatitis C virus infection.* Proc Natl Acad Sci U S A, 2006. **103**(15): p. 6001-6.
25. Meylan, E., et al., *Cardif is an adaptor protein in the RIG-I antiviral pathway and is targeted by hepatitis C virus.* Nature, 2005. **437**(7062): p. 1167-72.
26. Seth, R.B., et al., *Identification and characterization of MAVS, a mitochondrial antiviral signaling protein that activates NF-kappaB and IRF 3.* Cell, 2005. **122**(5): p. 669-82.
27. Xu, L.G., et al., *VISA is an adapter protein required for virus-triggered IFN-beta signaling.* Mol Cell, 2005. **19**(6): p. 727-40.
28. Horner, S.M., et al., *Mitochondrial-associated endoplasmic reticulum membranes (MAM) form innate immune synapses and are targeted by hepatitis C virus.* Proc Natl Acad Sci U S A, 2011. **108**(35): p. 14590-5.
29. Jiang, F., et al., *Structural basis of RNA recognition and activation by innate immune receptor RIG-I.* Nature, 2011. **479**(7373): p. 423-7.
30. Kowalinski, E., et al., *Structural basis for the activation of innate immune pattern-recognition receptor RIG-I by viral RNA.* Cell, 2011. **147**(2): p. 423-35.
31. Rothenfusser, S., et al., *The RNA helicase Lgp2 inhibits TLR-independent sensing of viral replication by retinoic acid-inducible gene-I.* J Immunol, 2005. **175**(8): p. 5260-8.
32. Bruns, A.M. and C.M. Horvath, *Activation of RIG-I-like receptor signal transduction.* Crit Rev Biochem Mol Biol, 2012. **47**(2): p. 194-206.
33. Venkataraman, T., et al., *Loss of DExD/H box RNA helicase LGP2 manifests disparate antiviral responses.* J Immunol, 2007. **178**(10): p. 6444-55.
34. Satoh, T., et al., *LGP2 is a positive regulator of RIG-I- and MDA5-mediated antiviral responses.* Proc Natl Acad Sci U S A, 2010. **107**(4): p. 1512-7.
35. Belgnaoui, S.M., S. Paz, and J. Hiscott, *Orchestrating the interferon antiviral response through the mitochondrial antiviral signaling (MAVS) adapter.* Curr Opin Immunol, 2011. **23**(5): p. 564-72.
36. Liu, H.M., et al., *The mitochondrial targeting chaperone 14-3-3epsilon regulates a RIG-I translocon that mediates membrane association and innate antiviral immunity.* Cell Host Microbe, 2012. **11**(5): p. 528-37.
37. Ohman, T., et al., *Actin and RIG-I/MAVS signaling components translocate to mitochondria upon influenza A virus infection of human primary macrophages.* J Immunol, 2009. **182**(9): p. 5682-92.
38. Zemirli, N. and D. Arnoult, *Mitochondrial anti-viral immunity.* Int J Biochem Cell Biol, 2012. **44**(9): p. 1473-6.
39. Shih, J.W. and Y.H. Lee, *Human DExD/H RNA helicases: Emerging roles in stress survival regulation.* Clin Chim Acta, 2014. **436C**: p. 45-58.
40. Hornung, V., et al., *5'-Triphosphate RNA is the ligand for RIG-I.* Science, 2006. **314**(5801): p. 994-7.
41. Plumet, S., et al., *Cytosolic 5'-triphosphate ended viral leader transcript of measles virus as activator of the RIG I-mediated interferon response.* PLoS One, 2007. **2**(3): p. e279.
42. Habjan, M., et al., *Processing of genome 5' termini as a strategy of negative-strand RNA viruses to avoid RIG-I-dependent interferon induction.* PLoS One, 2008. **3**(4): p. e2032.
43. Luthra, P., et al., *Activation of IFN-β expression by a viral mRNA through RNase L and MDA5.* Proc Natl Acad Sci U S A, 2011. **108**(5): p. 2118-23.

44. Roth-Cross, J.K., S.J. Bender, and S.R. Weiss, *Murine coronavirus mouse hepatitis virus is recognized by MDA5 and induces type I interferon in brain macrophages/microglia.* J Virol, 2008. **82**(20): p. 9829-38.
45. McCartney, S.A., et al., *MDA-5 recognition of a murine norovirus.* PLoS Pathog, 2008. **4**(7): p. e1000108.
46. Kato, H., et al., *Differential roles of MDA5 and RIG-I helicases in the recognition of RNA viruses.* Nature, 2006. **441**(7089): p. 101-5.
47. Gitlin, L., et al., *Essential role of mda-5 in type I IFN responses to polyriboinosinic:polyribocytidylic acid and encephalomyocarditis picornavirus.* Proc Natl Acad Sci U S A, 2006. **103**(22): p. 8459-64.
48. Fredericksen, B.L., et al., *Establishment and maintenance of the innate antiviral response to West Nile Virus involves both RIG-I and MDA5 signaling through IPS-1.* J Virol, 2008. **82**(2): p. 609-16.
49. Saito, T., et al., *Innate immunity induced by composition-dependent RIG-I recognition of hepatitis C virus RNA.* Nature, 2008. **454**(7203): p. 523-7.
50. Schnell, G., et al., *Uridine composition of the poly-U/UC tract of HCV RNA defines non-self recognition by RIG-I.* PLoS Pathog, 2012. **8**(8): p. e1002839.
51. Pichlmair, A., et al., *RIG-I-mediated antiviral responses to single-stranded RNA bearing 5'-phosphates.* Science, 2006. **314**(5801): p. 997-1001.
52. Ablasser, A., et al., *RIG-I-dependent sensing of poly(dA:dT) through the induction of an RNA polymerase III-transcribed RNA intermediate.* Nat Immunol, 2009. **10**(10): p. 1065-72.
53. Chiu, Y.H., J.B. Macmillan, and Z.J. Chen, *RNA polymerase III detects cytosolic DNA and induces type I interferons through the RIG-I pathway.* Cell, 2009. **138**(3): p. 576-91.
54. Marques, J.T., et al., *A structural basis for discriminating between self and nonself double-stranded RNAs in mammalian cells.* Nat Biotechnol, 2006. **24**(5): p. 559-65.
55. Goubau, D., et al., *Antiviral immunity via RIG-I-mediated recognition of RNA bearing 5'-diphosphates.* Nature, 2014.
56. Kato, H., et al., *Length-dependent recognition of double-stranded ribonucleic acids by retinoic acid-inducible gene-I and melanoma differentiation-associated gene 5.* J Exp Med, 2008. **205**(7): p. 1601-10.
57. Pichlmair, A., et al., *Activation of MDA5 requires higher-order RNA structures generated during virus infection.* J Virol, 2009. **83**(20): p. 10761-9.
58. Saito, T. and M. Gale, Jr., *Differential recognition of double-stranded RNA by RIG-I-like receptors in antiviral immunity.* J Exp Med, 2008. **205**(7): p. 1523-7.
59. Peisley, A., et al., *Cooperative assembly and dynamic disassembly of MDA5 filaments for viral dsRNA recognition.* Proc Natl Acad Sci U S A, 2011. **108**(52): p. 21010-5.
60. Peisley, A., et al., *Kinetic mechanism for viral dsRNA length discrimination by MDA5 filaments.* Proc Natl Acad Sci U S A, 2012. **109**(49): p. E3340-9.
61. Berke, I.C., et al., *MDA5 assembles into a polar helical filament on dsRNA.* Proc Natl Acad Sci U S A, 2012. **109**(45): p. 18437-41.
62. Zust, R., et al., *Ribose 2'-O-methylation provides a molecular signature for the distinction of self and non-self mRNA dependent on the RNA sensor Mda5.* Nat Immunol, 2011. **12**(2): p. 137-43.
63. Errett, J.S., et al., *The essential, nonredundant roles of RIG-I and MDA5 in detecting and controlling West Nile virus infection.* J Virol, 2013. **87**(21): p. 11416-25.
64. Kato, H., K. Takahasi, and T. Fujita, *RIG-I-like receptors: cytoplasmic sensors for non-self RNA.* Immunol Rev, 2011. **243**(1): p. 91-8.
65. Sun, Z., et al., *Phosphorylation of RIG-I by casein kinase II inhibits its antiviral response.* J Virol, 2011. **85**(2): p. 1036-47.

66. Gack, M.U., et al., *Phosphorylation-mediated negative regulation of RIG-I antiviral activity.* J Virol, 2010. **84**(7): p. 3220-9.
67. Maharaj, N.P., et al., *Conventional protein kinase C-alpha (PKC-alpha) and PKC-beta negatively regulate RIG-I antiviral signal transduction.* J Virol, 2012. **86**(3): p. 1358-71.
68. Nistal-Villan, E., et al., *Negative role of RIG-I serine 8 phosphorylation in the regulation of interferon-beta production.* J Biol Chem, 2010. **285**(26): p. 20252-61.
69. Wies, E., et al., *Dephosphorylation of the RNA sensors RIG-I and MDA5 by the phosphatase PP1 is essential for innate immune signaling.* Immunity, 2013. **38**(3): p. 437-49.
70. Gack, M.U., *Mechanisms of RIG-I-like receptor activation and manipulation by viral pathogens.* J Virol, 2014. **88**(10): p. 5213-6.
71. Gack, M.U., et al., *TRIM25 RING-finger E3 ubiquitin ligase is essential for RIG-I-mediated antiviral activity.* Nature, 2007. **446**(7138): p. 916-920.
72. Oshiumi, H., et al., *Riplet/RNF135, a RING finger protein, ubiquitinates RIG-I to promote interferon-beta induction during the early phase of viral infection.* J Biol Chem, 2009. **284**(2): p. 807-17.
73. Oshiumi, H., et al., *The ubiquitin ligase Riplet is essential for RIG-I-dependent innate immune responses to RNA virus infection.* Cell Host Microbe, 2010. **8**(6): p. 496-509.
74. Peisley, A., et al., *Structural basis for ubiquitin-mediated antiviral signal activation by RIG-I.* Nature, 2014. **509**(7498): p. 110-4.
75. Friedman, C.S., et al., *The tumour suppressor CYLD is a negative regulator of RIG-I-mediated antiviral response.* EMBO Rep, 2008. **9**(9): p. 930-6.
76. Cui, J., et al., *USP3 inhibits type I interferon signaling by deubiquitinating RIG-I-like receptors.* Cell Res, 2014. **24**(4): p. 400-16.
77. Fan, Y., et al., *USP21 negatively regulates antiviral response by acting as a RIG-I deubiquitinase.* J Exp Med, 2014. **211**(2): p. 313-28.
78. Arimoto, K., et al., *Negative regulation of the RIG-I signaling by the ubiquitin ligase RNF125.* Proc Natl Acad Sci U S A, 2007. **104**(18): p. 7500-5.
79. Lin, R., et al., *Negative regulation of the retinoic acid-inducible gene I-induced antiviral state by the ubiquitin-editing protein A20.* J Biol Chem, 2006. **281**(4): p. 2095-103.
80. Inn, K.S., et al., *Linear ubiquitin assembly complex negatively regulates RIG-I- and TRIM25-mediated type I interferon induction.* Mol Cell, 2011. **41**(3): p. 354-65.
81. Wang, L., et al., *USP4 positively regulates RIG-I-mediated antiviral response through deubiquitination and stabilization of RIG-I.* J Virol, 2013. **87**(8): p. 4507-15.
82. Pauli, E.K., et al., *The ubiquitin-specific protease USP15 promotes RIG-I-mediated antiviral signaling by deubiquitylating TRIM25.* Sci Signal, 2014. **7**(307): p. ra3.
83. Jacobs, J.L. and C.B. Coyne, *Mechanisms of MAVS regulation at the mitochondrial membrane.* J Mol Biol, 2013. **425**(24): p. 5009-19.
84. Dixit, E., et al., *Peroxisomes are signaling platforms for antiviral innate immunity.* Cell, 2010. **141**(4): p. 668-81.
85. Hiscott, J., J. Lacoste, and R. Lin, *Recruitment of an interferon molecular signaling complex to the mitochondrial membrane: disruption by hepatitis C virus NS3-4A protease.* Biochem Pharmacol, 2006. **72**(11): p. 1477-84.
86. Horner, S.M., H.S. Park, and M. Gale, Jr., *Control of innate immune signaling and membrane targeting by the Hepatitis C virus NS3/4A protease are governed by the NS3 helix alpha0.* J Virol, 2012. **86**(6): p. 3112-20.
87. Lin, R., et al., *Dissociation of a MAVS/IPS-1/VISA/Cardif-IKKepsilon molecular complex from the mitochondrial outer membrane by hepatitis C virus NS3-4A proteolytic cleavage.* J Virol, 2006. **80**(12): p. 6072-83.

88. Higgs, R. and C.A. Jefferies, *Targeting IRFs by ubiquitination: regulating antiviral responses.* Biochem Soc Trans, 2008. **36**(Pt 3): p. 453-8.
89. Oshiumi, H., et al., *DEAD/H BOX 3 (DDX3) helicase binds the RIG-I adaptor IPS-1 to up-regulate IFN-beta-inducing potential.* Eur J Immunol, 2010. **40**(4): p. 940-8.
90. Paz, S., et al., *Ubiquitin-regulated recruitment of IkappaB kinase epsilon to the MAVS interferon signaling adapter.* Mol Cell Biol, 2009. **29**(12): p. 3401-12.
91. Paz, S., et al., *A functional C-terminal TRAF3-binding site in MAVS participates in positive and negative regulation of the IFN antiviral response.* Cell Res, 2011. **21**(6): p. 895-910.
92. Saha, S.K., et al., *Regulation of antiviral responses by a direct and specific interaction between TRAF3 and Cardif.* EMBO J, 2006. **25**(14): p. 3257-63.
93. Tang, E.D. and C.Y. Wang, *TRAF5 is a downstream target of MAVS in antiviral innate immune signaling.* PLoS One, 2010. **5**(2): p. e9172.
94. Wang, Y.Y., et al., *WDR5 is essential for assembly of the VISA-associated signaling complex and virus-triggered IRF3 and NF-kappaB activation.* Proc Natl Acad Sci U S A, 2010. **107**(2): p. 815-20.
95. Cui, J., et al., *NLRC5 negatively regulates the NF-kappaB and type I interferon signaling pathways.* Cell, 2010. **141**(3): p. 483-96.
96. Moore, C.B., et al., *NLRX1 is a regulator of mitochondrial antiviral immunity.* Nature, 2008. **451**(7178): p. 573-7.
97. Mikkelsen, S.S., et al., *RIG-I-mediated activation of p38 MAPK is essential for viral induction of interferon and activation of dendritic cells: dependence on TRAF2 and TAK1.* J Biol Chem, 2009. **284**(16): p. 10774-82.
98. Liu, S., et al., *MAVS recruits multiple ubiquitin E3 ligases to activate antiviral signaling cascades.* Elife, 2013. **2**: p. e00785.
99. Pham, A.M. and B.R. Tenoever, *The IKK Kinases: Operators of Antiviral Signaling.* Viruses, 2010. **2**(1): p. 55-72.
100. Yoboua, F., et al., *Respiratory syncytial virus-mediated NF-kappa B p65 phosphorylation at serine 536 is dependent on RIG-I, TRAF6, and IKK beta.* J Virol, 2010. **84**(14): p. 7267-77.
101. Michallet, M.C., et al., *TRADD protein is an essential component of the RIG-like helicase antiviral pathway.* Immunity, 2008. **28**(5): p. 651-61.
102. Blander, J.M., *A long-awaited merger of the pathways mediating host defence and programmed cell death.* Nat Rev Immunol, 2014. **14**(9): p. 601-18.
103. Rajput, A., et al., *RIG-I RNA helicase activation of IRF3 transcription factor is negatively regulated by caspase-8-mediated cleavage of the RIP1 protein.* Immunity, 2011. **34**(3): p. 340-51.
104. Koshiba, T., et al., *Mitochondrial membrane potential is required for MAVS-mediated antiviral signaling.* Sci Signal, 2011. **4**(158): p. ra7.
105. Onoguchi, K., et al., *Virus-infection or 5'ppp-RNA activates antiviral signal through redistribution of IPS-1 mediated by MFN1.* PLoS Pathog, 2010. **6**(7): p. e1001012.
106. Liu, X.Y., et al., *Tom70 mediates activation of interferon regulatory factor 3 on mitochondria.* Cell Res, 2010. **20**(9): p. 994-1011.
107. Fitzgerald, K.A., et al., *IKKepsilon and TBK1 are essential components of the IRF3 signaling pathway.* Nat Immunol, 2003. **4**(5): p. 491-6.
108. Vitour, D., et al., *Polo-like kinase 1 (PLK1) regulates interferon (IFN) induction by MAVS.* J Biol Chem, 2009. **284**(33): p. 21797-809.
109. Johnsen, I.B., et al., *The tyrosine kinase c-Src enhances RIG-I (retinoic acid-inducible gene I)-elicited antiviral signaling.* J Biol Chem, 2009. **284**(28): p. 19122-31.

110. Song, T., et al., *c-Abl tyrosine kinase interacts with MAVS and regulates innate immune response.* FEBS Lett, 2010. **584**(1): p. 33-8.
111. Zhong, B., et al., *The E3 ubiquitin ligase RNF5 targets virus-induced signaling adaptor for ubiquitination and degradation.* J Immunol, 2010. **184**(11): p. 6249-55.
112. You, F., et al., *PCBP2 mediates degradation of the adaptor MAVS via the HECT ubiquitin ligase AIP4.* Nat Immunol, 2009. **10**(12): p. 1300-8.
113. Maelfait, J. and R. Beyaert, *Emerging role of ubiquitination in antiviral RIG-I signaling.* Microbiol Mol Biol Rev, 2012. **76**(1): p. 33-45.
114. Ye, J. and T. Maniatis, *A prion-like trigger of antiviral signaling.* Cell, 2011. **146**(3): p. 348-50.
115. Hou, F., et al., *MAVS forms functional prion-like aggregates to activate and propagate antiviral innate immune response.* Cell, 2011. **146**(3): p. 448-61.
116. Fullam, A. and M. Schroder, *DExD/H-box RNA helicases as mediators of anti-viral innate immunity and essential host factors for viral replication.* Biochim Biophys Acta, 2013. **1829**(8): p. 854-65.
117. Pyle, A.M., *RNA helicases and remodeling proteins.* Curr Opin Chem Biol, 2011. **15**(5): p. 636-42.
118. Umate, P., N. Tuteja, and R. Tuteja, *Genome-wide comprehensive analysis of human helicases.* Commun Integr Biol, 2011. **4**(1): p. 118-37.
119. Schroder, M., M. Baran, and A.G. Bowie, *Viral targeting of DEAD box protein 3 reveals its role in TBK1/IKKepsilon-mediated IRF activation.* EMBO J, 2008. **27**(15): p. 2147-57.
120. Gu, L., et al., *Human DEAD box helicase 3 couples IkappaB kinase epsilon to interferon regulatory factor 3 activation.* Mol Cell Biol, 2013. **33**(10): p. 2004-15.
121. Soulat, D., et al., *The DEAD-box helicase DDX3X is a critical component of the TANK-binding kinase 1-dependent innate immune response.* EMBO J, 2008. **27**(15): p. 2135-46.
122. Zhang, Z., et al., *DHX9 pairs with IPS-1 to sense double-stranded RNA in myeloid dendritic cells.* J Immunol, 2011. **187**(9): p. 4501-8.
123. Sadler, A.J., et al., *An antiviral response directed by PKR phosphorylation of the RNA helicase A.* PLoS Pathog, 2009. **5**(2): p. e1000311.
124. Yoo, J.S., et al., *DHX36 enhances RIG-I signaling by facilitating PKR-mediated antiviral stress granule formation.* PLoS Pathog, 2014. **10**(3): p. e1004012.
125. Zhang, Z., et al., *DDX1, DDX21, and DHX36 helicases form a complex with the adaptor molecule TRIF to sense dsRNA in dendritic cells.* Immunity, 2011. **34**(6): p. 866-78.
126. Miyashita, M., et al., *DDX60, a DEXD/H box helicase, is a novel antiviral factor promoting RIG-I-like receptor-mediated signaling.* Mol Cell Biol, 2011. **31**(18): p. 3802-19.
127. Liu, Y., et al., *The interaction between the helicase DHX33 and IPS-1 as a novel pathway to sense double-stranded RNA and RNA viruses in myeloid dendritic cells.* Cell Mol Immunol, 2014. **11**(1): p. 49-57.
128. Ma, Z., et al., *DDX24 negatively regulates cytosolic RNA-mediated innate immune signaling.* PLoS Pathog, 2013. **9**(10): p. e1003721.
129. Taylor, K.E. and K.L. Mossman, *Recent advances in understanding viral evasion of type I interferon.* Immunology, 2013. **138**(3): p. 190-7.
130. Nagy, P.D. and J. Pogany, *The dependence of viral RNA replication on co-opted host factors.* Nat Rev Microbiol, 2012. **10**(2): p. 137-49.
131. Ariumi, Y., et al., *DDX3 DEAD-box RNA helicase is required for hepatitis C virus RNA replication.* J Virol, 2007. **81**(24): p. 13922-6.
132. Randall, G., et al., *Cellular cofactors affecting hepatitis C virus infection and replication.* Proc Natl Acad Sci U S A, 2007. **104**(31): p. 12884-9.

133. Yedavalli, V.S., et al., *Requirement of DDX3 DEAD box RNA helicase for HIV-1 Rev-RRE export function.* Cell, 2004. **119**(3): p. 381-92.
134. Andersen, J., et al., *IRF-3-dependent and augmented target genes during viral infection.* Genes Immun, 2008. **9**(2): p. 168-75.
135. Diamond, M.S. and M. Farzan, *The broad-spectrum antiviral functions of IFIT and IFITM proteins.* Nat Rev Immunol, 2013. **13**(1): p. 46-57.
136. Borden, E.C., et al., *Interferons at age 50: past, current and future impact on biomedicine.* Nat Rev Drug Discov, 2007. **6**(12): p. 975-90.
137. Goodbourn, S., L. Didcock, and R.E. Randall, *Interferons: cell signalling, immune modulation, antiviral response and virus countermeasures.* J Gen Virol, 2000. **81**(Pt 10): p. 2341-64.
138. Vladimer, G.I., M.W. Gorna, and G. Superti-Furga, *IFITs: Emerging Roles as Key Anti-Viral Proteins.* Front Immunol, 2014. **5**: p. 94.
139. Daffis, S., et al., *Cell-specific IRF-3 responses protect against West Nile virus infection by interferon-dependent and -independent mechanisms.* PLoS Pathog, 2007. **3**(7): p. e106.
140. Pichlmair, A., et al., *IFIT1 is an antiviral protein that recognizes 5'-triphosphate RNA.* Nat Immunol, 2011. **12**(7): p. 624-30.
141. Brass, A.L., et al., *The IFITM proteins mediate cellular resistance to influenza A H1N1 virus, West Nile virus, and dengue virus.* Cell, 2009. **139**(7): p. 1243-54.
142. Lu, J., et al., *The IFITM proteins inhibit HIV-1 infection.* J Virol, 2011. **85**(5): p. 2126-37.
143. Smith, S.E., et al., *Chicken interferon-inducible transmembrane protein 3 restricts influenza viruses and lyssaviruses in vitro.* J Virol, 2013. **87**(23): p. 12957-66.
144. Zhang, W., et al., *Respiratory Syncytial Virus Infection is Inhibited by Interferon-Induced Transmembrane Proteins.* J Gen Virol, 2014.
145. Zhu, X., et al., *IFITM3-containing exosome as a novel mediator for anti-viral response in dengue virus infection.* Cell Microbiol, 2014.
146. Haller, O. and G. Kochs, *Human MxA protein: an interferon-induced dynamin-like GTPase with broad antiviral activity.* J Interferon Cytokine Res, 2011. **31**(1): p. 79-87.
147. Gao, S., et al., *Structure of myxovirus resistance protein a reveals intra- and intermolecular domain interactions required for the antiviral function.* Immunity, 2011. **35**(4): p. 514-25.
148. Mitchell, P.S., et al., *Evolution-guided identification of antiviral specificity determinants in the broadly acting interferon-induced innate immunity factor MxA.* Cell Host Microbe, 2012. **12**(4): p. 598-604.
149. Goujon, C., et al., *Human MX2 is an interferon-induced post-entry inhibitor of HIV-1 infection.* Nature, 2013. **502**(7472): p. 559-62.
150. Kristiansen, H., et al., *The oligoadenylate synthetase family: an ancient protein family with multiple antiviral activities.* J Interferon Cytokine Res, 2011. **31**(1): p. 41-7.
151. Munir, M. and M. Berg, *The multiple faces of proteinkinase R in antiviral defense.* Virulence, 2013. **4**(1): p. 85-9.
152. Gale, M., Jr. and M.G. Katze, *Molecular mechanisms of interferon resistance mediated by viral-directed inhibition of PKR, the interferon-induced protein kinase.* Pharmacol Ther, 1998. **78**(1): p. 29-46.
153. Diamond, M.S. and M. Gale, Jr., *Cell-intrinsic innate immune control of West Nile virus infection.* Trends Immunol, 2012. **33**(10): p. 522-30.
154. International Committee on Taxonomy of Viruses. and A.M.Q. King, *Virus taxonomy : classification and nomenclature of viruses : ninth report of the International Committee on Taxonomy of Viruses*. 2012, London ; Waltham, MA: Academic Press. x, 1327 p.

155. Parida, M., et al., *Japanese Encephalitis Outbreak, India, 2005.* Emerg Infect Dis, 2006. **12**(9): p. 1427-30.
156. Pialoux, G., et al., *Chikungunya, an epidemic arbovirosis.* Lancet Infect Dis, 2007. **7**(5): p. 319-27.
157. Geiss, B.J., et al., *Focus on flaviviruses: current and future drug targets.* Future Med Chem, 2009. **1**(2): p. 327-44.
158. Erickson, A.K., S. Seiwert, and M. Gale, Jr., *Antiviral potency analysis and functional comparison of consensus interferon, interferon-alpha2a and pegylated interferon-alpha2b against hepatitis C virus infection.* Antivir Ther, 2008. **13**(7): p. 851-62.
159. Stapleton, J.T., et al., *The GB viruses: a review and proposed classification of GBV-A, GBV-C (HGV), and GBV-D in genus Pegivirus within the family Flaviviridae.* J Gen Virol, 2011. **92**(Pt 2): p. 233-46.
160. Fields, B.N., D.M. Knipe, and P.M. Howley, *Fields virology*. 5th ed. 2007, Philadelphia: Wolters Kluwer Health/Lippincott Williams & Wilkins. 2 v. (xix, 3091, 86 p.).
161. Kapoor, A., et al., *Identification of a pegivirus (GB virus-like virus) that infects horses.* J Virol, 2013. **87**(12): p. 7185-90.
162. Horner, S.M. and M. Gale, Jr., *Intracellular innate immune cascades and interferon defenses that control hepatitis C virus.* J Interferon Cytokine Res, 2009. **29**(9): p. 489-98.
163. Horner, S.M. and M. Gale, Jr., *Regulation of hepatic innate immunity by hepatitis C virus.* Nat Med, 2013. **19**(7): p. 879-88.
164. Li, K. and S.M. Lemon, *Innate immune responses in hepatitis C virus infection.* Semin Immunopathol, 2013. **35**(1): p. 53-72.
165. Saito, T. and M. Gale, Jr., *Regulation of innate immunity against hepatitis C virus infection.* Hepatol Res, 2008. **38**(2): p. 115-22.
166. Keller, B.C., et al., *Resistance to alpha/beta interferon is a determinant of West Nile virus replication fitness and virulence.* J Virol, 2006. **80**(19): p. 9424-34.
167. Suthar, M.S., et al., *IPS-1 is essential for the control of West Nile virus infection and immunity.* PLoS Pathog, 2010. **6**(2): p. e1000757.
168. Lanciotti, R.S., et al., *Origin of the West Nile virus responsible for an outbreak of encephalitis in the northeastern United States.* Science, 1999. **286**(5448): p. 2333-7.
169. Lanciotti, R.S., et al., *Complete genome sequences and phylogenetic analysis of West Nile virus strains isolated from the United States, Europe, and the Middle East.* Virology, 2002. **298**(1): p. 96-105.
170. Hayes, E.B., et al., *Virology, pathology, and clinical manifestations of West Nile virus disease.* Emerg Infect Dis, 2005. **11**(8): p. 1174-9.
171. Beasley, D.W., A.D. Barrett, and R.B. Tesh, *Resurgence of West Nile neurologic disease in the United States in 2012: What happened? What needs to be done?* Antiviral Res, 2013. **99**(1): p. 1-5.
172. Gray, T.J. and C.E. Webb, *A review of the epidemiological and clinical aspects of West Nile virus.* Int J Gen Med, 2014. **7**: p. 193-203.
173. Deen, J.L., et al., *The WHO dengue classification and case definitions: time for a reassessment.* Lancet, 2006. **368**(9530): p. 170-3.
174. Normile, D., *Tropical medicine. Surprising new dengue virus throws a spanner in disease control efforts.* Science, 2013. **342**(6157): p. 415.
175. Pagni, S. and A. Fernandez-Sesma, *Evasion of the human innate immune system by dengue virus.* Immunol Res, 2012. **54**(1-3): p. 152-9.
176. Rajapakse, S., C. Rodrigo, and A. Rajapakse, *Treatment of dengue fever.* Infect Drug Resist, 2012. **5**: p. 103-12.
177. Lauer, G.M. and B.D. Walker, *Hepatitis C virus infection.* N Engl J Med, 2001. **345**(1): p. 41-52.

178. Simmonds, P., *Genetic diversity and evolution of hepatitis C virus--15 years on.* J Gen Virol, 2004. **85**(Pt 11): p. 3173-88.
179. Feld, J.J. and J.H. Hoofnagle, *Mechanism of action of interferon and ribavirin in treatment of hepatitis C.* Nature, 2005. **436**(7053): p. 967-72.
180. Wyles, D.L., *Antiviral resistance and the future landscape of hepatitis C virus infection therapy.* J Infect Dis, 2013. **207 Suppl 1**: p. S33-9.
181. Suthar, M.S., M. Gale, Jr., and D.M. Owen, *Evasion and disruption of innate immune signalling by hepatitis C and West Nile viruses.* Cell Microbiol, 2009. **11**(6): p. 880-8.
182. Diamond, M.S., *Mechanisms of evasion of the type I interferon antiviral response by flaviviruses.* J Interferon Cytokine Res, 2009. **29**(9): p. 521-30.
183. Debing, Y., D. Jochmans, and J. Neyts, *Intervention strategies for emerging viruses: use of antivirals.* Curr Opin Virol, 2013. **3**(2): p. 217-24.
184. Myong, S., et al., *Cytosolic viral sensor RIG-I is a 5'-triphosphate-dependent translocase on double-stranded RNA.* Science, 2009. **323**(5917): p. 1070-4.
185. Sugimoto, N., et al., *Helicase proteins DHX29 and RIG-I cosense cytosolic nucleic acids in the human airway system.* Proc Natl Acad Sci U S A, 2014. **111**(21): p. 7747-52.
186. Matsumiya, T., et al., *The levels of retinoic acid-inducible gene I are regulated by heat shock protein 90-alpha.* J Immunol, 2009. **182**(5): p. 2717-25.
187. Mosallanejad, K., et al., *The DEAH-box RNA helicase DHX15 activates NF-kappaB and MAPK signaling downstream of MAVS during antiviral responses.* Sci Signal, 2014. **7**(323): p. ra40.
188. Lu, H., et al., *DHX15 senses double-stranded RNA in myeloid dendritic cells.* J Immunol, 2014. **193**(3): p. 1364-72.
189. Foy, E., et al., *Regulation of interferon regulatory factor-3 by the hepatitis C virus serine protease.* Science, 2003. **300**(5622): p. 1145-8.
190. Li, K., et al., *Immune evasion by hepatitis C virus NS3/4A protease-mediated cleavage of the Toll-like receptor 3 adaptor protein TRIF.* Proc Natl Acad Sci U S A, 2005. **102**(8): p. 2992-7.
191. Keller, A., et al., *Empirical statistical model to estimate the accuracy of peptide identifications made by MS/MS and database search.* Anal Chem, 2002. **74**(20): p. 5383-92.
192. Nesvizhskii, A.I., et al., *A statistical model for identifying proteins by tandem mass spectrometry.* Anal Chem, 2003. **75**(17): p. 4646-58.
193. Perkins, D.N., et al., *Probability-based protein identification by searching sequence databases using mass spectrometry data.* Electrophoresis, 1999. **20**(18): p. 3551-67.
194. Lin, R., Y. Mamane, and J. Hiscott, *Structural and functional analysis of interferon regulatory factor 3: localization of the transactivation and autoinhibitory domains.* Mol Cell Biol, 1999. **19**(4): p. 2465-74.
195. Fouraux, M.A., et al., *The human La (SS-B) autoantigen interacts with DDX15/hPrp43, a putative DEAH-box RNA helicase.* RNA, 2002. **8**(11): p. 1428-43.
196. Martin, A., S. Schneider, and B. Schwer, *Prp43 is an essential RNA-dependent ATPase required for release of lariat-intron from the spliceosome.* J Biol Chem, 2002. **277**(20): p. 17743-50.
197. Negash, A.A., et al., *IL-1beta production through the NLRP3 inflammasome by hepatic macrophages links hepatitis C virus infection with liver inflammation and disease.* PLoS Pathog, 2013. **9**(4): p. e1003330.
198. Tanaka, N., A. Aronova, and B. Schwer, *Ntr1 activates the Prp43 helicase to trigger release of lariat-intron from the spliceosome.* Genes Dev, 2007. **21**(18): p. 2312-25.

199. Vashist, S., D. Bhullar, and S. Vrati, *La protein can simultaneously bind to both 3'- and 5'-noncoding regions of Japanese encephalitis virus genome.* DNA Cell Biol, 2011. **30**(6): p. 339-46.
200. Kim, Y.K. and S.K. Jang, *La protein is required for efficient translation driven by encephalomyocarditis virus internal ribosomal entry site.* J Gen Virol, 1999. **80 ( Pt 12)**: p. 3159-66.
201. Liu, Y., et al., *Autoantigen La promotes efficient RNAi, antiviral response, and transposon silencing by facilitating multiple-turnover RISC catalysis.* Mol Cell, 2011. **44**(3): p. 502-8.
202. Honda, M., T. Shimazaki, and S. Kaneko, *La protein is a potent regulator of replication of hepatitis C virus in patients with chronic hepatitis C through internal ribosomal entry site-directed translation.* Gastroenterology, 2005. **128**(2): p. 449-62.
203. Ireton, R.C. and M. Gale, Jr., *RIG-I like receptors in antiviral immunity and therapeutic applications.* Viruses, 2011. **3**(6): p. 906-19.
204. Morrison, J., S. Aguirre, and A. Fernandez-Sesma, *Innate immunity evasion by Dengue virus.* Viruses, 2012. **4**(3): p. 397-413.
205. Garcia-Sastre, A., *Induction and evasion of type I interferon responses by influenza viruses.* Virus Res, 2011. **162**(1-2): p. 12-8.
206. Marsili, G., et al., *HIV-1, interferon and the interferon regulatory factor system: an interplay between induction, antiviral responses and viral evasion.* Cytokine Growth Factor Rev, 2012. **23**(4-5): p. 255-70.
207. Bale, S., et al., *Ebolavirus VP35 coats the backbone of double-stranded RNA for interferon antagonism.* J Virol, 2013. **87**(18): p. 10385-8.
208. Leung, D.W., et al., *Structural basis for dsRNA recognition and interferon antagonism by Ebola VP35.* Nat Struct Mol Biol, 2010. **17**(2): p. 165-72.
209. Luthra, P., et al., *Mutual antagonism between the Ebola virus VP35 protein and the RIG-I activator PACT determines infection outcome.* Cell Host Microbe, 2013. **14**(1): p. 74-84.
210. Qiu, X., et al., *Reversion of advanced Ebola virus disease in nonhuman primates with ZMapp.* Nature, 2014. **514**(7520): p. 47-53.
211. Piot, P., J.J. Muyembe, and W.J. Edmunds, *Ebola in west Africa: from disease outbreak to humanitarian crisis.* Lancet Infect Dis, 2014.
212. Bedard, K.M., et al., *Isoflavone agonists of IRF-3 dependent signaling have antiviral activity against RNA viruses.* J Virol, 2012. **86**(13): p. 7334-44.
213. Kato, T., et al., *Cell culture and infection system for hepatitis C virus.* Nat Protoc, 2006. **1**(5): p. 2334-9.
214. Gentleman, R.C., et al., *Bioconductor: open software development for computational biology and bioinformatics.* Genome Biol, 2004. **5**(10): p. R80.
215. Smyth, G.K., *Linear models and empirical bayes methods for assessing differential expression in microarray experiments.* Stat Appl Genet Mol Biol, 2004. **3**: p. Article3.
216. Chen, E.Y., et al., *Enrichr: interactive and collaborative HTML5 gene list enrichment analysis tool.* BMC Bioinformatics, 2013. **14**: p. 128.
217. Sumpter, R., Jr., et al., *Viral evolution and interferon resistance of hepatitis C virus RNA replication in a cell culture model.* J Virol, 2004. **78**(21): p. 11591-604.
218. Lohmann, V., et al., *Viral and cellular determinants of hepatitis C virus RNA replication in cell culture.* J Virol, 2003. **77**(5): p. 3007-19.
219. Krishnan, M.N., et al., *RNA interference screen for human genes associated with West Nile virus infection.* Nature, 2008. **455**(7210): p. 242-5.